EFFECTS OF THE NOVEL IDO INHIBITOR DWG-1036 ON THE BEHAVIOUR AND NEUROCHEMISTRY OF THE TRIPLE TRANSGENIC MOUSE MODEL OF ALZHEIMER'S DISEASE

by

Emre Fertan

Submitted in partial fulfilment of the requirements for
the degree of Master of Science

at

Dalhousie University
Halifax, Nova Scotia
August 2017

DEDICATION PAGE

First, I dedicate this thesis to my mother and father who loved and supported me unconditionally.

Second, to my grandparents, I wish they were here to see it.

And third, all the patients who are dealing with dementia; and their loved ones.

TABLE OF CONTENTS

LIST OF TABLES

LIST OF FIGURES

ABSTRACT

Alzheimer's disease (AD) is a neurodegenerative disorder causing memory loss as well as deficits in speech, motor performance and mood. Although the exact mechanisms causing the disease or how it progresses are not completely understood, amyloid beta 42 and tau are shown to be involved in neurodegeneration. In this thesis, we studied the role of the kynurenine pathway (KP) in the progression of behavioural and neurochemical deficits seen in AD. KP breaks down tryptophan, yet some of the by-products are known to be neurotoxic and involved in AD mechanisms, moreover KP is upregulated by amyloid beta 42. By inhibiting KP with a novel compound in the triple-transgenic mice and then testing them in a battery involving anxiety, cognition, motor and depression related tests, as well as studying their brains, for AD markers and KP metabolites using ELISA assays, we were able to further understand the role of KP in AD.

LIST OF ABBRIVIATIONS AND SYMBOLS USED

3HK: 3-hydroxykynurenine
3xTg-AD: Triple transgenic mouse model of Alzheimer's disease
5-HT: 5-hydroxytryptophan (Serotonin)
5xFAD: Five times familial mouse model of Alzheimer's disease
95% CI: Ninety-five percent confidence intervals
α: alpha
β: beta
μ: Mean
γ: gamma
ABAD: Amyloid beta-binding alcohol dehydrogenase
AD: Alzheimer's disease
Aβ: Amyloid beta
ACh: Acetylcholine
AIC: Akaike information criterion
AMPA: 3-hydroxy-5-methyl-4-isoxazolepropionate
ANOVA: Analysis of varience
APLP: Amyloid precursor like protein
ApoE: Apolipoprotein E
APP: Amyloid precursor protein
AUC: Area under the curve
BBB: Blood brain barrier
BDNF: Brain derived neurotrophic factor
BM: Barnes maze
CD: Cluster of differentiation
CNS: Central nervous system
CSF: Cerebrospinal fluid
DD: Death domain
DF: Degrees of freedom
DNA: Deoxyribonucleic acid
DS: Down syndrome
DSM: Diagnostic and Statistical Manual of Mental Disorders
E2: Exon 2
EDTA: Ethylenediaminetetraacetic acid
ELISA: Enzyme-linked immunosorbent
EOAD: Early onset Alzheimer's disease
EPM: Elevated plus maze
FAD: Familial Alzheimer's disease
FST: Forced swim test
GM-CSF: Granulocyte-macrophage colony-stimulating factor

HIV: Human immunodeficiency virus
ICD-10: 10th International Statistical Classification of Diseases and Related Health Problems
IDL: Intermediate-density lipoproteins
IDO: Indoleamine 2,3-Dioxygenase
IFN-γ: Interferon gamma
I-L: interleukin
KA: Kynurenic acid
KB: Kilobase
KP: Kynurenine pathway
LC/MSMS: Liquid chromatography-mass spectrometry
LDH: Lactate dehydrogenase
LR: Likelihood ratio
LTP: Long term potentiation
MAP: Microtubule associated protein
MAPT: Microtubule associated protein tau
mRNA: Messenger ribonucleic acid
MRT: Mean residence time
MWM: Morris water maze
NAD: Nicotinamide adenine dinucleotide
NCD: Neuro cognitive disorder
NINCDS/ADRDA: National Institute of Neurological and Communicative Diseases and Stroke/Alzheimer's Disease and Related Disorders Association
NMDA: n-methyl, d-aspartate
NO: Nitric oxide
NSAID: Non-steroidal anti-inflammatory drug
O2: Superoxide ion
OA: Open arm
OF: Open field
OH: Hydroxyl racidcal
p75(NTR): p75 neurotrophin receptor
PAG: Periaqueductal grey
PBS: Phosphate-buffered saline
PCR: Polymerase chain reaction
PK: Pharmacokinetics
PolyI:C: Polyriboinosinic-polyribocytidilic acid
PS1: prensilin1
PSEN: Presenilin
qPCR: Qualitative polymerase chain reaction
QA: Quinolinic acid
RAGE: Receptor for advanced glycosylation end products

RIPA: Radio-immunoprecipitation assay
ROS: Reactive oxygen species
RNA: Ribonucleic acid
SAP: Stretch attend posture
SEM: Standard error of mean
TFC: Trace fear conditioning
TLR: Toll-like receptor
TMB: Tetramethylbenzidine
TNF: Tumour necrosis factor
TREM2: Myeloid cells 2
Trp: Tryptophan
TST: Tail suspension test
TXNIP: Thioredoxin-interacting protein
VLDL: Very low-density lipoproteins
WT: Wild type
WHO: World Health Organization

ACKNOWLEDMENTS

I would like to thank Dr. Richard E. Brown for helping me to become a scientist by providing extraordinary guidance during the last 5 years.

Dr. Sultan Darvesh and Dr. Ian Weaver for sitting on my committee and all their help with the neurochemical analyses.

Dr. Donald Weaver, members of the Krembil Research Institute, and especially Dr. Kurt Stover for providing DWG-1036 and performing the tissue analysis for the PK study, as well as their helpful comments and contributions throughout the study.

Dr. Aimée A. Wong for her tremendous help during the entire study. Dr. Austin Korgan for his help during brain dissections. Thalia Garvock-de Montbrun and Nicole Woodland for their help during the data collection, and the entire Brown lab for their support.

.

CHAPTER 1: INTRODUCTION

1.1 The Epidemiology and Phenotype of Alzheimer's Disease

Alzheimer's disease (AD), which is the most common cause of dementia, is an age-related and progressive neurodegenerative disorder with cognitive and behavioural symptoms. The total number of dementia patients worldwide was 24.3 million in 2013 and this number is predicted to double every twenty years (Hampel at al., 2011; Prince et al., 2016), with a new diagnosis every 7 seconds (Ferri et al., 2005). In 2016, there was a total of 564,000 dementia cases in Canada, with the majority of them being AD. A total of 1.1 million Canadians are currently affected by the disease, and the annual financial cost of the disease to the society is estimated to be 10.4 billion Canadian dollars (Alzheimer's Society of Canada, 2016). The average life expectancy of an individual who has been diagnosed with AD at the age of 65 is 8.3 years, and this drops to 3.4 years if the patient is diagnosed at the age of 90 (Brookmeyer et al., 2002). Since patients with AD have a relatively long expected lifespan, they, as well as their relatives, must endure physical and psychological difficulties for a long period of time. There are studies showing that caregivers may develop symptoms of anger, anxiety, social withdrawal, and/or health and sleep problems as a consequence of caring for someone with AD (Simpson and Carter, 2014; Dauphinot et al., 2014). Therefore, AD is a debilitating condition that affects the individual, their families, and society as a whole, making it essential to gain knowledge about the disease and develop effective treatments that can delay and reverse the symptoms.

AD was first described by the German psychiatrist Aloysius (Alois) Alzheimer in 1907. The first documented case was seen in Auguste Deter, who was 51 years old when

the first symptoms of hallucinations, paranoia, and memory loss became apparent; her condition worsened over the next four years, until her death in 1906. When Alzheimer autopsied her brain, he observed unusual neurofibril formations inside the cells, which could be stained with dyes that normal fibrils did not react with. Moreover, there was severe neuronal loss in her cortex particularly in the upper layers, and formations of "miliary foci" (seed like formations which can be observed without staining), which were caused by the deposition of a "special substance". Alzheimer concluded his autopsy report by stating that, "Considering everything, it seems we are dealing here with a special illness…There are certainly more psychiatric illnesses than are listed in our textbooks" (Alzheimer, 1907 as translated by Stelzmann et al., 1995). Today, these unusual fibril formations are known as tau tangles, and the "special substance" has been characterized as amyloid beta (Aβ) fragments (Glenner and Wong, 1984). Together, the Aβ plaques ("miliary foci") and tau tangles are the neuropathological hallmarks of AD.

Although AD is typically recognized as an age-related disease, it is not solely restricted to the elderly population. About 17% of AD cases occur before the age of 65 and are defined as early onset Alzheimer's disease (EOAD) (Panegyres and Chen, 2013). Studies have shown that EOAD may have a more aggressive progression than late onset AD, with increased neuronal and synaptic loss (Nochlin et al., 1993), as well as more severe peripheral (Yasuno et al., 1998) and cognitive (Smits et al., 2012) defects. EOAD symptoms can appear as early as 24 years of age (Filley et al., 2007). Furthermore, as recognized by the DSM-V, there is a familial type of AD (FAD) that is often inherited with autosomal dominant gene mutations. About 60% of EOAD patients have a relative who has suffered from the same disease, and approximately 13% of them carry an

autosomal dominant mutation associated with AD (Campion et al., 1999). On occasion, relatives of people with late onset sporadic AD can also get EOAD (Brickell et al., 2006); these cases are less common and not as well understood, but nevertheless important as they indicate complex genetic causes of sporadic AD.

AD is most commonly described and studied as a cognitive disorder characterized by memory problems, which develop as a result of neurodegeneration (Nasrallah and Wolk, 2014) and synaptic dysfunction (Tu et al., 2014). Neuronal deficits typically start in medial temporal lobe structures such as the hippocampus and entorhinal cortex and spread throughout the basal forebrain to the neo-cortex (Thambisetty et al., 2010). As a result of this, hippocampal dysfunction is usually the first deficit seen in AD patients, often preceding other dementia symptoms by as many as 6 years (Small et al., 2000; Backman et al., 2001). The main function of the hippocampus appears to be episodic and spatial memory formation (Scoville and Milner, 1957). It has been suggested that the right hippocampus is involved in learning and navigating novel environments, and the left hippocampus is important for episodic memory formation (Burgess et al., 2002). As a result of hippocampal dysfunction, anterograde amnesia is the most common and is usually the initial symptom of AD. Episodic memory deficits are often followed by language problems in AD patients (Klimova et al., 2015). This is one of the most debilitating symptoms as it impairs the communication between patients and their caregivers. The underlying cause of the difficulty in verbal communication may be the loss of semantic memories rather than a neurological inability to produce speech (i.e. aphasia). In other words, when AD patients see a picture of a lion, they cannot name it because they do not recognize the animal (Weintraub et al., 2012). This was shown by

experiments of category fluency (naming things in a specific category) versus letter fluency, in which AD patients performed better in the latter task (Henry et al., 2004). As the disease progresses through the cortex, especially in the pre-frontal areas, working memory, executive function, and attentional deficits also become apparent (Weintraub et al., 2012).

Many "non-cognitive" symptoms are also associated with AD, and although they do not receive as much attention as the cognitive symptoms, they may be just as debilitating for patients and their caregivers. For example, motor dysfunctions occur in many AD patients, even before the appearance of cognitive symptoms (Buchman and Bennett, 2011). Dysphagia, which is an impairment in swallowing, is a common motor problem seen in later stages of AD. It is the most common cause of death in AD as the patient may choke on their food or die of aspiration pneumonia (Humbert et al., 2010). Another interesting "non-cognitive" change seen in AD patients is their pain response. There is actually a decrease in the pain medication prescribed for AD patients compared to age-matched controls (Pickering et al., 2005). This is due to the belief that people with AD have a lower pain sensitivity (Scherder et al., 2003). However, Cole et al. (2011) found higher connectivity between the brain areas responsible for pain sensation and response such as the dorsal-lateral pre-frontal cortex, thalamus, and the periaqueductal grey matter, as well as prolonged activation of these areas after painful stimulation. Together, these results indicate a potential detrimental situation in which AD patients are in fact experiencing more pain but are receiving less help to manage it. Behavioural deficits such as depression, anxiety, irritability, apathy, agitation, euphoria, and disinhibition, as well as psychotic symptoms such as delusions and hallucinations are also

commonly reported in advanced stages of AD (Monastero et al., 2009; Raudino, 2013). However, these symptoms may be caused by impairments in cognitive functioning (Fernandez et al., 2010). For example, depression may arise in the early stages of the disease as a result of the patient recognizing that their memory is beginning to decline. Similarly, at later stages when the patient is unable to recognize their caregivers, being surrounded by "unfamiliar people" may cause anxiety.

1.2 Diagnosis of AD

Dementia is described as a loss of memory function, accompanied with at least one more cognitive deficit (DSM-IV). Four of the most common forms of dementia, which make up 90% of all cases are AD, vascular dementia, fronto-temporal dementia and dementia with Lewy bodies (Parkinsonism) (Bolla et al., 2000). Since early diagnosis and appropriate treatment is crucial for slowing down the progression of AD, it is important to define and diagnose the condition with high accuracy and distinguish it from other types of dementia (Karantzoulis and Galvin, 2011).

There are various definitions of AD: The World Health Organization (WHO) described four different subtypes of AD in the 10th International Statistical Classification of Diseases and Related Health Problems (ICD-10). Those subtypes are (1) early onset AD, which shows symptoms before the age of 65; (2) late onset AD, which shows symptoms after the age of 65; (3) AD with atypical or delayed form, and (4) Alzheimer dementia without any specification (ICD-10 World Health Organization, 2001). On the other hand, the DSM-V (2013) categorizes AD under "neurocognitive disorders" (NCDs)

alongside dementia syndrome, delirium, amnesic syndrome, and other cognitive disorders. In this definition, AD has two mutually exclusive subdivisions: intensity (major vs. mild), and the absence or presence of a family history and genetic markers (sporadic vs. familial). Yet, there seems to be a number of problems with the definition used in the DSM-V. Firstly, it is not practical to group NCDs together, as the diseases listed in this category are quite distinct from each other in terms of cause, symptoms, and treatment. Furthermore, the given boundaries of mild and major AD are not clear enough to group the patients efficiently and provide distinct treatment options (Cornutiu, 2015). Lastly, recent studies have shown that there is a strong genetic component of sporadic AD, even though it is not as clearly understood as it is in familial AD cases (Piaceri et al., 2013). The final definition of AD comes from the National Institute of Neurological and Communicative Diseases and Stroke/Alzheimer's Disease and Related Disorders Association (NINCDS/ADRDA), whose diagnostic criteria for AD involves histopathological markers in addition to behavioural and cognitive symptoms (McKhann et al., 1984).

As demonstrated by the variety of definitions, AD is clinically heterogeneous in presentation and progression, demonstrating variable topographic distributions of atrophy. For example, focal temporal lobe dysfunction is associated with an amnestic syndrome, slow decline, with tangles limited largely to the medial temporal region including the entorhinal cortex. Moreover, while left parietal atrophy is associated with language symptoms, younger age of onset, and faster rate of decline; right parietal lobe atrophy is associated with a similar syndrome but with visuospatial symptoms replacing impaired

language function. Finally, the rare frontal variant is associated with executive dysfunction in addition to memory decline and behavioural deficits (Lam et al., 2013).

Even today, AD can only be diagnosed with total confidence after the analysis of the post-mortem brain by confirming the existence of plaques and tangles as described by Alzheimer (Joachim et al., 1988). However, there are some methods for early diagnosis of dementia while the patient is still alive. For example, a six-step evaluation test can be performed to diagnose mild dementia (Feldman et al., 2008). This test includes the patients' self-reported history as well as reports from primary caregivers in the absence of the patient. Past experiences of stroke, head trauma, or increasing memory loss and depression-like symptoms are used to evaluate the state of the patient. Next, a physical examination and brief cognitive tests are administered. If a decline in cognitive performance does exist, basic laboratory tests measuring blood levels of vitamin B12, erythrocytes, homocysteine, as well as Aβ levels in the cerebrospinal fluid (CSF) can be performed. Structural imaging tests for the brain are also applied to separate treatable causes of dementia such as renal failure, brain tumour, normal pressure hydrocephalus, subdural hemorrhages, and vascular dementia. Vascular dementia is another form of dementia, responsible for 5-20% of all the dementia cases (Igoumenou and Ebmeier, 2012), defined as the loss of cognitive function due to decreased blood flow to the cerebrum (Iemolo et al., 2009; Feldman et al., 2008). For a review of National Institute of Aging-Alzheimer's Association workgroups on diagnostic guidelines of AD see McKhann et al. (2011).

There is a growing interest in the peripheral changes in AD patients, and there are many studies focusing on the early effects of the disease on the immune system

(Serpentene et al., 2014), metabolic function (de la Monte and Tong, 2014), the gut-brain axis (Qiu and Zhu, 2014), as well as the microbiome (Shoemark and Allen, 2015). These peripheral changes could possibly be used to diagnose the disease by measuring metabolic, cell-based, and blood-based changes seen in AD (Khan and Alkon, 2015). The relationship between diabetes and AD is currently being studied extensively (Kroner et al., 2009). In addition to its role in glucose metabolism, insulin also acts as an important neuromodulator in the brain (Duarte et al., 2012). Some studies showed that decreased insulin levels affect neurotransmitter release and disturb plasticity (Izumi et al., 2003). Furthermore, Aβ and insulin are both amyloidogenic peptides sharing a common sequence recognition motif and can bind to the same receptor. This suggests that as the Aβ levels increase, it may compete with insulin for binding to the receptor (Xie et al., 2002). This may be one of the links between Aβ and formation of tangles, as decreased insulin signaling is known to cause tau hyperphosphorylation (Deng et al., 2009).

1.3 AD Mechanisms:

1.3.1 Amyloid Beta: AD is often described as the most complex of all neurological disorders, and the exact cause of the disease remains unclear. One of the oldest and most prominent theories is the amyloid cascade hypothesis. Glenner and Wong (1984) first suggested the involvement of a "novel cerebrovascular amyloid protein" in the pathogenesis of AD after they measured it in the beta sheet fibrils that Dr. Alzheimer called the miliary foci. Following this, various labs formulated the cascade hypothesis in the early 1990's (Hardy and Allsop, 1991; Selkoe, 1991). According to this hypothesis, the increasing imbalance of Aβ fragment production (especially $A\beta_{42}$) compared to its clearance is the first and primary cause of AD. This increased Aβ deposition results in

gliosis, oxidative stress, tau hyperphosphorylation, and eventually neuronal death (Figure 1; Selkoe and Hardy, 2016).

There is a great deal of evidence supporting the amyloid cascade hypothesis, such as the existence of Aβ plaques in post mortem brains and the fact that mutations increase the amount of $A\beta_{42}$ cause FAD. Furthermore, $A\beta_{42}$ itself has been shown to be neurotoxic: it binds to the cell surface p75 neurotrophin receptor (p75(NTR)) and activates its intracellular death domain (DD). In turn, the DD activates caspase-8, which then activates caspase-3, initiating apoptosis (Chiarini et al., 2006). Moreover, it has been shown that $A\beta_{42}$ can bind to α7 nicotinic receptors and get endocytosed (Nagele et al., 2002). Intracellular $A\beta_{42}$ is also known to increase phosphor-p53(ser15) expression by binding to the promoter and causing apoptosis in a Bax-dependent manner (Ohyagi et al., 2005; Fogarty et al., 2010). It has been shown that $A\beta_{42}$ starts to kill nerve cells as soon as two hours after exposure (Mann et al., 1996). Another strong piece of evidence for the crucial role of Aβ in AD comes from Down syndrome (DS), which is caused by an extra copy of chromosome 21 (Desai, 1997). During the first half of the 20th century the average life expectancy for children with DS was 9 years (Penrose, 1949), but now patients can live much longer. These patients, however, almost always develop AD in later stages of life. This is caused by over-expression of amyloid precursor protein (APP), which is located on the chromosome 21 (Wiseman et al., 2015). Furthermore, in some rare cases called translocation DS, which is caused by sections (not including the APP region) of an extra chromosome 21 being attached to one of the original copies (Bornstein et al., 2010), individuals do not develop AD later in life (Prasher et al., 1998). On the other hand, if the section carrying the APP gene is duplicated and not the rest of the

chromosome, individuals do not show signs of DS but do develop AD (Rovelet-Lecrux et al., 2006). All of these findings support the amyloid cascade hypothesis and indicate the causative role of Aβ in AD; however, the amyloid cascade hypothesis is not unchallenged (Morris et al., 2014).

The strongest anti-Aβ arguments are the presence of plaques in the post-mortem brains of individuals who did not show any signs of the disease while they were alive (Price et al., 2009) and the findings that decreasing Aβ levels do not always cure the cognitive symptoms (Mullane and Williams, 2013). When both arguments are considered, it is important to realize that there is a period between the increase of Aβ, neuronal loss, and the resulting cognitive decline. Some studies show that the brain pathology in AD may be evident years before the behavioural deficits (Morris et al., 1996; Perrin et al., 2009). This suggests that those individuals with the neuropathological symptoms of AD may have died “too early", before they developed any behavioural symptoms. Indeed, the post-mortem brain analysis of individuals with DS who died in their twenties show high plaque loads even though they did not have symptoms of AD. This also suggests that when AD symptoms appear, the neurological damage has already occurred and cannot be reversed, hence when someone goes to their physician with memory problems, it is already too late to reverse the symptoms by decreasing Aβ levels. Finally, although plaques were initially believed to be the damaging structures of Aβ, currently it is generally accepted that they are just byproducts of its overproduction and that the actual neurodegenerative form of Aβ are the oligomers (DaRocha-Souto et al., 2011).

Even though the role of APP in the development of AD has been extensively studied, surprisingly little is known about this molecule in terms of its natural function

(Dawkins and Small, 2014). APP is a single pass, transmembrane glycoprotein, belonging to the family of amyloid precursor-like proteins (APLP1 and APLP2) and has a large extracellular domain containing the N-terminus and a shorter intra-cellular domain containing the C-terminus (O'Brien and Wong, 2011). Alternative splicing of the 18 exons making up the gene may generate eight different isoforms. The 695-amino acid isoform is predominantly found in the central nervous system (CNS), while the 770 and 751 amino acid isoforms are found in other tissues and may be used as peripheral AD markers (Vignini et al., 2011). Although the exact physiological function of APP is unknown, it has been suggested that increasing the levels of APP may have positive effects on cell growth (Oh et al., 2009). Moreover, studies have found that APP may be important for neuronal survival and recovery after traumatic brain injury (Thornton et al., 2006). Although studies using APP knockout mice showed that the protein is not crucial for survival, these mice were more susceptible to ischemia-related death (Koike at al., 2012). APP knockout mice also had age-related deficits in passive avoidance learning (Senechal et al., 2008) and abnormalities in the pre-synaptic sites (Laßek et al., 2014), suggesting that APP is also involved in synaptogenesis and synaptic function. Other studies showed that APP promotes neurite outgrowth in cell cultures (Small et al., 1994; Allinquant et al., 1995) and its expression is upregulated in axons in response to injury (Gentleman et al., 1993), as well as during critical periods of synaptogenesis (Wang et al., 2009).

APP has structural similarities to the developmentally important protein Notch and has the ability to bind to Notch receptors, which suggests that APP and Notch may have similar functions in early development (Chen et al., 2006). APP is produced in high

quantities by the endoplasmic reticulum and transported to the axon endings using fast axonal transport (Koo et al., 1990). It is also rapidly metabolized and there is only a small amount of APP present on the cell surface at any given time (O'Brien and Wong, 2011), as summarized in Figure 2. There are multiple ways that APP can be cleaved and metabolized (Figure 3), and it is still not clear what determines which metabolic pathway APP will follow. The non-amyloid pathway in the cell membrane involves alpha (α) and gamma (γ) secretases. First, α-secretase cuts the protein within the amyloid sequence, releasing the ectodomain. Later, γ-secretase cleaves the trans-membrane domain of the protein (Nunan and Small, 2000). APP may also be endocytosed and taken to the Golgi apparatus and lysosomes, where it is cleaved by beta (β) secretase at the N-terminus and γ-secretase at the trans-membrane domain (Tam et al., 2014). This second pathway produces Aβ fragments at different lengths, with $A\beta_{40}$ and $A\beta_{42}$ being the most common (Winton et al., 2011), which are named according to their lengths in number of base pairs. As shown by Zhang et al., (2002), the smaller polypeptide chain ($A\beta_{40}$) has no neurotoxic effects but the insoluble $A\beta_{42}$ kills nerve cells as soon as two hours after exposure and accumulates over time to form plaques (Mann et al., 1996). Recently, a third cleavage pathway involving the α and β secretases has been described by Portelius et al. (2011). This cleavage pathway produces much smaller Aβ fragments that are only 15-16 amino acids act as an agonist for the pre-synaptic α7 nicotinic receptors, increasing calcium release and enhancing long term potentiation (LTP) and memory in a contextual fear conditioning task (Lawrance et al., 2014).

As with APP, the exact physiological role of Aβ is still unclear. Even though AD appears much later than the usual age of reproduction and therefore is not affected by the

rules of natural selection, evolutionary biology suggests that Aβ must have a beneficial purpose and increase fitness. Recent studies have shown that Aβ may be working as an anti-microbial agent in the brain, which is immunoprivileged. Kumar et al. (2016) showed that when the one-month-old five times familial mouse model of AD (5xFAD) and wild type (WT) littermates are intracerebrally injected with *salmonella typhimurium* bacteria, the 5xFAD mice showed significantly stronger disease resistance and reduced mortality. Later, they replicated these results using transgenic AD models of *Caenorhabditis elegans* and human cell lines expressing $A\beta_{42}$ and $A\beta_{40}$. Interestingly, in the human cell studies the survival rate was higher in the cells expressing $A\beta_{42}$ compared to $A\beta_{40}$. Moreover, when brains of the *S. typhimurium* infected 5xFAD mice were stained with Aβ and bacteria markers, co-localization was observed, showing higher amounts of Aβ in the infected cells. Brains of the 5xFAD mice which were not injected with the bacteria showed no staining for Aβ, consistent with the literature that Aβ deposition is detectable in this model around 1.5 months of age (Oakley et al., 2006). These findings provide strong evidence for the anti-microbial role of Aβ and indicate that infections may cause an increased production of Aβ.

Recent findings, indicate that the amyloid cascade hypothesis can explain some of the older theories of AD and bring researchers closer to a unified theory. For example, the cholinergic hypothesis of AD is one of the earliest attempts to explain the disease (Bartus et al., 1982). This theory is based on evidence that cholinergic neurons found in the basal forebrain, collectively called the Basal Nucleus of Meynert, are some of the earliest parts of the brain showing degeneration (Davies and Maloney, 1976). Acetylcholine (ACh) is an important neuromodulator with neuroprotective properties (Thompson et al., 2006;

Akaike et al., 2010), as well as being involved in learning and memory (Blokland, 1995; Hasselmo, 2006). Taken together, these findings suggest a strong involvement of cholinergic dysfunction in the pathogenesis of AD. As discussed below, there is strong evidence for the role of α7 nicotinic receptors in Aβ mediated toxicity in AD (Parri et al., 2011). Therefore, it is not surprising that along with n-methyl, d-aspartate (NMDA) receptor blockers such as memantine (Oliveras et al., 2012), cholinergic agonists and acetylcholinesterase inhibitors are the most commonly prescribed types of medication for AD (Ibach and Haen, 2004). As shown by Dr. Margaret Fahnestock's laboratory at McMaster University, degeneration of cholinergic neurons in the nucleus of Meynert is also related to Aβ deposition. Brain derived neurotrophic factor (BDNF) is an important growth factor for the survival and behaviour dependent plasticity of neurons (Lipsky and Marini, 2007). Levels of BDNF have been shown to decrease both in Aβ treated human neuroblastoma cells (Garzon and Fahnestock, 2007) and mouse models of AD (Peng et al., 2009). Since the BDNF input to the basal forebrain cholinergic neurons from the hippocampus is essential for their survival, Aβ induced decrease of BDNF release may be a key factor in the loss of these ACh neurons (Fahnestock et al., 2002).

Other disease mechanisms involving the cholinergic system are based on Aβ overstimulation of neurons or glial cells. In particular, the α7 nicotinic receptors seem to be highly involved in $A\beta_{42}$ mediated neuroregulation (Craig et al., 2011). Recent studies have shown that ACh is involved in maintaining proper Aβ levels and may have neuroprotective or neurodegenerative effects, depending on the amount of synaptic stimulation (Ovsepian and Herms, 2013). Aβ may bind to the α7 receptors on astrocytes and activate them, which causes a calcium influx into glial cells, causing them to release

glutamate to activate the extra-synaptic NMDA receptors (Talantova et al., 2013). These extra-synaptic NMDA receptors, unlike the synaptic NMDA receptors, are associated with neuronal damage and apoptosis (Parsons and Raymond, 2014). The activation level of α7 receptors on the neuron can have bi-directional effects (Bencherif et al., 2014). Controlled levels of stimulation promote neuronal survival (Marrero and Bencherif, 2009) but overstimulation decreases cognitive abilities (Boccia et al., 2010) and causes cell death (Gimonet et al., 2003).

1.3.2 Tau: In addition to Aβ, tau is an important molecule implicated in AD. Tau was discovered by Weingarten et al. (1975) and unlike Aβ, its physiological function is well understood: tau is a microtubule-associated protein (MAP). Along with the microfilaments and intermediate (neuro) filaments, microtubules are important structures that make up the cytoskeleton that supports neurons and many other cell types (Fletcher and Mullins, 2010; Kapitein and Hoogenraad, 2015). Microtubules are very dynamic during proliferation and eventually get stabilized by MAP's such as MAP1A, MAP1B, MAP2, and tau (Maccioni and Cambiazo, 1995). Tau is found in many species including *C. elegans*, *Drosophila*, goldfish, bullfrogs, rodents, bovines, monkeys, and humans (Buee et al., 2000). In humans, the microtubule associated protein tau (MAPT) gene is located on chromosome 17, extends over 100 kilobases (KB), and contains at least 16 exons (Andreadis et al., 1992). Tau is predominantly expressed in the axons, yet it can be traced in peripheral cells and glia (Kahlson and Kenneth, 2015). Tau in glial cells has been associated with some disorders (Berry et al., 2001). It has been shown that tau is not only involved in microtubule stabilization but also neurite growth, axonal transport (Avila et al., 2004), and nucleic acid protection (Violet et al., 2014). Interestingly, and similar to

APP knockouts, tau knockout mice are viable and only show minor deficits in terms of microtubule organization (Harada et al., 1994), muscle weakness, hyperactivity, and impairments in the contextual fear conditioning task (Ikegami et al., 2000). The survival and relatively normal phenotype of the tau knockout mice can be explained by increase of other MAP's such as MAP1A (Harada et al., 1994).

The tau protein has six different isoforms, resulting from the alternative splicing of exons 2 (E2), 3 and 10. Alternative splicing of E2 and E3 affects the N-terminal of the protein and results in the absence of 2 inserts, producing the 2N (longest with both inserts), 1N, and 0N (shortest without the inserts) isoforms. In the adult brain, the proportions of 2N, 1N, and 0N isoforms is approximately 54%, 37%, and 9% respectively (Goedert and Jakes, 1990), and these ratios change during different stages of development. For example, the shortest isoform is the only one present in the fetal human brain (Kosik et al., 1989). On the other hand, the alternative splicing of E10 affects the C-terminal, which is the microtubule binding site. This either adds or subtracts an additional binding repeat, producing the 4R or 3R isoforms (Liu and Gong, 2008). The proportion of these isoforms are similar in the adult human brain and the changes in the ratio often indicate disease (D'Souza and Schellenberg, 2005). There are as many as 85 potential phosphorylation sites (80 Ser, 80 Thr, and 5 Tyr) in the 2N4R (longest) isoform of tau, and most of these are accessible due to its unfolded structure, which makes tau a phosphoprotein (Wang and Mandelkow, 2016). While normal phosphorylation of tau is important for decreasing its binding to the microtubules and promoting structural dynamism, hyperphosphorylation is involved with various disorders. When hyperphosphorylated, tau detaches from microtubules, becomes hydrophobic, and forms

aggregates. This dysfunctional form of tau is seen in many neurological diseases, collectively called tauopathies. These include progressive supranuclear palsy, corticobasal degeneration, agyrophilic grain disease, Pick's disease, Huntington disease, frontotemporal dementia with Parkinsonism-17 and AD (Kovacs, 2015).

Dr. Alzheimer first observed the involvement of tau in AD, as he described "unusual neurofibril formations" in the brain of Aguste Deter (Alzheimer, 1907 as translated to English by Stelzmann et al., 1995). Hyperphosphorylation of tau does not only make it insoluble and detach from microtubules, but also significantly slows down its degradation, causing a buildup (Poppek et al., 2006). This may explain the formation of tangles as a defence mechanism against excess tau (Iqbal et al., 2010). Although the exact relationship between Aβ aggregation and tau-mediated toxicity is not completely understood, various *in vivo* and cell culture studies showed that tau is involved (if not essential) for Aβ-induced neuronal loss (Bloom, 2014). In one study, researchers crossed JNPL3 transgenic mice expressing a mutant tau protein with Tg2576 mice expressing mutant APP. The resulting offspring started showing Aβ pathology at the same age as the Tg2576 mice, but tau pathology was significantly more aggressive than in the JNPL3 mice, showing that Aβ contributes to tau dysfunction (Lewis et al., 2001). Similarly, when Roberson et al. (2007) crossed tau knockout mice with hAPPJ20 mice that over-express human APP, plaque accumulation in the offspring was similar to the hAPPJ20 mice. However, the loss of tau genes protected the hybrids against the learning and memory deficits and the excitotoxicity characteristic of the parental strain. These results were also supported by cell culture studies: when $A\beta_{40}$ was applied to mouse neuronal cultures, degeneration was observed. Later, when the same treatment was applied to cells

from tau knockout mice, there was no degeneration, yet the degenerative effect of $A\beta_{40}$ was rescued in these cells by expressing human tau (Rapoport et al., 2002). Collectively, these results suggest the role of tau in Aβ-induced toxicity.

Interestingly, there is evidence suggesting that tangles are not the toxic form of tau but instead smaller oligomeric aggregates formed by hyperphosphorylated tau are responsible for neurodegeneration (Ward et al., 2012). This is similar to the current idea that Aβ oligomers are the toxic form of Aβ, instead of the plaques. Hence, the two hallmarks of the disease seem to be "easier to detect by-products" of the actual toxic forms. Using specific antibodies for the oligomeric tau, LaPointe et al. (2009) showed that the N-terminus of insoluble tau can inhibit fast axonal transport in the anterograde direction, but monomers cannot. Dysfunctional tau aggregates seem to be involved in synaptic dysfunction, one of the most important factors for memory deficits in AD. By using neuronal cultures, Frandemiche et al. (2014) showed that tau is normally localized in the axonal dendritic shafts during resting conditions. Yet, synaptic activity via chemical and electrophysiological LTP (Bliss and Lomo, 1973) protocols relocate tau to the synaptic terminals and spines, interacting with actin. Yet, when Aβ was added to the cultures, tau was translocated to the synapse in the resting state and both tau and actin levels were decreased after synaptic activity, showing the exact opposite of normal physiological conditions. Finally, when Frandemiche et al. (2014) looked at the phosphorylation state of synaptic tau after the LTP protocol and Aβ induced translocation, they found differences in phosphorylated sites. Altogether, these findings suggest that while both Aβ and tau are essential for the development of AD, Aβ acts more like a trigger initiating the deficits and tau is like the bullet which causes the effect.

However, there are several other "components of the gun" which are involved in the disease.

1.3.3 Immune Response and Inflammation: The role of the immune system and neuro-inflammation in AD has long been recognized. There is microglia activation in AD (Solito and Sastre, 2012), and some evidence indicating a protective role of long time non-steroidal anti-inflammatory drug (NSAID) use (Vlad et al., 2008). Yet, the exact mechanisms regulating the immune response and the role of Aβ in the processes are not fully understood. Traditionally, microglia activation and inflammation has been linked to Aβ deposition. As proposed by the cascade hypothesis, microglia activity was considered a response to increased Aβ in the later stages of the disease (Lim et al., 2000; Wyss-Coray, 2006). However, some recent evidence suggests that immune activity may precede Aβ pathology: mutations in genes encoding triggering receptors expressed on myeloid cells 2 (TREM2) and microglia cell surface antigen CD33 have been linked to AD (Jonsson et al., 2013; Bradshaw et al., 2013). When Krstic et al. (2012) stimulated the immune system of pregnant mice at the late gestation period with polyriboinosinic-polyribocytidilic acid (PolyI:C), which is a synthetic analog of double stranded viral RNA (Lever et al., 2015), they observed AD-like symptoms in the offspring at later stages of life such as increased APP expression, altered tau phosphorylation, and working memory deficits. If the immune system of these mice was challenged again during adulthood, the phenotype became even more evident.

The relationship between the immune response and Aβ becomes even more complex when the antimicrobial role of Aβ is considered. If Aβ itself is present to fight infections in the CNS, it is paradoxical that it would induce an immune response. Perhaps

Aβ is working alongside microglia to clear infections but as the cascade hypothesis suggests, Aβ may stop being beneficial after a certain concentration and starts being detrimental, creating the need of clearance. Aβ binds to a number of proteins on the surface of microglia including cluster of differentiation 14 (CD14), CD36, CD47, α6β1 integrin, class A scavenger receptor, receptor for advanced glycosylation end products (RAGE), and toll-like receptors (TLRs) and cause production of inflammatory cytokines and chemokines such as interleukin-1 (IL-1), IL-6, granulocyte-macrophage colony-stimulating factor (GM-CSF), IL-12 and IL-23, and tumour necrosis factor (TNF) (Heppner et al., 2015). In addition to the production of inflammatory modulators, receptor-mediated phagocytosis of Aβ by the microglia has been shown *in vitro* (Koenigsknecht and Landreth, 2004).

1.3.4 Mitochondrial Dysfunction and Oxidative Stress: Reactive oxygen species (ROS) are the byproducts of aerobic respiration. They are rich in free radicals, which are molecules with unpaired electrons, making them highly reactive with other molecules around them. Several ROS including superoxide ion (O2(•-)), hydroxyl radical (OH(•)), and nitric oxide (NO(•)) serve important physiological purposes in cell signaling (Thannickal and Fanburg, 2000; Vara and Pula, 2014). The balance between their production and clearance is very important, as accumulation of ROS causes oxidative stress by binding to nucleic acids, proteins, and lipids, causing their oxidation (Kohen and Nyska, 2002). ROS are cleared by antioxidant enzymes; and either an increase in ROS production or a decrease in antioxidant enzyme levels can tip the delicate balance. All of these deficits have been observed in AD brains, in multiple regions including the hippocampus, entorhinal cortex, and the amygdala (Wang et al., 2014). Moreover, marks

of oxidative stress can be seen in the earlier stages of AD before significant plaque and tangle accumulation (Pratico at al., 2002). However, this does not mean that these symptoms precede or cause Aβ pathology: studies done with DS patients showed increased oxidative stress in earlier stages of life before developing AD symptoms (Pallardo et al., 2006), suggesting that Aβ is still involved in the ROS imbalance. Similarly, the occurrence of oxidative damage in FAD (Velez-Pardo et al., 1998) supports the theory that Aβ is a driving factor in ROS elevation.

Mitochondria are the major sources of ROS production due to the inevitable electron leakage during the electron transport chain of cellular respiration. Not surprisingly, deficits in all mitochondrial functions have been reported in AD, even in the early stages (Wang et al., 2009). Reduced glucose metabolism is shown to be caused by reduced expression of genes encoding subunits of the mitochondrial electron transport chain (Gibson et al., 1998; Rhein et al., 2009). Mitochondria are also prominent sources of intracellular calcium and heavily involved in apoptotic pathways (Giorgi et al., 2012). Hence, mitochondrial damage caused by Aβ overload is not only detrimental to the neurons due to the decreased energy production, but also due to increased oxidative stress, disrupted signaling pathways, and the potential to cause apoptotic neuronal loss. One enzyme involved in Aβ-mediated mitochondrial dysfunction and eventually neuronal loss is amyloid beta-binding alcohol dehydrogenase (ABAD). This enzyme is predominantly found in the mitochondria and interacts with Aβ. Furthermore, elevated levels of ABAD have been found in post-mortem analyses of human brains with AD and the brains of mouse models of AD. This interaction is shown to increase cytochrome *c* release, DNA fragmentation, lactate dehydrogenase (LDH) release, and generation of

ROS in cortical neurons (Chen and Yan, 2007). Furthermore, spatial learning and memory deficits in the radial-arm water maze are seen in the mAPP/ABAD mouse model of AD (Lustbader et al., 2004). Taken together, these findings suggest that Aβ is an important factor in mitochondrial dysfunction, damaging the energy metabolism of the neurons, increasing ROS, and eventually causing apoptosis. Interestingly, physiological levels of Aβ are shown to have anti-oxidant properties, neutralizing ROS (Kontush, 2001). This may be additional evidence for the amyloid cascade hypothesis, as an increase in Aβ causes mitochondrial dysfunction and increases oxidative stress, which in turn increases Aβ, which decreases oxidative stress, creating a negative-feedback loop.

1.3.5 Genetic Factors in AD: Many genetic mutations may accelerate the onset of AD and cause the symptoms to appear before the age of 60 (Alberici et al., 2014). Some of these mutations may be inherited in an autosomal dominant fashion and cause Familial Alzheimer's Disease (Campion et al., 1999) which represents about 5% of all AD cases (Wu et al., 2012). Mutations in three specific genes have been associated with FAD: 24 different mutations are described for the *APP* gene on chromosome 21; 185 mutations are described for the *Presenilin 1* (PSEN1) gene on chromosome 14, and 14 mutations are described for the *Presenilin 2* (PSEN2) gene on chromosome 1 (Tanzi, 2012). While the *APP* mutations increase the total Aβ production as well as the $A\beta_{42}$:$A\beta_{40}$ ratio by modifying specific cleavage sites, PSEN1 and PSEN2 are both subunits of γ-secretase and increase $A\beta_{42}$ production. Interestingly, γ-secretase is also involved in Notch cleavage (O'Brien and Wong, 2011), but the effects of *presenilin* mutations on Notch signaling is not well understood. Some studies suggest γ-secretase inhibitors may disrupt Notch signaling and help prevent some types of cancer (Olsauskas-Kuprys et al., 2013).

Recently, Muller et al. (2013) restudied the brain of Dr. Alzheimer's patient Auguste Deter and found that the first documented AD patient was suffering from an autosomal dominant *PSEN1* mutation. Since her family record did not indicate relatives suffering from dementia, Auguste Deter cannot be diagnosed with FAD but the mutation could be the reason behind the early onset of the symptoms, even though the findings of Muller et al. (2013) are still controversial (Rupp et al., 2014).

Although mutations seen in AD are most commonly associated with the familial form of the disease, some genetic mutations are also involved in the sporadic form. Mutations in apolipoprotein E (ApoE) are some of the most common mutations associated with sporadic AD. Discovered in the early 1970s, ApoE is a lipoprotein involved in the transport of lipids among cells and in the clearance of very low-density lipoproteins (VLDL) and intermediate-density lipoproteins (IDL) from the plasma. There are three different isoforms of ApoE: while ApoE3, the most common isoform, is considered to be the "normal form", ApoE2 and ApoE4 differ from ApoE3 by a single amino acid substitution at position 112 or 158 (Huang and Mahney, 2014). Recently, Thomas Sudhof's lab showed that these isoforms play different roles in the development of AD (Huang et al., 2017). By using trans-differentiated human embryonic stem cells into excitatory neurons, either cultured with or without glial cells, they first showed that the presence of glia increases Aβ production significantly. In order to investigate the role of glia in Aβ production, they added specific glial proteins to the cultured neurons, one at a time, and determined that ApoE, Igf2, and IgfBP2 were responsible for the increase in Aβ. To investigate the role of glial ApoE in this process, they expressed the three different ApoE isoforms on the cultures individually and found that all three of them

increased the levels of both $A\beta_{40}$ and $A\beta_{42}$ without changing the levels of the secretases involved in APP cleavage, suggesting an overall increase in APP levels. Furthermore, they found that the three ApoE isoforms have different potencies in increasing Aβ levels in the order of ApoE4 > ApoE3 > ApoE2. ApoE activation starts a signaling cascade causing increased ERK1/2 phosphorylation in the same order of ApoE4 > ApoE3 > ApoE2. Eventually this cascade activates the AP-1 transcription factor and increase APP transcription. These results were also supported by qualitative polymerase chain reaction (qPCR) studies, as adding ApoE increased the levels of APP mRNA. Together these findings show the involvement of ApoE in the pathogenesis of AD and how mutations increasing the ApoE4 production may be a risk factor. Furthermore, as ApoE is involved in lipid transfer, its effect of increasing APP also provides insight for the physiological role of APP. As discussed earlier, APP is a membrane protein, increased during growth and after injuries. Therefore, glial ApoE may be the regulator of this increase, providing the necessary APP for the growing neuronal membrane and Aβ may be the byproduct of this process.

1.4 The Kynurenine Pathway and AD:

The main objective of this thesis is to understand the role of the kynurenine pathway (KP) on the progression of AD-like symptoms in the behaviour and brain chemistry of the triple transgenic (3xTg-AD) mouse model. Tryptophan (Trp) is one of the nine essential amino acids that the human body cannot synthesize and must acquire through diet (Moffett and Namboodiri, 2003). Once absorbed by the body, Trp travels through the circulatory system either bound to albumin or in free form, with the albumin-bound form accounting for up to 90% (McMenamy et al., 1965). Trp can only be transported across

the blood brain barrier in its free form by the competitive and non-specific L-type amino acid transporter (Hargreaves et al., 1988). Once in the CNS, Trp acts as a precursor to various metabolic pathways producing proteins, serotonin, and kynurenines (Ruddick et al., 2006). In both the peripheral and central systems, the KP is a major route for the metabolism of Trp, breaking down 95% of the Trp into nicotinamide adenine dinucleotide (NAD), one of the major electron carriers in cellular respiration (Soliman et al., 2010). Trp is also heavily involved in the immune response. Trp is required for T-cell survival and proliferation. Most of the information about the role of Trp in this process comes from KP studies, as catabolism of Trp within this pathway significantly decreases T-cell activity (Munn et al., 1999; Moffett and Namboodiri, 2003). As shown in Figure 4, there are many steps in the KP, each producing various byproducts.

Indoleamine 2,3-Dioxygenase (IDO) is the first and rate-limiting enzyme in the KP (Soliman et al., 2010). It is 407 amino acids in length and is transcribed by the INDO gene, which is located on the 8th chromosome in humans. IDO is expressed in the lungs, gut, kidneys, plasmacytoid dendritic cells within draining lymph nodes, spleen, and brain (Soliman et al., 2010). It was initially studied for its role in pregnancy (Munn et al., 1998) and cancer (Moon et al., 2015), as it is upregulated in both cases. This is due to the immune activating function of Trp: during pregnancies, the placenta releases IDO in order to break down Trp and stop the immune system from attacking the foreign embryo. In cancer, tumours release IDO in order to stop the body from killing the cancerous cells and allow the tumor to grow. IDO also inhibits Vav1, a guanine nucleotide exchange factor, involved in the signaling of the activated T-cell receptor through the MAPK/ERK pathways (Li et al., 2009). Under normal physiological conditions, IDO expression is

balanced by a negative feedback loop: kynurenine, one of the KP metabolites, increases IL-6 expression that in turn suppresses the promoter region of INDO (Dinatale et al., 2010). There are other modulators of IDO expression, which alter the balance between IDO and Trp in various diseases. Various cytokines and inflammatory molecules, such as lipopolysaccharides and human immunodeficiency virus (HIV) proteins (Fujigaki et al., 2001), increase IDO expression. However, its most potent stimulant is interferon gamma (IFN-γ), which is able to both induce the expression and increase the enzymatic activity of IDO-1 (Yasui et al., 1986; Dai et al., 1990; Taylor and Feng, 1991). Since INF-γ is released from activated T-cells in the immune response, (Chen and Guillemin, 2009), there seems to be another negative-feedback regulation of Trp. Interestingly, $A\beta_{42}$ has also been shown to increase IDO expression in microglia (Guillemin et al., 2003b). As discussed earlier, microglia are heavily involved in the immune response seen in AD. Moreover, the relationship between AD, Aβ, and INF-γ is also quite complex. Yamada et al. (2009) showed that IDO expression and KP activity were only increased by INF-γ in cell cultures pre-treated with $A\beta_{42}$ and INF-γ, as $A\beta_{40}$ pre-treatment had no such effect. Secondly, pre-treating neuronal cultures with INF-γ significantly increased apoptosis caused by $A\beta_{42}$ treatment, compared to INF-γ alone (Bate et al., 2006). Another study showed that nitric oxide (which is a ROS), is increased in the moderate stages of AD in an IFN-γ and tumour necrosis factor alpha (TNF-α) dependent manner (Belkhelfa et al., 2014), indicating the role of INF-γ in oxidative stress. By using a Swedish-APP mutant transgenic mouse lacking the IFN-γ receptor type I, Yamamoto et al. (2007) showed the importance of IFN-γ in Aβ plaque buildup. These mice had significantly fewer amyloid plaques and gliosis at 14 months of age compared to the ones with functional IFN-γ receptors. In addition, they also showed that IFN-γ and TNF-α up-regulate the expression

of β-secretase. Although most of the evidence suggests a detrimental role of INF-γ in AD, one study using 3xTg-AD mice (which are also used in the current study), showed that 10 months of chronic intra-hippocampal expression of IFN-γ through delivery of a serotype-1 recombinant adeno-associated virus vector increased microglia activation and Aβ pathology, but also decreased the levels of hyperphosphorylated tau and even increased neurogenesis (Mastrangelo et al., 2009).

Based on the complex relationships between IDO regulating INF-γ and AD, and the direct role of $A\beta_{42}$ in IDO expression, the KP is an important mediator in the development of AD. In the healthy brain, tryptophan, IDO, and KP metabolite levels are balanced, but in AD, KP activity is increased which raises the concentration of metabolites produced (Chen and Guillemin, 2009). This has two main effects on brain physiology: (1) tryptophan levels decrease, and since tryptophan is necessary for immune activation, the immune activity of the AD brain is decreased (Corona et al., 2013). (2) Due to the increase of IDO, KP metabolites 3-hydroxykynurenine (3HK), quinolinic acid (QA), and kynurenic acid (KA) are increased, which are associated with AD in different ways. 3HK acts as a neurotoxin; once taken into the cells with transporters for large neutral amino acids, it increases oxidative stress and initiates apoptotic pathways (Okuda et al., 1998). This toxicity appears to be region specific, possibly due to differential transporter activity. One study showed increased 3HK levels in the post-mortem striatal tissue of Huntington's disease patients, but not in AD brain cortices (Pearson and Reynolds, 1992). However, a recent study showed increased 3HK levels in the serum of AD patients (Schwarz et al., 2013). Since 3HK can pass through the blood brain barrier (Fukui et al., 1991), it is not clear why the levels were not significantly different in

cortical neurons.

Quinolinic acid is a NMDA receptor agonist, causing excitotoxicity at high levels (Stone et al., 1981). The cortical levels of QA are normally lower compared to peripheral tissues (Hayes et al., 1997), but QA is significantly increased during the immune response, mostly by microglia and dendritic cells (Hayes et al., 1996). Neurons and astrocytes, on the other hand, are not capable of producing QA as they lack the enzyme kynurenine hydroxylase (Moffrett et al., 1993). Instead, they uptake QA and convert it to NAD, which is non-toxic (Guillemin et al., 2007). However, this system is rapidly exhausted in pathological conditions, such as AD, causing significantly high levels of QA (Guillemin et al., 2005). Direct application of QA onto neuronal cultures cause neuronal death (Kim et al., 1987), and injection of QA into distinct regions of the rat brain cause axonal lesions (Schwarcz et al., 1983). QA has a significant implication in AD, in that it is associated with the hyperphosphorylation of tau. When added to human neuronal cultures, QA significantly increased the levels of phosphorylated tau. Furthermore, this system seems to be NMDA-dependent since adding memantine, an NMDA antagonist used as a therapeutic in AD, blocked the phosphorylation. Polymerase chain reaction (PCR) studies showed that QA affects the expression of 10 genes involved in AD; six associated with tau phosphorylation pathways and four with neuroprotective properties (Rahman et al., 2009).

On the other hand, kynurenic acid is neuroprotective and even functions as an antagonist for QA. In low concentrations, it binds to and inhibits the glycine-modulatory site of NMDA receptors, and in high concentrations it binds to the glutamate-binding site of NMDA and 3-hydroxy-5-methyl-4-isoxazolepropionate (AMPA) receptors (Stone,

1993). In addition, it also antagonizes the α7 receptors (Hilmas et al., 2001), which selectively activates a G-protein coupled receptor, GPR35 (Wang et al., 2006), which is involved in inflammatory pain (Cosi et al., 2011). Increased KA has anticonvulsant and sedative effects (Carpenedo et al., 1994), and is protective against ischemic damage (Cozzi et al., 1999). Moreover, KA has also been shown to decrease the levels of TNF-α and nitric oxide (Morini et al., 2007). Although KA appears to be reversing the adverse effects of 3HK and QA, its levels are too low compared to the other metabolites (1:15), and therefore fails to act as a full protective agent in diseases such as AD (Moroni et al., 1988).

Wu et al. (2013) studied the production of kynurenine metabolites in the brains of 3xTg-AD mice and AD patients. They showed a slight increase in IDO mRNA levels in the hippocampi of 2-4, 6-8, and 10-12-month-old 3xTg-AD mice compared to WT controls. IDO levels are significantly higher in the cerebellum of all mice at all ages compared to the hippocampus and cortex. On the other hand, an age-related increase of QA levels was reported in the hippocampi of 3xTg-AD mice. Significantly higher levels of hippocampal IDO were reported in human AD patients compared to age and sex-matched controls. These results show that although a similar IDO pathology exists in the 3xTg-AD model, it is not as robust as in humans.

To our knowledge, the only study done to treat a mouse model of AD with an IDO inhibitor was performed by Yu et al. (2015). They used coptisine, a chemical widely used in Chinese medicine, which has been shown to inhibit IDO activity. They treated 8-month-old APP/PS1 mice with coptisine for one month followed by testing in the Morris water maze (MWM) and studied their brains. Results showed that coptisine reversed the

performance deficits in the MWM and decreased the plaque formation and microglia activation.

1.5 Mouse Models of AD

The most effective method for developing new AD treatments would be to test novel drugs on AD patients and observe the effects of these drugs on their brains; however, due to obvious ethical and experimental control concerns, it is not possible to do these types of studies on humans. Therefore, the development and testing of animal models that mimic aspects of AD are necessary. Many mouse models of AD have been developed, mostly by inserting or knocking out different genes that are related to APP, Aβ, or tau production (Wong at al., 2002). Five widely used models in laboratories around the world were reviewed by Bilkei-Gorzo (2013) and are described briefly below.

The single transgenic *Tg2576*, and *APP23* mouse models carry the Swedish mutation (with different promoters in each model), which increases the production of APP and eventually the amount of insoluble $A\beta_{42}$ protein. This causes an age-related increase in the presence of amyloid plaques. Structures of the limbic system and noradrenergic neurons are mainly affected in these models (Bondolfi et al., 2002; Guerin et al., 2009). These mice show cognitive deficits as well as disturbed circadian rhythms, yet these symptoms are less severe than seen in humans with AD. The *APP/PS1* double transgenic model also show increased $A\beta_{42}$ levels, but these mice carry an extra mutation on the *Presenilin 1* gene in addition to the Swedish mutation, which significantly increases the amount of $A\beta_{42}$ produced. Neural degeneration starts as early as 6-8 weeks of age in these mice (Manook et al., 2012), followed by cognitive deficits (Lagadec et al., 2012) as well as motor and behavioural symptoms (Pugh et al., 2007). However, these

impairments are relatively lower compared to humans with AD which, as with *Tg2576* and *APP23* models, which decreases the face value of the model. All of these models show the Aβ pathology that is crucial for the development of AD, but as mentioned above, it is not the only neurohistological hallmark of AD, as tau tangles are also found in the brains of AD patients. *P301L* mice, engineered as a model for frontotemporal dementia, were the first model that showed tau pathology due to the over expression of the tau gene (Lewis et al., 2000). At 6 months of age, these mice showed tangle formations in the brain and the spinal cord, as well as up to a 50% loss in neuronal density in the spinal cord. Moderate motor problems were demonstrated in these mice at about 10 months of age, with the majority of these mice dying around 13 months before showing significant cognitive deficits (Gotz et al., 2007).

The 5xFAD mouse model was engineered by Oakley et al. (2006) by introducing mutations to the *APP* and *PSEN1* genes of C57BL/6 x SJL F1 mice: (1) the K670N/M671L substitution, which is known as the Swedish mutation, was first identified by Mullan et al. (1992) and is associated with some FAD cases in Sweden. This mutation affects the β-secretase cleavage site and increases the overall Aβ production (Haass et al., 1995). (2) The I716V or the "Florida" mutation was described by Eckman et al. (1997) and is associated with the γ-secretase cleavage site. (3) The *V717I*, which is known as the "London" mutation (Goate et al., 1991), also acts on the γ-secretase cleavage site and increases the $A\beta_{42}$:$A\beta_{40}$ ratio. A recent case study on two Italian families with multiple members suffering from early onset AD reported that all individuals who had the disease also carried the autosomal dominant London mutation (Talarico et al., 2010). Finally, (4) the M146L and (5) the L286V transgenes were added to *PSEN1*. It has been shown that

these five mutations act in an additive manner and accelerate $A\beta_{42}$ formation in the brain (Citron et al., 1998). Studies using 5xFAD mice have shown that intracellular $A\beta_{42}$ plaques form as early as 1.5 months of age, followed by extracellular $A\beta_{42}$ plaques at 2 months of age (Oakley et al., 2006).

To our knowledge, the only transgenic mouse model showing both Aβ and neurofibrillary tangle pathology is the triple transgenic mouse (3xTg-AD) which is a powerful model to investigate the neurobiological and behavioural aspects of AD. The 3xTg-AD mouse model was originally generated by Oddo et al. (2003) by co-microinjecting APP_{Swe} and tau_{P301L} to single-cell embryos of homozygous $PS1_{M146V}$ knock-in mice. These mice are reported to show intracellular Aβ buildup in the cortex starting at three months of age, which extends to the hippocampus between three and six months, followed by extracellular plaque formation around six months. While the first traces of hyperphosphorylated tau can be measured at six months of age in the hippocampus, the tangle pathology becomes severe around nine months of age (Oddo et al., 2003).

The M146V mutation on the presenilin1 (PS1) gene increases Aβ levels by altering APP cleavage. PS1 is a component of γ-secretase, which cleaves APP with β-secretase in the $A\beta_{42}$ pathway. In addition to AD, the M146V mutation is also associated with store-operated calcium channel activity (Ryazantseva et al., 2013), which may contribute to excitotoxicity. It is also involved in neurotrophin receptor p75NTR cleavage by γ-secretase (Hatchett et al., 2007). Since this receptor is found on basal cholinergic neurons, the M146V mutation may be contributing to the cholinergic deficits in AD in an Aβ-irrelevant fashion. This mutation is also involved in developmental processes, as

Tokuhiro et al. (1998) showed that the mutant PS1 attenuates the neuronal differentiation of NTera 2 cells. Lastly, Deasi et al. (2012) showed that when treated with $A\beta_{42}$, M146V mutant cell cultures show oligodendrocyte dysfunction and loss of myelination. This suggests that PS1 is not only involved in increasing $A\beta_{42}$ levels, but also involved in other disease mechanisms.

As explained earlier, the Swedish mutation is associated with FAD and increases overall Aβ levels. On the other hand, tau_{P301L} is a frontotemporal dementia mutation. It was first described by Hutton et al. (1998) and was named after its effects of changing cytosine to thymine at codon 301, resulting in the substitution of proline instead of leucine in the translated protein. In 1999, Mirra et al. described a family with this mutation who suffered from dementia. Although they were initially diagnosed with AD during their lifetime, post-mortem analyses showed frontotemporal dementia pathology with tau tangles as well as neuronal and glial inclusions, neuropil threads, and astrocytic plaques. Since the P301L mutation is on the 10th exon, only the 4R isoforms of tau are affected (Kar et al., 2007). As explained above, mice carrying the P301L mutation develop age-related tau pathology as well as behavioural deficits (Lewis et al., 2000). Interestingly, it has been shown that in the earlier stages of tau pathology, mice show superior motor performance on the Rotarod and balance beam tasks compared to WT controls, yet as the mice age, this enhanced motor performance is reversed and P301L mice start showing motor deficits (Morgan et al., 2011). A similar phenotype was also shown in the 3xTg-AD mice by our lab: Stover et al. (2015) tested six-month-old 3xTg-AD mice on a test motor battery and showed significantly enhanced performance on the Rotarod compared to the WT controls. Yet, when the same battery was repeated with

naive mice at 16 months of age, the enhanced motor phenotype was less apparent (Garvock-de Montbrun et al., paper in progress). These findings suggest that the improved motor performance seen in young 3xTg-AD mice may be caused by the P301L mutation, and earlier stages of tau pathology may be beneficial for motor performance. Finally, injection of $A\beta_{42}$ fibrils into the brains of P301L mutant tau transgenic mice caused a five-fold increase in the amount of tau tangles (Götz et al., 2001), supporting the accelerating role of Aβ in tau dysfunction predicted by the cascade hypothesis.

Both the APP_{Swe} and tau_{P301L} transgenes are expressed under the Thy-1 promoter in 3xTg-AD mice. Thy-1 or CD90 is a murine antigen, a cell surface glycoprotein from the immuno-globulin superfamily (Williams and Gagnon, 1982), and is anchored to the cell surface by a phospholipid tail. It is expressed in high levels in all neurons (Spanopoulou et al., 1988), which makes it a useful promoter for expressing transgenes in the CNS. Thy-1 is also expressed in high levels in immune cells, including T-lymphocytes (Kollias et al., 1987) and spleen cells (Dennert and Hyman, 1980; Borrello and Phipps, 1996). Furthermore, there is some evidence showing an age- and sex-related differentiation of Thy-1 expression in C57B1/6 mice (Barrat et al., 1997). Finally, it has been shown that Thy-1 expression significantly increases in microglia during immune responses (Busshoff et al., 2001). Altogether, these studies suggest that Thy-1 may not be the best choice for expressing the AD promoting genes in 3xTg-AD mice, especially when the role of the immune system in AD is considered. Many of the behavioural and neurochemical studies performed using this model may be confounded by the presence of Aβ in immune cells and by the interaction between the natural immune response caused by AD pathology and the activity of the Thy-1 promoter. A very recent study showed

higher susceptibility to infection and an increased pro-inflammatory response, such as higher levels of tTNF-α, IL-6, CCL5, and CXCL-1, as well as an increase in immune cell infiltration to the sites of infection (Montacute et al., 2017). Moreover, increased peripheral immune reactivity and spleen function were also shown (Subramanian et al., 2010). These results should be discussed very carefully, as the AD pathology in the brain may not be responsible, as Aβ itself is expressed in these peripheral tissues. Our lab has recently discovered altered spleen anatomy and physiology in 3xTg-AD mice: more specifically, we have reported significantly enlarged spleens in the 3xTg-AD mice compared to WT controls and the 5xFAD mouse model (Wheeler et al., in progress).

Our lab, in addition to others, has extensively studied the behaviour and neuropathology of 3xTg-AD. Stover et al. (2015) studied 3xTg-AD mice at six months of age to determine the most sensitive cognitive task to assess their deficits. They found significantly more spontaneous alternations in the Y-maze, significantly more freezing in the contextual fear-conditioning task, and no differences in the cued version of the fear-conditioning task, nor in the novel object recognition task. The greatest difference was found in the Barnes maze: although 3xTg-AD mice did not spend more time searching for the escape hole during the acquisition phase, they made significantly more errors. In addition, 3xTg-AD mice spent significantly less time near the correct hole during the probe trial, indicating memory deficits (Stover et al., 2015). As mentioned earlier, Stover et al. (2015) also found significantly better motor performance on the Rotarod at six months of age. Leanne Stevens did a cross-sectional study with 3xTg-AD mice, testing them between 2 and 15 months of age. Using the 8-arm radial maze, she showed working memory deficits starting as early as two months of age, which did not worsen with age

(Stevens and Brown, 2015). Sterniczuk et al. (2010) studied circadian rhythm function in 3xTg-AD mice and reported greater locomotor activity during the day and shorter free-running periods prior to the onset of AD-pathology in males, and decreased activity levels during the active phase for females. They also studied cognitive and behavioural deficits and acquired some results suggesting a decreased anxiety profile in the 3xTg-AD mice, spending more time in the centre of the open field (OF) and more time in the open arms of the elevated plus maze (EPM). Yet they did not find any significant differences in active and passive avoidance tasks. Attar et al. (2013) used a five-day training protocol version of the Barnes maze (BM) and showed deficits in the probe trial but not in the acquisition trials at four months of age. This suggests that 3xTg-AD mice have memory problems instead of learning problems, and overtraining might mask them. Some synaptic deficits were also shown in this model: by using hippocampal slices from two and four-month-old 3xTg-AD mice, Grigoryan et al. (2014) showed significantly reduced LTP compared to WT controls, which decreased further if the mice experienced early stress.

1.6 Hypotheses to be Tested in this Thesis

Based on the evidence discussed above, we hypothesize that the elevated levels of $A\beta_{42}$ in AD are directly (and indirectly by increasing INF-γ) responsible for the over-activation of the KP by elevating IDO levels. This alters the immune reactivity of neurons by decreasing Trp and increasing KP metabolites. While 3HK and QA are collectively contributing to the disease progression by increasing oxidative stress and tau phosphorylation, neuroprotective KA levels are not reaching high enough levels to reverse these processes. Hence, the over-activity of KP is an important contributing factor of AD pathogenesis, causing neuronal loss and behavioural dysfunction.

Treatment of the 3xTg-AD mice with an IDO-inhibitor should (1) decrease the levels of oligomeric tau by decreasing the levels of QA, which is involved in the tau pathology, and (2) reduce the behavioural deficits, but (3) should have no effect on Aβ plaque levels, as it is upstream of the KP.

In order to test these hypotheses, we treated 3xTg-AD and WT control (129C57BL/6) mice with a novel IDO-inhibitor (DWG-1036) or vehicle control (distilled water), from two to six months of age and then evaluated them on a comprehensive test battery measuring cognitive, motor, and emotional deficits (Chapter 3). Later, we quantified $A\beta_{40}$ and $A\beta_{42}$, QA, INF-γ, immune marker thioredoxin-interacting protein (TXNIP), Trp, and oligomeric tau, in the post-mortem brains (Chapter 4).

CHAPTER 2: PRELIMINARY STUDIES

Before testing the behavioural and neurochemical effects of DWG-1036 on 3xTg-AD mice, two pilot studies were completed to determine the maximum tolerable dose and pharmacokinetics (PK) of DWG-1036. In the tolerability study, DWG-1036 was administered to male WT and male and female 3xTg-AD mice for 20 days. During this time, the body weight and overall wellbeing of the mice were recorded daily. At the end of 20 days, mice were euthanized for further tissue analysis. For the PK study, different doses of DWG-1036 were administrated to the mice at different time points prior to euthanasia. The brain and plasma samples were then analyzed in order to determine the brain penetration and half-life dynamics of DWG-1036.

2.1 Development of DWG-1036

DWG-1036 is a novel IDO inhibitor developed by Dr. Donald Weaver's lab in the Krembil Research Institute, Toronto, Ontario and provided to our lab for the behavioural and neurochemical analyses on 3xTg-AD mice. Prior to administration, the enzymatic inhibition properties of the compound were studied by Dr. Weaver's group. The IC50 value was determined as 80μm with an *in vitro* assay, and 7μm in the cell based assay (Figure 5).

Details of the chemical preparation procedure were provided by Dr. Weaver's lab as the following: A 500 mL round bottom flask was charged with the 3-pyridyl acetic acid (HCl salt, 13.7 g, 78 mmol) then anhydrous 1,3-dioxane (200 mL). Triethylamine (28 mL, 200 mmol) was added dropwise at room temperature, and the mixture was stirred for 30 min. The 5-Fluoroindole-3-carboxaldehyde (10.9 g, 66.8 mmol) was then added, followed by piperidine (14.5 mL, 147 mmol). The reaction mixture was stirred at 110 °C

for 18 hr. The reaction mixture was cooled to room temperature and an additional aliquot of 3-pyridyl acetic acid (HCl salt, 2.32 g, 13.4 mmol) and piperidine (1.3 mL, 13.4 mmol) was added. The reaction mixture was heated at 110 °C for an additional 18 hr. The reaction mixture was cooled to room and then partitioned between aqueous ammonium chloride (100 mL) and ethyl acetate (200 mL). The organic fraction was separated then washed with brine and dried with Na_2SO_4. After filtration, silica gel was added and the solution was concentrated in vacuo. Automated flash column chromatography (100:0 to 1:1 hexanes:ethyl acetate gradient) afforded 12.5 g of free base. The free base was suspended in water (1 mL per 20 mg of compound), 5% aqueous HCl (≈ 1 eq.) was added until most of the suspended material had dissolved. The reaction mixture was filtered, then concentrated via lyophilisation to provide 11.3 g of the compound as a bright yellow solid (62% yield). HPLC purity analysis was carried out using a Waters 1525EF Binary pump system equipped with a dual wavelength absorbance detector (254, 280 nm) and a manual injector. The stationary phase consisted of a Silicycle Silia Chrom SB C18 column (250 × 4.6 mm), and the mobile phase used water (0.1% trifluoroacetic acid) and acetonitrile (0.1% trifluoroacetic acid) at the following gradient system, eluting at 1 mL/min: 80% H_2O / 20% AcCN for 1 min., then a linear ramp to 5% H_2O / 95% AcCN over 7 min., hold at 5% H_2O / 95% AcCN for 4 min., then return a linear ramp to 80% H2O / 20% AcCN for 3 min. The chemical structure of DWG-1036 is shown in Figure 6.

After being synthesized in Dr. Weaver's laboratory, DWG-1036 was shipped to our lab in powder form. We prepared the solution by dissolving DWG-1036 in sterile distilled water in a dose of 80mg/kg (concentration 1.5 mg/ml). DWG-1036 was transported into sterile glass tubes by using a fine balance and spatula, and distilled water

was added through the latex bottle stopper with a 24-gage needle and 10ml syringe. Then the DWG-1036 was dissolved in distilled water first by shaking the tube by hand then on a vortex mixer (vortex genie) on high speed for two minutes. Then, the solution was drawn up into a clean 10ml syringe by using a new needle and then filtered into a new clean sterile glass bottle with a 0.22 micro-litre sterile micro filter. The solution was stored in a dark room at 22 °C.

2.2 Subjects:

A total of 11 transgenic (3xTg-AD, JAX #34830) and 23 WT control (129C57BL/6) mice were born in-house from breeding pairs purchased from Jackson Laboratories in Bar Harbor, Maine. Mice were housed in same sex groups of 2-4 in translucent polyethylene cages (13 × 30 × 15 cm) with wire food hoppers and microisolator filter lids, in a climate controlled (20 ± 2 °C) vivarium on a reversed 12:12 hr light/dark cycle with lights off at 10:00. The mice were fed Purina Laboratory Rodent Chow #5001 (Agribrand Purina, Strathroy, Ontario, Canada) and tap water, ad libitum. A black polyethylene tube (4cm diameter, 7.5cm length) was placed in the cages for environmental enrichment. Mice were transported to clean cages once a week. All of the subjects were treated according to Canadian Council on Animal Care guidelines and tested under a protocol approved by the Dalhousie University Committee on Laboratory Animals (16-016).

2.3 PK Study

2.3.1 Methods: In order to determine that DWG-1036 passes the blood brain barrier (BBB) and reaches the brain, as well as determining the half-life and distribution dynamics, a PK study was performed. Nine 3xTg-AD and 15 WT control mice were used in this study. The distribution of sexes, genotypes, time of sacrifice, and measured DWG-

1036 concentrations for each mouse is shown in Table 1. Twenty-two mice received DWG-1036 at a dose of 80mg/kg with an injection volume of 0.01ml/g, via oral gavage, using 1ml syringes and 22 gage gavage needles. The mice were sacrificed 0.25, 0.5, 1, 4, 8, or 12 hours after treatment for tissue and plasma analyses. Two additional mice were treated with the vehicle and sacrificed 0.5 hours after as negative controls.

All mice were anesthetized with gaseous isofluorane (1-5% in oxygen). A cardiac puncture was performed under anesthesia, after checking the toe-pinch reflex for signs of pain perception. 1ml syringes and 24 gage needles previously washed with ethylenediaminetetraacetic acid (EDTA) were used for the cardiac puncture and the blood was collected in 1.5ml micro-centrifuges tubes. Then the blood was centrifuged at 3,000 g at 4 °C for 15 minutes. The supernatant was transferred to another tube, frozen with dry ice and stored at -80 °C. Meanwhile, the mouse was perfused with 10% phosphate buffered solution (PBS) for 2 min. Then the carcasses were decapitated, the skin on top of the skull was removed and the skull opened, in order to collect the brain. Then the tissues were put in 1.5ml microcentrifuge tubes, frozen with dry ice and stored at -80°C for shipping to the Krembil Research Institute. The concentration of DWG-1036 in the plasma and brain was then quantified by liquid chromatography-mass spectrometry (LC/MSMS). The PK parameters were computed using the "PK" package with the R Statistical Computing software.

2.3.2 Results: Data from 21 mice were analyzed for the PK study with a between-within mixed factor ANOVA by using genotype and sex as between factors and compound administration time as the within factor. There were no differences between the genotypes ($F(1, 8) = 2.169$, $p = 0.179$) or the sexes ($F(1, 8) < 1.0$, $p = 0.998$), but the concentration

of DWG-1036 in the brains differed significantly based on the time of administration ($F(7, 8) = 7.801$, $p = 0.005$). As shown in Figure 8, the concentration of the compound in the brain was inversely proportional with the administration time.

Furthermore, DWG-1036 was at detectable levels ($\mu = 59{,}198$ ng/ml) in the brain 15 minutes after administration and reached the highest levels after ($\mu = 69{,}753$) half an hour. The half-life of DWG-1036 was calculated as 1.24 hr, the area under the curve (AUC) from 0 to last measured point ($AUC_{0\text{-last}}$) was 138,652 ng.h/mL, the AUC for 0 to infinity was ($AUC_{0\text{-}\infty}$) 138,760 ng.h/mL, and the mean residence time (MRT) was 1.79 hours.

2.4 Tolerability Study

2.4.1 Methods: After determining that DWG-1036 penetrates the brain tissue, we performed a tolerability study to determine any undesirable side effects of the compound. A total of two 3xTg-AD and 8 WT mice were used in this study. The distribution of sexes, genotypes, and treatment for each mouse is shown in Table 2. For 25 days, subjects were treated via oral gavage with (1) 30, 60 or 80 mg/kg DWG-1036 once a day, (2) vehicle, or (3) 80 mg/kg DWG-1036 twice a day. Weights of the mice were recorded daily, prior to treatment and their general well-being was measured with the mouse grimace scale (Miller and Leach, 2015).

2.4.2 Results: Data of weight change over the 25-day test period from 10 mice were analyzed for the tolerability study with a between-within mixed factor ANOVA by using genotype, sex and treatment volume as between factors and day as the within factor. There was a main effect of dose ($F(3, 99) = 33.699$, $p = 0.003$) as the mice receiving higher doses lost more weight. There was also a significant day by dose interaction F (60,

99) = 4.216, $p < 0.005$) as the mice receiving DWG-1036 at higher doses lost more weight over the 25-day period (Figure 9).

2.5 Conclusions of Preliminary Studies

Results of the PK study showed that the DWG-1036 is able to pass the blood brain barrier and reach the brain as early as 15 minutes after administration. Moreover, pharmacokinetics of DWG-1036 did not differ between the 3xTg-AD and the WT mice, or the two sexes. This showed that the compound could be administrated at the same amounts to every subject. The PK study also showed that DWG-1036 is being cleared from the brain rapidly, as the half-life of the compound is 1.24 hr and the amounts were below detectable levels after 12 hours. The area under the curve was calculated as 138,652 ng.h/mL, which represents the total amount of exposure until the compound is fully cleared from the brain (Sowunmi et al., 2011). Furthermore, the mean residence time of DWG-1036 was calculated as 1.79 hours, which means that a molecule of the compound spends less than 2 hours in the brain, on average (Cutler, 1987). Taken together, these results indicate that the most effective way of treatment would be administering DWG-1036 multiple times a day, in order to provide sufficient inhibition of IDO. However, the tolerability study showed that the maximum tolerable dose is 80 mg/kg once a day as the mice receiving more of the compound lost significant amounts of weight and were eventually dropped from the study.

CHAPTER 3: BEHAVIOURAL TESTS

After determining the pharmacokinetic profile and maximum tolerable dose of DWG-1036, male and female 3xTg-AD and WT control mice were treated with the compound between 2 and 6 months of age. We chose to begin administering DWG-1036 at 2 months because this is the earliest stage of detectable intracellular Aβ. Behavioural tests were completed at 6 months of age, as this is the earliest time point Stover et al. (2015) detected cognitive deficits. A total of six behavioural tests were administered in the following order: elevated plus maze (EPM), Barnes maze (BM), forced swim test (FST), tail suspension test (TST), Rotarod, and trace fear conditioning (TFC). Mice continued to be treated with DWG-1036 during behavioural testing and were sacrificed one day after TFC for neurochemical analyses.

3.1 Subjects and Treatment

A total of 21 transgenic (3xTg-AD, JAX #34830) and 53 WT control (129C57BL/6) mice were born in-house from breeding pairs purchased from Jackson Laboratories in Bar Harbor, Maine. As summarized in Table 3, 10 female 3xTg-AD mice received the DWG-1036 treatment and five female 3xTg-AD mice received the vehicle as control for the compound. While six male 3xTg-AD mice received DWG-1036, no male transgenic mice received the vehicle, due to breeding outcomes. Nineteen female and 13 male WT mice received the compound, and 11 female and 10 male WT mice were treated with vehicle. Breeding, housing conditions, and DWG-1036 preparation were the same as described in section 2.1.

All mice started compound (DWG-1036) or vehicle treatment at 2 months of age. Treatments were applied once a day by oral gavage, at a dose of 80mg/kg with an

injection volume of 0.01ml/g. 1 ml syringes and 22-gauge gavage needles were used and the gavage needles were covered with a flavoured (pomegranate and strawberry) edible lubricant (Sliquid Swirl®), purchased from the local adult entertainment store, for easier application in terms of increased lubrication and counterbalancing the unpleasant taste of DWG-1036. Treatments were applied daily around 4:30 pm and the weights of the mice were recorded before the application. If a mouse lost more than 1.5 grams since the prior day, no compound was administered that day. Mice that did not receive treatment five days in a row or 15 days in total were excluded from the study. After 120 days of treatment (when the mice reached 6 months of age), behavioural tests were performed in the order described below. DWG-1036 or vehicle treatment continued during behavioural testing. All subjects were treated according to Canadian Council on Animal Care guidelines and tested under a protocol approved by the Dalhousie University Committee on Laboratory Animals (16-017).

3.2 Methods and Hypotheses

3.2.1 Elevated Plus Maze: Using an elevated platform with an open and closed area to measure anxiety in rodents was first proposed by KC Montgomery in 1955. Pellow et al. (1985) modified Montgomery's Y-Maze design by using a plus-shaped elevated maze with two open and two closed arms, located at 90° angles from each other (Figure 7a). By using different pharmacological agents, Pellow et al. (1985) showed that more anxious subjects would spend more time in the closed arms, as they feel safer. On the other hand, due to the natural exploring instinct of the rodents, less anxious subjects would eventually visit the open arms and spend similar amounts of time in all 4 arms. However, some preference for the open arms has also been shown: Flanigan et al. (2015) observed that

5xFAD mice spent more time in the open arms of the maze, which is unusual. The authors found neuronal loss in the barrel field indicating painful whisker stimulation. Indeed, when they trimmed the whiskers, mice did spend more time in the closed arms. Based on Sterniczuk et al.'s (2010) findings, we are expecting that 3xTg-AD mice will spend more time in the open arms compared to the WT controls, and that this will be reversed by DWG-1036 administration.

The EPM apparatus and testing procedure described by Brown et al. (1999) were used. Mice were carried to a dark room, separated from the test room, in their home cages, with the water bottle removed. Then individual mice were carried to the EPM in a clean plastic container, while their cage mates remained in the holding room with ad-libitum food and water. The EPM consisted of a plus-shaped maze with two open arms (30 x 5 cm) with a 4-mm lip to prevent the mouse from slipping off, and two closed arms (30 x 5 cm) with transparent Plexiglas walls (15 cm high) located across from each other. The arms were connected by a centre square (5 x 5 cm). The floor of the maze was black Plexiglas and the walls of the closed arms were clear. Testing was completed in a room (2 x 5 m) illuminated by two 60 W white lightbulbs.

Each mouse was tested on one five-minute trial, and between mice the maze was cleaned with a Sparkleen® solution. At the beginning of the trial the mice were placed in the centre square. A camera 2.1 m above the maze recorded the movement of the mice throughout the trial. The time in the open and closed arms, and the distance travelled were analyzed with a computerized tracking system (EthoVivion, Noldus, Wageningen, The Netherlands). The duration of grooming, freezing (remaining completely immobile except for respiration), the number of bouts of rearing (removing forepaws from the floor of the

maze), stretch attend postures (SAP, extending its head and then returning to the previous position), and head dips (moving its head over the edge of the maze and pointing downwards) were recorded using a computerized tracking system (Limelight, Actimetrics Inc., Wilmette, IL). In the EPM, distance travelled, rears, and head dips are measures of locomotor behaviour, and the percentage of time in the closed arms, stretch attend postures, grooming, and time spent freezing are measures of anxiety (O'Leary et al., 2013).

3.2.2 Barnes Maze: The Barnes maze (Figure 7b) was developed by Dr. Carol Barnes, who worked at Dalhousie University (Barnes, 1979). It is an escape task based on the desire of mice for small, enclosed, dark, and quiet areas. Mice are placed on a circular platform elevated from the ground, brightly lit from above, and a loud buzzer plays in the background. Based on extra-maze cues, mice need to locate the correct escape hole on the edge of the maze. It has been shown that if the extra-maze cues are blocked by a curtain or wall around the maze, mice cannot locate the escape hole (O'Leary and Brown, 2013). Stover et al. (2015), found that the Barnes maze was the test that had the largest effect size when comparing 3xTg-AD mice with WT controls – therefore, we chose to use this test in our study. We are expecting deficits in both acquisition and probe trials for the 3xTg-AD mice, reversed by DWG-1036 administration.

The BM is a white polyethylene platform (122 cm diameter) elevated 48.4 cm from the floor with sixteen holes (4.45 cm diameter) equally spaced around the perimeter 1.3 cm from the edge, as described by O'Leary and Brown (2012). Four of the holes (4, 8, 12 and 16) were capable of having a black plastic escape box beneath them. A buzzer (0–37.2 kHz, 89 dB) and two 150W flood lamps placed 155 cm above the maze were used as aversive stimuli. A polyvinyl-chloride tube (8 cm diameter, 12.5cm height) was used to

hold the mouse in the centre of the maze before the trial began. A camera was mounted 1.7 m above the maze and the Limelight tracking system (Actimetrics) was used to track the location of the mice.

Mice were tested in groups of 3-5 and each mouse in the group was assigned a specific escape hole location. There were five phases in the test procedure: habituation, acquisition training, acquisition probe, reversal training, and reversal probe (O'Leary and Brown, 2013). During the habituation phase, mice were placed in a 2L glass beaker which was inverted over the assigned escape hole. The mice were then free to explore the escape hole, escape box, and the adjacent area for two minutes. The acquisition training phase consisted of two trials per day for 15 days. On each trial, mice were placed in the centre tube and after an interval of 5-10 seconds the tube was lifted and the buzzer was turned on. The mice were given 300 seconds to locate the escape hole, and if they did not enter the escape box within this time they were led to the escape hole with a plastic cup which was used to transport the mice. The maze was cleaned between trials with Sparkleen® solution to prevent odour cues from developing around the escape holes. The latency to enter the escape hole, distance travelled, and average speed were analyzed for each trial using Ethovision (Noldus, Wageningen, The Netherlands). The number of errors (when a mouse dips its head into a hole that is not the escape hole) and correct head dips were recorded by the experimenter. Repeated head-dips into the same hole were recorded as one head dip. The BM was rotated 90° between each group and all escape holes were cleaned.

The day after acquisition training the mice were given a five-minute memory probe trial with the buzzer turned off. During this trial, the escape box was removed and

the maze was rotated 45º so that a non-escape hole was in the correct escape hole location. For analysis of spatial memory, the maze was divided into 16 pie shaped zones and the number of entries and time spent in each zone were recorded. The following day mice were given a curtain probe trial using the same procedure with no spatial cues, as the maze was surrounded by a black curtain.

The mice were then given a five-day reversal training phase with the escape hole moved to the opposite side of the maze fallowed by a reversal probe trial (with no curtain) using the same procedure as during the acquisition probe trial. Latency to locate the escape hole in the acquisition trials was considered a measure of spatial learning and time spent by the correct hole in the probe trial was considered as a measure of memory (O'Leary and Brown, 2012). Performance in the curtain probe trial indicated the role of extra-maze spatial cues in learning the escape hole location.

3.2.4 Forced Swim: The forced swim test (FST) for mice (Figure 7c) was developed by Porsolt et al. (1977). It is based on the natural tendency of mice to try to escape water, but eventually become immobile, presumably due to learned helplessness. The duration of immobility in a six-minute test is considered a measure of "behavioral despair" or "depression". Although immobility in rodents in the FST does not mirror depressive symptoms in humans, it has shown good reliability and predictive validity in screening for putative antidepressant drugs (Petit-Demouliere et al., 2005), as the duration of immobility can be manipulated with various therapeutics used in humans to treat depression (Slattery and Cryan, 2012). Procedural differences such as cylinder diameter, depth of water, method of scoring, water temperature, age of mice, strain of mice, sex of mice, housing of mice, time of day, lab environment, and drug administration procedure

have been shown to affect immobility times in the FST and replicability between studies (Petit-Demouliere et al., 2005). Previous studies in our lab testing depression-like behaviour in the 3xTg-AD mice showed less time spent immobile for the 3xTg-AD and male mice, suggesting a lower depression profile (Fraser, 2013). Another study tested retention of learned helplessness in the 3xTg-AD mice by using a five-session training paradigm, followed by a later session after a four-week delay. Although the initial immobility levels were not different between the groups, the 3xTg-AD mice showed less immobility in the last session, suggesting the decreased retention of learned helplessness (Luo et al., 2017). Based on these finding, we are expecting shorter duration and less bouts of immobility in the 3xTg-AD mice compared to the WT controls.

Moreover, the relationship between KP and depression should also be considered (Wichers and Maes, 2004; Reus et al., 2015). Since KP breaks down Trp, over-activation of the pathway directly reduces serotonin (5-HT) levels. Although the relationship between 5-HT and depression is not fully understood (Cowen and Browning, 2015), most treatments for depression focus on increasing 5-HT levels in the synapse (Ramachandraih et al., 2011). Since DWG-1036 is an IDO blocker, we are expecting it to increase free Trp levels and reduce depression-like symptoms in both 3xTg-AD and WT mice receiving the compound.

The procedure described by Martin and Brown (2010) was used for the FST. A 2L glass cylinder (19 cm tall, 10 cm in diameter) was filled with tap water at room temperature (23 ± 2 °C) up to the 1.6L point and was allowed to sit overnight to achieve room temperature.

Mice were picked up from their home cages in a plastic container with holes in the bottom to drain water, and were carefully placed into the water, making sure their head was up. Mice were observed for immobility for one 6-min trial which was recorded with a video camera. The test was run under red light in an otherwise dark and quiet test room. After the trial was completed mice were scooped up from the glass cylinder with the plastic container and put in a holding cage filled with paper towel, and placed on a warming pad to dry for several minutes before being returned to their home cage.

3.2.4 Tail Suspension: Similar to the FST, the tail suspension test (TST, Figure 7d) was also developed as a measure of learned helplessness and depression-like behaviour for mice (Steru et al., 1985). We decided to use both tests as 3xTg-AD mice show better motor performance compared to WT controls in other tests, which may confound their swimming abilities. By comparing the results from the FST and TST, we will be able to get the most reliable measures for depression and the effect of DWG-1036.

The tail suspension test (Med Associates, St. Albans, VT, USA) consisted of a box (32 x 33 x 33 cm) that is open on one side to allow an observer to view the subjects or for video recording. An aluminum strip (11.5 x 2.2 x 0.15 cm) is suspended vertically from a strain gauge within the enclosure, which the mouse is attached to by its tail with duct tape.

After its weight was recorded, individual mice were placed on an upside-down cage located under the aluminum strip and their tails were gently attached to the strip. Then the holding cage was slowly removed to allow the mice hang from the strip by its tail. Mice were observed for immobility for one 6-min trial, which was recorded with a video camera. Testing was done in a quiet room lit by two 60-watt white light bulbs. At

the end of the trial the empty cage was once again placed under the mouse so it could stand on four feet without any pressure on the tail. Then the duct tape was carefully removed to free the tail and the mouse was carried back to its home cage.

3.2.5 Rotarod: The accelerating Rotarod (Jones and Roberts, 1968; Figure 7e) measures motor coordination and motor learning (LeMarec and Lalonde, 1997), as well as the effects of different drugs (Hymson and Hynes, 1982) and cerebellar function (Catson et al., 1999) on motor performance. It has also been used to compare the motor performance of different strains of inbred mice (Brown and Wong, 2007). Stover et al. (2015) showed increased performance in 3xTg-AD mice compared to WT controls at six months of age. We are expecting to replicate these results and hypothesize that water-treated 3xTg-AD mice will have significantly longer latencies compared to WT controls. Furthermore, we expect that this increase in motor performance will be reversed by DWG-1036 administration and that there will be no significant difference between the DWG-1036 treated 3xTg-AD mice and WT controls.

Mice were tested on the AccuRotor accelerating Rotarod (Accuscan Instruments Inc. Columbus Ohio), described by O'Leary (2013), to measure neuromuscular motor coordination and motor learning. The Rotarod consisted of a 44 cm long acrylic rod with a diameter of 3 cm, covered with rubber to provide better gripping. The rod was separated into four 11 cm sections by circular Plexiglas dividers (15 cm high), allowing four mice to be tested concurrently. There were four separate holding chambers 39 cm beneath each section of the rod. The latency of falling from the rod was measured with electronic timers embedded to the Rotarod, which automatically stopped when the mouse touched the surface of the holding chamber. The Rotarod was located in a 112 x 260 cm room, lit by a single 60-watt red light. The experimenter stood directly adjacent to the Rotarod

during all testing.

The water bottles were removed from the cages and the mice were carried to the testing room. Cages were located next to the Rotarod in the same order as the mice were positioned on the device. Mice were gently held by their tails and placed on the floor of the holding chamber. Once all 4 mice were in the Rotarod, they were placed on the rod, facing the opposite direction of the rotation as well as the experimenter. The maximum length of each trial was 360 seconds, and during the trial the rod gradually accelerated from 0 to 48 rotations per minute. After the last mouse fell from the rod, a 1-minute break was given before starting the next trial. Therefore, the inter-trial interval was 1-7 minutes, with mice that had fallen early in the previous trial receiving longer inter-trial intervals than mice that performed well, which helped to reduce fatigue in poorly performing animals. Mice completed 6 trials on the Rotarod per day for 5 consecutive days. The Rotarod was cleaned with soap and water after each group of mice (1-4 animals) completed a daily test session of 6 trials.

3.2.6 Trace Fear Conditioning: Blanchard and Blanchard (1969) first described a fear-conditioning paradigm using foot shocks (Figure 7f). Although there are many versions of the test, they are all based on the fact that a rodent will associate a chamber (context) or sound (cue) with a painful foot shock and when the same conditioned stimulus is presented again (even without the unconditioned stimulus, i.e. foot shock), the animal will react to it with a freezing reflex (Fanselow, 1980). Further studies showed that contextual fear conditioning requires spatial memory and the hippocampus as well as the amygdala to stimulate the periaqueductal grey (PAG) to initiate freezing (Maren et al., 2013; Kim et al., 2013), while the hippocampus is not needed for the cued test (Marschner et al., 2008).

A third version of the test, called trace fear conditioning (TFC) includes working memory, as there is a gap between the cue and the foot shock. It has been shown that the prefrontal cortex, which is associated with working memory, and the anterior cingulate cortex, which is involved in attention, are required for trace fear conditioning but not the cued or contextual versions (Runyan et al., 2004; Han et al., 2003). We are using the TFC to measure working memory deficits in the DWG-1036 or vehicle treated 3xTg-AD and WT control mice.

A previous study done in our lab using the 8-arm radial maze showed working memory deficits in 3xTg-AD mice as early as two months of age, as well as sex differences with male 3xTg-AD mice performing worse than females. Interestingly, there was no such sex difference for WT mice and the deficits did not increase with age (Stevens and Brown, 2015). Based on these results, we are expecting that 3xTg-AD mice treated with the vehicle will perform worse than WT controls, but there will be no difference for DWG-1036 treated 3xTg-AD mice. Moreover, we are expecting to see similar sex differences as observed by Stevens and Brown (2015) in vehicle treated 3xTg-AD mice.

Trace fear conditioning and testing took place in two identical MED Associates Inc. (St. Albans, VT) fear conditioning chambers, as described by Martin and Brown (2010). The front, top, and back of the chamber were transparent Plexiglas and the other two remaining were stainless steel. The floor of the chamber consisted of 36 3.2 mm stainless steel rods that were capable of delivering an electric shock. A speaker was attached to one of the stainless-steel walls and a video camera was mounted in front of one of the Plexiglas walls to record the behaviour of the mouse. The procedure consisted

of a training and test phase, which took place on two consecutive days. During the training phase, mice were placed in the chamber and their levels of baseline freezing were recorded for 774 seconds. During this time five 80 dB tone cues lasting 15 seconds were presented with 130 second intervals. Each tone cue was followed by a one-second 0.7 mA foot shock, delivered 30 seconds after the tone. Thirty-seconds after the last shock the mice were removed from the chamber and returned to their home cage and the chamber was cleaned with Sparkleen® solution.

In the working memory test phase, mice were placed in the same chamber used during training for 265 seconds. Black Plexiglas was placed over the floor of the chamber to cover the steel rods, the inside walls of the testing chamber were covered with black and white striped plastic, and a novel lemon odour was introduced into the chamber, in order to stop the mice from recognizing the chamber. The mice were then placed in this modified chamber and their freezing time was recorded for two minutes, followed by a 15-second-long 80dB tone identical to the one presented during training. After the tone, level of freezing was recorded for another 130 seconds. The increase in freezing after the cue was analyzed as a measure of working memory.

3.3 Statistical Analyses

Analysis of variance (ANOVA), linear regression, Pearson Correlation analyses, and generalized linear mixed model regressions were used to analyze the data from the behavioural and neurochemical tests (Chapter 4). “R: The R Project Statistical Computing®” version 3.4.0 (2017-04-21) -- "You Stupid Darkness” was used for all of the statistical analyses and the graphs were generated in “Graph Pad Prism IV”, using means and standard errors (SEM).

ANOVAs were used to analyze the data in the PK and tolerability studies as well as to compare the longevity and body weight data throughout DWG-1036 administration. Treatment condition (DWG-1036 or vehicle), genotype (3xTg-AD or WT), and sex (female, male) were the between factors and treatment day was the within factor. Degrees of freedom (DF), F values and p values were reported for the ANOVAs and the critical (α) value was taken as 0.05 for determining statistical significance.

Data from the behavioural tests EPM, FST, and TST as well as the ELISA assays were analyzed by linear regression by using treatment condition, genotype, and sex as between measures. In order to deal with unequal sample sizes, a Type 2 calculation of sums of squares was used (Langsrud, 2002). Akaike information criterion (AIC) scores (Wagenmakers and Farrell, 2004) and p values were reported. Due to the software used, a higher AIC score actually indicates a better model, as this score is for the model lacking that factor (ie. the AIC score for genotype is actually for the model lacking genotype). 95% confidence intervals (95% CI) were used to determine statistical significance, as a factor was considered significant if the 95% CI did not include 0. CI's are for the difference between the measures within a factor (ie. 95% CI for sex is the difference between female and male mice), for that measure (latency, frequency, etc.).

Data from the Barnes maze, Rotarod, and TFC were analyzed with generalized linear mixed model regressions by using treatment condition, genotype, and sex as the between factors and test day as the within factor. AIC scores and likelihood ratios (LR) are presented. LR is a measure of goodness of fit, used to compare statistical models (Kohn and Michaels, 2005). It shows how much the model including a specific factor is

better at explaining the variance than a model excluding that factor. 95% CIs were used to determine significance.

3.4 Results

3.4.1 Longevity and Body Weights: Although a total of 74 mice started treatment at 2 months of age, only 52 of them completed the 4-month treatment period and were able to be tested in the in the EPM, which was the first behavioural test, at 6 months of age. Of the 22 mice that died during treatment or were removed from the study due to weight loss, 4 of them were female 3xTg-AD mice receiving DWG-1036 (40% loss), 14 of them were female WT mice receiving DWG-1036 (73.68% loss), one of them was a female WT mouse, receiving vehicle (9% loss), 2 of them were male 3xTg-AD mice receiving DWG-1036, and one of them was a male WT mouse receiving DW. All of the mice from the other groups survived the treatment and made it to the behavioural test battery (Figure 10).

For the time of removal (either due to death or significant weight loss), there was a significant genotype effect ($F(1, 17) = 7.080$, $p = 0.016$), as the 3xTg-AD mice were removed during later stages (mean = 68 days). There was also a genotype by sex interaction ($F(1, 17) = 16.181$, $p < 0.005$), as female 3xTg-AD mice were dropped from the study later than female WT mice (mean = 83.75 and 36.80 days, respectively) but the opposite was the case for the male mice (mean = 5.00 and 70.00 days, respectively).

The weight of each mouse was also recorded throughout the 4 months of treatment (Figure 11). Changes within 5 day periods were analyzed by between-within mixed factor ANOVAs by using genotype, treatment, and sex as between factors and day of treatment as the within factor. There were significant effects of treatment condition (F

(1, 1169) = 116.998, $p < 0.0005$), genotype (F (1, 1169) = 363.978, $p < 0.0005$), sex (F (1, 1169) = 1123.969, $p < 0.0005$), and day (F (25, 1169) = 4.609, $p < 0.0005$), as well as significant treatment by genotype (F (1, 1169) = 74.770, $p < 0.0005$), treatment by sex (F (1, 1169) = 30.373, $p < 0.0005$), sex by genotype (F (1, 1169) = 7.758, $p = 0.054$), and treatment by day (F (25, 1169) = 2.471, $p < 0.0005$) interactions. Further analyses showed that male WT mice receiving vehicle weighed more than all the other mice and female 3xTg-AD mice receiving DWG-1036 weighed the least. Other groups ranked in between in the order of male-Tg-DWG-1036 > female-WT-vehicle > female-WT-DWG-1036 > male-Tg-DWG-1036 > female-Tg-vehicle.

Then we compared the differences between the end and start weights for each group by between measures ANOVAs, using genotype, treatment, and sex as factors. Although there were no significant genotype (F (1, 45) = 0.721, $p = 0.400$) or sex effects (F (1, 45) = 1.750, $p = 0.193$), there was a significant treatment effect (F (1, 45) = 43.959, $p < 0.0005$). Further analyses showed that female mice receiving DWG-1036 gained an average of 1.19 grams during the 4 months of treatment regardless of their genotype. On the other hand, all the other groups lost an average of 2.65 grams.

3.4.2 Elevated Plus Maze: Total distance, frequency of open arm (OA) visits, and total time spent in the OAs, as well as freezing, stretch attend posture (SAP), rearing, grooming, and head dip behaviours were compared between the groups by using linear regression. A total of 6 female-Tg-DWG-1036, 5 female-Tg-vehicle, 5 female-WT-DWG-1036, 10 female-WT-vehicle, 6 male-Tg-DWG-1036, 11 male-WT-DWG-1036, and 7 male-WT-vehicle mice were used in these analyses.

For total distance (Figure 12), there were no main effects of treatment condition (AIC = 659.64, p = 0.105), sex (AIC = 656.94, p = 0.691), or interactions between factors. There was a trend of WT mice moving more compared to 3xTg-AD mice (AIC = 660.03, p = 0.085), but the confidence intervals did not indicate significance (CI 95% = -42.840, 647.754).

For the frequency of OA visits (Figure 13), there were no significant main effects of genotype (AIC = 265.74, p = 0.385), treatment condition (AIC = 267.27, p = 0.130), or sex (AIC = 265.01, p = 0.857). Yet, there was a trend of WT female mice visiting the open arms more frequently compared to WT male mice, but the opposite was true for 3xTg-AD mice (AIC = 270.35, p = 0.099). However, the confidence intervals did not indicate significance (CI 95% = -35.391, 4.573).

For total time spent in OAs (Figure 14), there was a main effect of genotype (AIC = 485.71, $p < 0.005$). Confidence intervals showed that the 3xTg-AD mice spent more time in the OAs, compared to the WT mice (CI 95% = -188.031, -79.689). Furthermore, there was a trend of vehicle treated mice spending more time on the OAs compared to the DWG-1036 treated mice (AIC = 466.98, p = 0.091), but the confidence intervals showed that this difference was not significant (CI 95% = -9.337, 93.229). There was no significant difference between male and female mice (AIC = 465.11, p = 0.323).

For freezing frequency (Figure 15), there were no main effects of genotype ($p > 0.05$) or sex ($p > 0.05$), but there was a trend of DWG-1036 treated mice freezing more than vehicle treated controls (AIC = 131.04, p = 0.077). However, the confidence intervals showed that the difference is not significant (CI 95% = -3.621, 0.275).

For freezing duration (Figure 16), there were no significant main effects of genotype ($p > 0.05$) or sex ($p > 0.05$), but DWG-1036 treated mice froze longer than water treated controls (AIC = 339.92, $p = 0.041$, CI 95% = -27.615, 0.064). There was also a trend of WT female mice freezing less than 3xTg-AD mice, but there was no such difference for the male mice (AIC = 341.29, $p = 0.068$). However, the confidence intervals showed that the difference is not significant (CI 95% = -5.260, 68.663).

For SAP (Figure 17), there were no main effects of genotype, treatment, or sex, nor any significant interactions ($p > 0.05$ for all).

For rearing (Figure 18), there were no significant main effects of genotype or treatment condition, but there was a significant difference between the males and the females (AIC = 148.72, $p = 0.031$). According to the confidence intervals, male mice reared more than the female mice (CI 95% = 0.126, 4.624).

For grooming frequency (Figure 19), there were no significant main effects of genotype or treatment condition, but there was a trend of male mice freezing more frequently than females (AIC = 75.718, $p = 0.092$). However, the confidence intervals showed that the difference is not significant (CI 95% = -0.211, 2.087).

For grooming duration (Figure 20), there was a significant main effect of treatment condition (AIC = 187.57, $p = 0.025$). Confidence intervals showed that the vehicle treated mice groomed more than the DWG-1036 treated mice (CI 95% = 0.333, 6.853). There were no differences between the genotypes or sexes.

For the head dips (Figure 21), there were no main effects of genotype, treatment, or sex, nor any significant interactions ($p > 0.05$ for all).

3.4.3 Barnes Maze: The time to find the escape box over the 15-day period of acquisition and the 5-day period of the reversal acquisition, as well as the number of head dips in the correct and incorrect holes, and the time spent by the correct hole as well as the total distance travelled in the probe, curtain probe and reversal probe trials were compared between the treatment conditions, genotypes, and sexes with linear (for probe trials) and generalized linear mixed model regressions (for acquisition trials).

Data from 6 female-Tg-DWG-1036, 5 female-Tg-vehicle, 5 female-WT-DWG-1036, 10 female-WT-vehicle, 6 male-Tg-DWG-1036, 11 male-WT-DWG-1036, and 10 male-WT-vehicle mice were used for the latency to find the escape box during the acquisition phase as well as the number of correct and incorrect head dips. For escape latency (Figure 22), the best model included day (AIC = 18565, LR = 157.800). According to the confidence intervals, all mice got faster at locating the correct hole over the 15-day period (CI 95% = -6.876, -5.060). Moreover, the best model also included a sex by day interaction (AIC = 18398, LR = 8.6968), as female mice improved more over the 15-day period than males (95% CI = 0.975, 4.832, Figure 23). There was also a treatment by day interaction (AIC = 18398, LR = 8.944) as the DWG-1036 treated mice improved more over time than the vehicle treated mice (95% CI = 1.008, 4.832, Figure 24). A genotype by day interaction was involved in the best model (AIC = 18394, LR = 4.295), as 3xTg-AD mice improved more than WT mice (95% CI = 0.121, 4.337, Figure 25). The only three-way interaction involved in the best model was between genotype, sex and day (AIC = 18391, LR = 8.526), as the WT male mice improved more than the other groups (95% CI = -13.101, -2.582).

For the number of head dips in incorrect holes (Figure 26) over the 15-day period

of acquisition trial, the best model included day (AIC = 10687, LR = 306.359) and genotype (AIC = 10389, LR = 7.684) as the number of errors decreased over time for all mice (95% CI = -0.754, -0.609) and WT mice made less errors compared to 3xTg-AD mice (95% CI = -4.862, -0.879). The best model also included a genotype by day interaction (AIC = 10384, LR = 5.752) as the number of errors decreased more for 3xTgAD mice over the 15 days compared to WT controls (95% CI = 0.038, 0.376, Figure 27). There were also interactions between sex, genotype and day (AIC = 10368, LR = 5.154), and treatment, genotype, and day (AIC = 10367, LR = 4.167), as male and WT mice improved more than the other groups (95% CI = -0.909, -0.067), as well as the DWG-1036 treated WT mice (95% CI = 0.018, 0.861).

For the number of correct head dips (Figure 28) over the 15-day period of acquisition trial, the best model included day (AIC = 5028, LR = 75.181) as all mice deceased their number of head dips into the correct hole over the 15-day period (95% CI = -0.070, -0.045). A three-way treatment by genotype by day interaction was also included in the best model (AIC = 4958.8, LR = 5.203), as 3xTg-AD mice receiving DWG-1036 had a greater decrease in correct head dips over the 15-day period (95% CI = 0.012, 0.163).

Data from 6 female-Tg-DWG-1036, 5 female-Tg-vehicle, 5 female-WT-DWG-1036, 10 female-WT-vehicle, 4 male-Tg-DWG-1036, 10 male-WT-DWG-1036, and 10 male-WT-vehicle mice were used for the latency to find the escape box (Figure 29) during the reversal acquisition phase as well as the number of incorrect (Figure 30) and correct (Figure 33) head dips. For the latency, the best model only included the test day (AIC = 5809.8, LR = 41.190), and confidence intervals showed that all mice got faster

over the 5-day period (95% CI = -17.736, -9.570).

For the number of wrong head dips, the best model included main effects of day (AIC = 3083.7, LR = 32.318) and genotype (AIC = 3059.5, LR = 8.158). Confidence intervals showed that the number of wrong head dips decreased for all mice over the 5-day period (95% CI = -1.176, -0.580), and WT mice made less number of errors compared to 3xTg-AD mice (95% CI = -4.270, -0.840, Figure 31). There was also a treatment by day interaction (AIC = 3052.9 LR = 6.685), as vehicle treated mice improved more over the 5 days (95% CI = -1.437, -0.199, Figure 32). The best model included a three-way interaction between treatment, genotype and test day (AIC = 3050.5, LR = 3.908). The confidence intervals showed that WT mice treated with vehicle improved more (95% CI = 0.014, 3.382).

For the number of correct head dips, the best model included test day (AIC = 1161.3, LR = 8.803), as the number of correct hole head dips increased for all mice over the 5-day period (95% CI = 0.022, 0.108). There was also an interaction between treatment and genotype (AIC = 1162.3, LR = 4.495), as WT mice treated with DWG-1036 did more correct head dips compared to WT mice treated with the vehicle but 3xTg-AD mice treated with DWG-1036 did less correct head dips compared to 3xTg-AD mice treated with the vehicle (95% CI = -1.800, -0.074, Figure 34).

For the probe trial, data from 6 female-Tg-DWG-1036, 5 female-Tg-vehicle, 5 female-WT-DWG-1036, 10 female-WT-vehicle, 4 male-Tg-DWG-1036, 10 male-WT-DWG-1036, and 10 male-WT-vehicle treated mice were compared using linear regression. For the frequency of correct hole visits (Figure 35), the best model only

included a sex by genotype interaction (AIC = 164.80, p = 0.016). According to the confidence intervals, male 3xTg-AD mice visited the correct hole less than the other groups (95% CI = 1.108, 17.125).

For the total time spent at the correct hole (Figure 36), the best model included no main factors or interactions, suggesting that all groups spent similar amount of time at the correct hole.

For the total distance covered on the probe trial (Figure 37), the best model included a sex by genotype interaction (AIC = 705.76, p = 0.013), as female 3xTg-AD mice moved more compared to male 3xTg-AD mice but female WT mice moved less than male WT mice (95% CI = 308.229, 3876.784).

For the curtain probe trial, data from 6 female-Tg-DWG-1036, 5 female-Tg-vehicle, 5 female-WT-DWG-1036, 10 female-WT-vehicle, 4 male-Tg-DWG-1036, 11 male-WT-DWG-1036, and 10 male-WT-vehicle treated mice were compared with linear regression. For the frequency of correct hole visits (Figure 38), the best model included no main factors or interactions, suggesting that all groups visited the correct hole similar amount of times.

For the total time spent by the correct hole (Figure 39), the best model included no main factors or interactions, suggesting that all groups spent similar amount of time at the correct hole.

For the total distance covered on the curtain probe trial (Figure 40), the best model only included genotype (AIC = 684.56, p = 0.014). The confidence intervals showed that the 3xTg-AD mice moved more than the WT mice (95% CI = -1124.428, -104.094).

For the reversal probe trial, data from 6 female-Tg-DWG-1036, 5 female-Tg-vehicle, 5 female-WT-DWG-1036, 11 female-WT-vehicle, 4 male-Tg-DWG-1036, 10 male-WT-DWG-1036, and 9 male-WT-vehicle treated mice were compared using linear regression. For the frequency of correct hole visits (Figure 14), the best model included no main factors or interactions, suggesting that all groups visited the correct hole similar amount of times.

For the total time spent by the correct hole (Figure 42), the best model included no main factors or interactions, suggesting that all groups spent similar amount of time at the correct hole.

For the total distance traveled (Figure 43), the best model only included a genotype by sex interaction (AIC = 706.27, p = 0.046), as female 3xTg-AD mice moved more than male 3xTg-AD mice but female WT mice moved less than male WT mice (95% CI = -117.609, 3546.580).

We also performed a generalized linear mixed model regression to compare the three probe trials with each other. For the frequency of correct hole visits, the best model included the type of probe trial (AIC = 841.89, LR = 29.371), as mice visited the correct hole more times in the probe trial compared to the curtain and reversal probes (95% CI = 1.073, 3.325). The best model also included a probe type by genotype by sex interaction (AIC = 827.58, LR = 10.1943).

For the time spent by the correct hole the best model only included the type of probe trial (AIC = 1646.3, LR = 47.954), as all mice spent more time by the correct hole in the probe trial then the curtain and reversal probes (95% CI = 40.821, 77.129).

For the distance travelled in the probe trials, the best model included a main effect of probe type (AIC = 2478.1, LR = 34.610) as mice moved more in the curtain probe trial compared to the other two (95% CI = -666.175, -238.018). There was also a genotype by sex by probe type interaction (AIC = 2457.2, LR = 17.929).

3.4.4 Forced Swim: Time spent immobile and the frequency of immobile bouts were compared between the groups for the FST. A total of 6 female-Tg-DWG-1036, 5 female-Tg-vehicle, 5 female-WT-DWG-1036, 10 female-WT-vehicle, 3 male-Tg-DWG-1036, 9 male-WT-DWG-1036, and 10 male-WT-vehicle mice were used in these analyses.

For immobility frequency (Figure 44) in the FST, there was a significant main effect of genotype (AIC = 148.93, $p < 0.005$). Confidence intervals showed that WT control mice were more frequently immobile compared to 3xTg-AD mice (CI 95% = 4.147, 9.192). There were no significant differences between the treatment conditions or sexes. Furthermore, there was a trend of male mice receiving DWG-1036 becoming immobile more frequently compared to female mice receiving the compound, yet there was no such difference for mice receiving the vehicle (AIC = 130.63 $p = 0.059$). The confidence intervals showed that the treatment by sex interaction is not significant (CI 95% = -9.746, 0.6125).

For duration of immobility (Figure 45) in the FST, there was a significant main effect of genotype (AIC = 427.80, $p < 0.005$). Confidence intervals showed that WT control mice were immobile for longer periods of time compared to 3xTg-AD mice (CI 95% = 110.035, 186.505). However, there were no significant differences between the treatment conditions or sexes. Furthermore, male mice receiving DWG-1036 were

immobile for longer periods of time compared to female mice receiving the compound, yet there was no such difference for mice receiving the vehicle (AIC = 391.58, p = 0.021, CI 95% = -160.675, -6.540).

3.4.5 Tail Suspension: Time spent immobile and the frequency of immobile bouts were compared between the groups for the TST. A total of 6 female-Tg-DWG-1036, 5 female-Tg-vehicle, 5 female-WT-DWG-1036, 10 female-WT-vehicle, 3 male-Tg-DWG-1036, 9 male-WT-DWG-1036, and 10 male-WT-vehicle mice were used in these analyses.

For immobility frequency (Figure 46) in the TST, there were no main effects of treatment condition, genotype, or sex, but there was a significant treatment by genotype interaction, as 3xTg-AD mice receiving DWG-1036 were immobile less frequently than 3xTg-AD mice receiving the vehicle, but there was no such difference for WT mice (AIC = 137.43, p = 0.041, 95% CI = -12.797, 0.308).

For immobility duration (Figure 47) in the TST, there was a significant difference between 3xTg-AD and WT mice (AIC = 368.32, p = 0.011). The confidence intervals showed that 3xTg-AD mice were immobile for longer periods of time (95% CI = -72.209, -8.202). Moreover, there was also a significant treatment by sex interaction as male mice receiving DWG-1036 were immobile for longer periods of time compared to male mice receiving the vehicle, but there was no such difference for female mice (AIC = 366.66, p = 0.030, 95% CI 95% = -131.943, -0.876). There were also trends of 3xTg-AD mice receiving DWG-1036 being immobile for longer periods of time compared to 3xTg-AD mice receiving the vehicle, which was not the case for WT mice (AIC = 365.44, p = 0.063), and female 3xTg-AD mice being immobile for longer periods of time compared

to male 3xTg-AD mice, but there was no such sex difference for WT control mice (AIC = 365.48, p = 0.061). Yet, neither of these interactions reached statistical significance according to the confidence intervals (95% CI for genotype x treatment = -10.051, 139.267), 95% CI for genotype x sex = -10.723, 155.945).

3.4.6 Rotarod: Latency to fall down from the accelerating Rotarod (Figure 48) was measured for 5 days. Differences between the treatment conditions, genotypes, sexes and weight were compared over the 5 days with generalized linear mixed model regressions. A total of 6 female-Tg-DWG-1036, 5 female-Tg-vehicle, 5 female-WT-DWG-1036, 9 female-WT-vehicle, 3 male-Tg-DWG-1036, 9 male-WT-DWG-1036, and 10 male-WT-vehicle mice were used in this analysis.

The best model included a main effect of day (AIC = 2386.4, LR = 32.697). According to the confidence intervals, all mice improved over the 5-day period (95% CI = 5.211, 10.325).

The model also included trends of female 3xTg-AD mice performing better than the male 3xTg-AD mice (AIC = 2360.0, LR = 2.733) and a steeper learning curve for the DWG-1036 treated mice compared to the vehicle treated mice over the 5 days (AIC = 2360.6, LR = 3.314). Confidence intervals showed that neither of these interactions were significant (95% CI for genotype x sex = -12.160, 140.478. 95% CI for treatment x day = -0.444, 11.934).

The best model also included a three-way interaction of genotype, weight and day (AIC = 2351.6, p = 8.488). Furthermore, there was also a three-way interaction between genotype, sex, and day (AIC = 2358.1, p = 15.042).

3.4.7 Trace Fear Conditioning: Time spent frozen before (baseline) and after the tone were compared between the treatment conditions, genotypes, sexes with a generalized linear mixed model regression (Figure 49). A total of 6 female-Tg-DWG-1036, 5 female-Tg-vehicle, 4 female-WT-DWG-1036, 9 female-WT-vehicle, 3 male-Tg-DWG-1036, 9 male-WT-DWG-1036, and 10 male-WT-vehicle mice were used in this analysis. The best model included the trial condition (AIC = 871.00, LR = 49.933) as all the mice spent more time frozen after the cue (95% CI = -35.034, -22.837). Treatment condition was also included in the best model (AIC = 825.91, LR = 4.839) as the DWG-1036 treated mice spent more time frozen compared to the DW treated mice (95% CI = -24.711, -1.492).

3.5 Conclusions of the Behavioural Tests

3.5.1 Longevity and Body Weights: When we looked at the changes in body weight during the 4 months of compound administration, almost all the mice lost some weight during the first few days. Various studies have shown that handling and restraining rodents, as well as oral gavage, may cause a stress response (Brown et al., 2000; Turner et al., 2012), which may be responsible for the weight loss (Chotiwat et al., 2010). Apart from the weight loss, acute stress caused by the daily oral gavage may actually be increasing IDO levels. Dostal et al. (2017) showed that restraint stress increase IDO1 and KP metabolites, selectively in the astrocytes. This is interesting because as explained in the introduction, unlike microglia, astrocytes and neurons cannot produce QA, but metabolize the upstream byproducts of KP into NAD.

Furthermore, there were differences between DWG-1036 and vehicle treated mice, and between sexes as the female mice receiving the compound lost more weight and eventually died or were removed from the study. The difference in treatment

condition may be explained by the way DWG-1036 feels or acts. Since the compound is slightly acidic, it may be burning the mouth and digestive tract of the subjects causing stress and decreasing food intake, or it may have side effects such as nausea. Furthermore, as discussed above, due to the pharmacodynamics of DWG-1036, the IDO levels may actually be increasing, which in turn decreases Trp levels and suppresses the immune system, making the subjects more susceptible to infections. On the other hand, higher weight loss and mortality rates in the female mice can be explained by the start weights. DWG-1036 is a fat-soluble compound; hence the adipocyte levels may affect the way it acts. As the females have less fat to begin, with the compound may have affected them differently. Furthermore, since the starting weight was lower for the females, the loss caused by treatment may have affected them more and reached critical levels.

3.5.2 Elevated Plus Maze: According to O'Leary et al. (2013), the EPM measures anxiety and locomotor activity in mice. While frequency of open arm (OA) entry, total time spent in the OAs, frequency and duration of freezing and grooming, frequency of SAPs, and head dips are considered measures of anxiety, total distance travelled on the EPM and frequency of rearing are considered measures of locomotion. Based on the findings of Sterniczuk et al. (2010), we hypothesized a lower anxiety profile in 3xTg-AD mice, which would be reversed by DWG-1036 treatment.

In the current study, 3xTg-AD mice spent more time in the OAs of the EPM compared to WT mice. As explained above, more time spent in the OA is considered exploratory behaviour and indicates low levels of anxiety, as a nervous mouse would spend most of its time in the safer closed arms. However, if a mouse is exploring the maze, it would spend about equal time in the open and closed arms. Spending more than

50% of the total test duration in the OAs indicates an avoidance of the closed arms. The trend of female 3xTg-AD mice freezing for longer durations and the lack of genotype differences in other anxiety measures such as grooming and SAPs, indicate that the reason behind 3xTg-AD mice spending more time in the OAs was not lower levels of anxiety, but instead a preference for the OAs over the closed arms. Filali et al. (2012) found similar results when they tested 3xTg-AD mice on the EPM, as WT mice entered the closed arms more frequently than 3xTg-AD mice.

This situation can either be explained as an avoidance of the closed arms or as a preference for OAs. Multiple studies using another mouse model of AD, the 5xFAD mice, found similar results as the transgenic mice spent significantly longer periods of time in the OAs (Jawhar et al., 2012; Flanigan et al., 2014). When Flanigan et al. (2014) further studied this abnormal behaviour, they found a loss of GABAergic interneurons in the barrel field, which is the somatosensory area responsible for vibrissae sensation (Rice and Van der Loos, 1977). With further electrophysiological measures, they showed that whiskers of the 5xFAD mice are oversensitive to touch and the closed arms of the EPM were in fact causing the mice pain. When they shortened the whiskers by clipping them, 5xFAD mice spent less time in the OAs. A similar condition may be true for the 3xTg-AD mice and oversensitive whiskers may explain the avoidance of the closed arms of the EPM.

The explanation for the preference of OAs comes from human cases. Ha et al. (2012), showed altered risk taking behaviour in AD patients. When faced with a decision which may have negative consequences, AD patients made riskier decisions compared to healthy controls. Furthermore, loss of inhibition has also been shown in humans with AD

(Müller-Spahn, 2003) in forms of increase in aggression and sexual behaviours. A preference for OAs of the EPM may be a reflection of these behavioural disturbances for 3xTg-AD mice. Yet once again, the lack of differences in other anxiety-related behaviours, especially the head dips, show that this explanation is less likely than the avoidance of the closed arms. As a future direction, shortening the whiskers of 3xTg-AD mice similar to Flanigan et al. (2014), as well as studying the barrel field may provide more clarity about the preference for the OAs of 3xTg-AD mice.

There was also a trend of WT mice travelling more in the EPM than 3xTg-AD mice. Hypoactivity in 3xTg-AD mice was previously shown by Filali et al. (2012) by using the open field test. Although they explained this by a decrease in cortical activity, we think that it can also be explained by the OA preference of 3xTg-AD mice. 3xTg-AD mice may be moving less since they are predominantly in the OAs, in which there is a risk of falling. In order to decrease this risk, they may be moving less. The trend of female 3xTg-AD mice freezing more than female WT mice also supports this idea, as they may be avoiding movement to prevent falling down from the maze.

The DWG-1036 treated mice spent more time frozen, which indicates higher levels of anxiety. This was also supported by trends of higher freezing frequencies and less OA visits. The relationship between IDO, KP, and anxiety is complicated and most of the evidence comes from studies manipulating levels of 5-HT and Trp. Although some studies show anxiolytic effects of 5-HT (Takeuchi et al., 2010), others show decreased levels of anxiety in mice deficient in brain 5-HT (Mosienko et al., 2012). A study done by Bell et al. (2014) showed that both agonists and antagonists have anxiolytic effects compared to the vehicle treatment in the elevated zero maze. Andersen and Teicher

(1999) even showed that higher levels of 5-HT in the right amygdala compared to the left is correlated with higher anxiety. Our findings show that increasing Trp levels by inhibiting the KP, which breaks it down, increases levels of anxiety, supporting the findings of a positive correlation between 5-HT and anxiety.

In conclusion, our findings in the EPM regarding the genotype agrees with the literature and supports our hypothesis. The results also suggest that factors such as neuronal loss in specific brain regions may be masking the anxiety profile of 3xTg-AD mice. On the other hand, we failed to show a genotype by treatment interaction as all the subjects treated with DWG-1036 showed higher levels of anxiety, regardless of their genotype.

3.5.3 Barnes Maze: The BM is an escape-based task measuring spatial learning and memory (O'Leary and Brown, 2013). Spatial learning is regulated by the hippocampus in mice (Broadbent et al., 2004; Vorhees and Williams, 2014). Since hippocampal dysfunction is one of the first symptoms appearing in AD (Henneman et al., 2009), performance in the BM is crucial for validating the 3xTg-AD mouse as a model of AD and evaluating DWG-1036 as a therapeutic against AD. However, once something is learned, activity in the hippocampus is decreased and cortical activity is increased, suggesting that the memories are kept in the cortex, instead of the hippocampus (Frankland and Bontempi, 2005). For the retrieval of those memories the pre-fontal (Preston and Eichenbaum, 2013) and cingulate (Einarsson and Nader, 2012) cortices are required. When Stover et al. (2015) tested 3xTg-AD mice in the BM at 6 months of age, they showed decreased latencies both for 3xTg-AD and WT control mice over the 15-day

period and female mice of both genotypes were faster at locating the escape hole compared to males.

In our experiment, all mice got better over the 15-day learning period suggesting that 3xTg-AD mice are capable of learning the location of the escape box, agreeing with the findings of Stover et al. (2015). Furthermore, we also replicated the findings regarding sex differences as female mice got faster than male mice over the 15-day period. This does not agree with the literature, as in both humans and mice, males are known to perform better at spatial learning tasks (Shore et al., 2001; Monfort et al., 2015). Moreover, the number of head dips into the wrong hole decreased more for males than females. This may suggest that the better performance of females may be caused by an enhancement in performance instead of learning (Soderstrom and Bjork, 2015).

Our results also showed that 3xTg-AD mice improved more than WT mice over the acquisition period for their latencies of locating the escape box as well as decreasing the number of head dips into the wrong hole. We have previously seen this enhancement of performance in 3xTg-AD mice in the Hebb-Williams maze (Hebb and Williams, 1946), when we tested 4 and 9 months old subjects (Fertan et al., in progress). As shown by McDonald and White (1993), there are multiple memory systems in the brain which often work in opposition. Experiments have shown increased performance in the cued Morris Water Maze (MWM) task when the hippocampi of the subjects were removed. Although the escape box was cleaned between the trials to get rid of any olfactory cues, mice might have still used the smell of the box to find the correct location. Since the hippocampal function is decreased in 3xTg-AD mice, their learning strategy may be

shifted to cue association. Pietropaolo et al. (2009) showed better performance in the cued version of the MWM for 3xTg-AD mice.

Furthermore, the performance on day 15 is similar for all groups, yet WT mice have shorter latencies in the first part of acquisition. This shows that WT mice are reaching their peak performance around day 8, which is earlier than 3xTg-AD mice. This results in a greater increase of performance throughout the full 15-day period for 3xTg-AD mice. The acquisition phase of the BM may be too long to detect genotype differences in this model.

There was also a difference between the DWG-1036 and vehicle treated mice, as the mice receiving the compound improved more, suggesting that inhibiting the KP may have enhancing effects of spatial learning. This result was expected for 3xTg-AD mice, as increased levels of QA cause tau phosphorylation and eventually neuronal loss, which is responsible for deficits in spatial learning. Hence, our results show that DWG-1036 is effective at reversing the adverse effects of over-activity in the KP caused by the AD mutations.

On the other hand, the increased performance in the WT mice treated with the compound compared to the WT mice receiving the vehicle can be explained by the increase of KP metabolites due to chronic stress. As explained in the introduction, 3HK, one of the KP metabolites, has neurotoxic properties similar to QA. Yet unlike QA, it is produced in astrocytes, in which IDO levels are increased due to stress (Dostal et al., 2017) caused by daily gavage. Thus, some neuronal loss may have happened in vehicle-

treated WT mice which affected learning, and mice treated with DWG-1036 may have been protected from this by balancing the 3HK levels with the inhibition of IDO.

The number of correct head dips also decreased for all the mice over the 15-day period. Although this result may seem controversial, it makes sense as a head dip is recorded when the mouse briefly puts its head into the escape hole but then takes it out and moves away from the hole. The buzzer is only stopped when the mouse fully enters the escape area. Hence, this is actually a measure of how fast the mice can learn how the maze works: as the subjects get faster at locating and entering the escape hole, they no longer do head dips. These results validate the BM as a measure of spatial learning as the subjects eventually stop randomly searching for the escape hole by head dipping into every hole and begin to navigate towards the correct one using learned cues.

The reversal learning phase of the BM also relies on the hippocampus as it requires spatial learning. Yet in addition, it requires the activity of the indirect dopaminergic pathway and D2 receptor activity (Keeler et al., 2014) as reward predicting cues lose their value. There was only a day effect in this phase, as all mice decreased their latencies of locating the escape hole over the 5-day period. This contradicts findings from Stover et al. (2015), as they showed that in addition to a reduction of escape latencies over the 5-day period, 3xTg-AD mice and female mice of both genotypes were significantly faster at locating the escape hole. As explained above, WT control mice reached their peak performance around day 8 in the acquisition phase. Hence, the 5-day duration of the reversal acquisition phase may not have been long enough for the subjects to reach their peak performance, masking genotype and treatment condition effects. This is also supported by the results from correct head dips. Unlike the initial acquisition

phase, the frequency of correct head dips increased for all the subjects over the 5-day period. This indicates that mice were still trying to learn the correct location of the escape box at the end of the reversal acquisition period and did not reach their peak performance. On the other hand, WT control mice had a smaller number of wrong head dips compared to 3xTg-AD, which agrees with Stover et al.'s (2015) and suggest a spatial learning deficit in 3xTg-AD mice.

The escape box is removed in the probe trials and the time spent near the hole which used to be above the escape box, is compared between the groups as a measure of spatial memory. In this test Stover et al. (2015) found less time spent by the correct hole for 3xTg-AD mice compared to WT controls. In our experiment, there was a sex by genotype interaction, as male 3xTg-AD mice visited the correct hole less frequently than other subjects yet all mice spent similar amounts of time by the correct hole. This suggests that male 3xTg-AD mice might have spent more time at each hole. It is important to note that all male 3xTg-AD mice analyzed for the probe trial were treated with DWG-1036, so these results may not be accurate, as they could not be compared with mice of the same sex and genotype treated with the vehicle.

There were no differences between the groups for frequency or duration of correct hole visits in the reversal probe trial. Stover et al. (2015) also did not find any significant differences for the duration, yet 3xTg-AD mice visited the correct zone more frequently. The results for both measures were significantly lower for all subjects compared to the first probe trial and close to chance levels. This also supports the idea that the reversal acquisition phase is not long enough to learn the location of the escape hole.

The curtain probe trial was done one day after the acquisition probe trial with the same escape hole locations to show that the subjects are actually using spatial cues to locate the escape box. There were no treatment, genotype, or sex differences in this test. Furthermore, subjects spent about 20 seconds near the correct hole. Since there are 16 holes in total and the test duration is 300 seconds, subjects did not have an actual preference for the correct hole but they spent about equal amounts of time at each hole. This is important for validating the BM as a spatial task.

In conclusion, our results from the BM suggest that 3xTg-AD mice may be using a cued learning strategy to locate the escape hole in the BM by using odour cues from the escape box, which is compensating for the spatial learning deficits. Inhibiting the KP enhances spatial learning and this may be caused by decreasing neuronal loss caused by QA in 3xTg-AD mice and 3-HK in WT controls. Lastly, the duration of the acquisition phases may be masking the differences between the groups: we think that an 8-day period for both the first and reversal acquisition phase would increase the validity of the test to measure spatial learning.

3.5.4 Depression Tests: Along with the TST, the FST was done in order to measure depression-like behaviour. Both tests are based on exposing mice to an uncomfortable and unescapable situation in which the frequency and duration of immobile bouts are measured. Based on previous findings, we were expecting a decreased depression profile in 3xTg-AD mice compared to WT controls (Fraser, 2013). Moreover, due to the relationship between depression and 5-HT we were expecting lower frequency and duration of immobile bouts in mice treated with DWG-1036 compared to the vehicle treated subjects, as they would have higher levels of Trp and 5-HT.

There was a genotype difference in the FST, as 3xTg-AD mice were almost never immobile and in cases where they were, it was for much shorter periods of time. Aman et al. (2016) showed reduced thermal sensitivity in the APPswe × PS1.M146V mouse model of AD. Although it is not the same model, the APP and PS1 mutations are the same, suggesting that 3xTg-AD mice may also have reduced thermal sensitivity. As shown by Petit-Demouliere et al. (2005), water temperature is an important factor in the FST, as the immobility decreases when the water is not cold enough to make the mice uncomfortable. Hence the possibly reduced thermal sensitivity of 3xTg-AD mice may have made the test more tolerable for them.

Our results also showed that male mice receiving DWG-1036 stayed immobile for longer periods of time compared to females receiving the compound. Since 3xTg-AD mice stayed immobile for very short periods of time, the treatment condition effect is mostly due to the differences in WT mice. This difference may be explained by the interaction between the female steroidal hormone progesterone and the KP. De Bie et al. (2016) showed that in the presence of IFN-γ, progesterone alters the KP by decreasing the levels of QA and increasing the neuroprotective metabolite KA. Studies of humans have shown increased levels of QA in the anterior cingulate gyrus of severely depressed patients (Steiner et al., 2011). Moreover, reduction of KA to QA ratio was also shown in major depressive disorder (Savitz et al., 2015). When combined with the IDO inhibition by DWG-1036, these progesterone - KP interactions in female mice may have lowered the immobility durations compared to males.

Unlike the FST, 3xTg-AD mice did not show reduced depression-like symptoms in the TST. There was a treatment by genotype interaction, as 3xTg-AD mice treated with DWG-1036 became immobile less frequently than those treated with the vehicle. This supports our hypothesis of DWG-1036 increasing Trp levels by inhibiting the KP and decreasing the symptoms of depression. For the duration of immobility, WT mice had lower duration times than 3xTg-AD mice, which again contradicts with the findings in the FST and suggests that the transgenic mice have higher levels of learned helplessness compared to WT controls.

In conclusion, the tests of depression-like behaviour provide opposing results for the depression profile of 3xTg-AD mice. This may be due to the design of the FST, as the thermal sensitivity of 3xTg-AD mice is altered, making them more resilient. On the other hand, the DWG-1036 treatment in both tests seems to decrease depressive symptoms. Sex differences affecting the KP and increased Trp levels may be responsible for this.

3.5.5 Rotarod: The Rotarod is a measure of motor learning and coordination, based on the latency of subjects to remain on an accelerating rod. Although our lab has shown significantly better performance in 3xTg-AD mice starting at 2 months of age (Fraser, 2013; Stover et al., 2015), there are conflicting findings in the literature. For example, Sterniczuk et al. (2010) found no differences between 3xTg-AD and WT mice.

In the current study there was a significant day effect in the Rotarod, as all mice improved over the 5-day period. However, we did not find any genotype differences. This may be a side effect of the daily gavage treatment. In Stover et al. (2015), most mice reached an average of 200 seconds over the 5-day period, but in our study the average

latency was about 150 seconds which suggests that the treatment may have caused discomfort and negatively impacted the performance of the mice, masking possible genotype or treatment condition effects. This is also supported by differences in the body weights of the mice between Stover et al. (2015) and our study. In their study, the average weight for the mice was around 30 grams, but in our study the average weight of the subjects was around 25 grams, even though the mice in our study were about one month older.

3.5.6 Trace Fear Conditioning: Working memory was tested in the trace fear conditioning: during the gap between the tone and the electric shock, the subjects had to remember the tone and associate it with the shock. Based on the results of Stevens and Brown (2015), we were expecting working memory deficits in 3xTg-AD mice, which would be improved by DWG-1036 treatment.

In the current study all the subjects froze more after the cue, which validates the test and shows that they were all capable of associating the tone with the shock. However, we did not find any differences between 3xTg-AD and WT mice, which contradicts our hypothesis. This may be caused by differences between the tests used by Stevens and Brown (2015) and our study. They used the 8-arm radial maze which requires spatial working memory. According to Baddeley (1998), three main components of working memory are the visuospatial sketchpad, the phonological loop, and the central executive. These regions are all located in the pre-frontal cortex (Müller and Knight, 2006). Yet the hippocampus is also involved in spatial working memory tasks such as the 8-arm radial maze (Spellman et al., 2015). On the other hand, the trace fear conditioning test used in

our study uses a tone cue instead of a spatial cue. As discussed above for the BM, 3xTg-AD mice do not seem to have deficits in cued learning.

On the other hand, DWG-1036 treated mice were frozen for longer periods of time compared to the vehicle treated ones. This suggests a working memory improvement due to the treatment, since the baseline duration (before the tone) of freezing did not differ between the groups. Chess et al. (2007) showed working memory deficits caused by increasing KA. On the other hand, increasing Trp in healthy humans have shown to increase working memory function (Luciana et al., 2001). Hence decreasing KA and increasing Trp by inhibiting the KP may have helped to improve the performance in the trace fear conditioning task, suggesting that DWG-1036 is an effective treatment against working memory deficits.

CHAPTER 4: NEUROCHEMICAL TESTS

After the completion of the behavioural tests, mice were sacrificed and their brains were harvested for further analyses. Multiple enzyme-linked immunosorbent (ELISA) assays were performed to measure the levels of $A\beta_{40}$ and 42 and oligomeric tau, as well as tryptophan, KP metabolite quinolinic acid, IFN-γ, and TXNIP.

Since the overproduction of Aβ in 3xTg-AD mice is achieved by introducing transgenes, and it is upstream of KP dysfunction, we are expecting elevated levels of Aβ in both DWG-1036 and vehicle treated 3xTg-AD mice compared to WT controls. Similarly, we hypothesize that IFN-γ will be increased as a response to $A\beta_{42}$ causing immune reactivity, thus we hypothesize that IFN-γ as well as the immune marker TXNIP will be similar in both DWG-1036 and vehicle treated 3xTg-AD mice, but lower in WT controls. Since IDO is implicated in supressing the innate immune system, we expect WT mice treated with DWG-1036 will also have higher amounts of IFN-γ and TXNIP compared to the vehicle treated WT mice. Secondly, due to the IDO-inhibition by DWG-1036, we expect the KP will be less active in 3xTg-AD mice treated with the compound, therefore Trp levels will be increased, while the levels of QA and oligomeric tau will be decreased.

4.1 Methods

4.1.1 Post Mortem Tissue Collection and Preparation: All of the mice were euthanized within 1-3 days post-behavioural tests and they continued receiving treatment in the meantime. On the day of sacrifice, all subjects received the compound or vehicle 1.5 hours before tissue collection. All mice were anesthetized with gaseous isofluorane (1-5% in oxygen). A cardiac puncture was performed under anesthesia, after checking the toe-

pinch reflex for signs of pain perception. 1 ml syringes and 24 gage needles previously washed with EDTA were used for the cardiac puncture and the blood was collected in 1.5 ml micro-centrifuges tubes. The blood was centrifuged at 3 000 g at 4°C for 15 minutes. The supernatant was transferred to another tube, frozen with dry ice and then stored at -80°C. Meanwhile, the mouse was perfused with 10% PBS for 2 minutes. The carcass was decapitated, the skin on top of the skull was removed and the skull opened, and the brain was removed. The brain was divided into two hemispheres and one of the hemispheres was further dissected to individually collect the cerebellum, brain stem, hippocampus, and the pre-frontal cortex. These parts were frozen with dry ice and shipped to Toronto to be further analyzed by Dr. Donald Weaver's lab. Remaining brain regions were put in 1.5 ml micro-centrifuge tubes, frozen with dry ice and stored at -80°C.

In preparation of the tissue samples for enzyme-linked immunosorbent assay (ELISA), hippocampal and cortical tissue was extracted from the frozen hemispheres of each animal and allowed to thaw. 89-170 mg of wet tissue was homogenized with the aid of a plastic pestle in ice-cold radio-immunoprecipitation assay (RIPA) lysis and protein extraction buffer containing protease-inhibitors (300 µl/sample; one cOmplete™, Mini, EDTA-free protease inhibitor cocktail tablet (Merck) per 10 mL of RIPA buffer). All procedures were performed on ice, and all the tools were cleaned with alcohol (70%) between the samples to avoid contamination. The homogenates were centrifuged (12 000 rpm, 20 min, 4°C) to remove debris and insoluble material. Total protein in the supernatant was quantified (~274-335 ng/ul) with a Take3™ Micro-volume Plate on an Epoch Spectrophotometer (BioTek Instruments INC). The supernatants were then aliquoted (3x100 µl) and stored at -80°C until use.

4.1.2 ELISA Kit Preparation: The ELISA kits for $A\beta_{40}$ and $A\beta_{42}$ were purchased from BioLegend® (Catalog # 841301 and 842401, respectively). The detection range for both kits was 7.4 - 250 pg/mL. The kit for QA was purchased from Aviva Systems Biology® (Catalog # OKCD02284). The detection range for this assay was 1.23-100 ng/mL. The assay for IFN-γ was purchased from Cloud-Clone Corp.® (Catalog # SEA049Mu). This assays detection range was 15.6-1000 pg/mL. The assay for TXNIP was purchased from CUSABIO® (Catalog # CSB-EL025383MO). The detection range for this assay was 28-1800 pg/mL.

The standard curves were prepared by following the instructions provided by the ELISA kit manuals and differed slightly between kits. A general summary is provided below and the parts that differed significantly between the kits are mentioned.

A stock of 100 ng/mL standard was prepared by adding 1 mL standard diluent into 100 ng Lyophilized standard. The mixture was allowed to sit at room temperature for 15 minutes.

Later, the 6 serially diluted standards were prepared by adding 600 µl of the standard diluent to Tubes 2-6, and adding 300 µl of the standard to Tube 2 and shaking it. Then, 300 µl of the solution from Tube 2 was added to Tube 3 and 300 µl of the solution from Tube 3 to Tube 4. Tube 5 was prepared with the same procedure, but Tube 6 was left "blank" as only standard diluent was put in it and no solution from Tube 5.

The biotin complex was prepared by adding 150 µl biotin reconstitution buffer into the 100X Biotin Complex. This mixture was diluted 100x with the Complex Diluent.

The Avidin-HRP Conjugate was prepared by diluting the 100X Avidin-HRP Conjugate 100 times with the Conjugate Diluent.

The was buffer was prepared by mixing 20 mL of 30X Wash Buffer with 580 mL of pure water. This mixture was gently mixed, sealed with parafilm and stored in 4°C.

To establish the amount of supernatant to load in each well, 50 µl of serially titrated standards were loaded into 12 wells (2 of each) with 12 tissue samples from the mouse brains diluted in the same concentrations. Fifty µl's of 1X Biotin Complex was then added onto each plate, the wells were covered with the clear lid and the plate was incubated at 37°C for one hour (incubation period was 12 hours in 4°C for the amyloid beta assays). After incubation, the liquid inside the wells was cleared and the wells were washed with 350 µl of wash buffer for 2 minutes, 4 times. Then, 100 µl of Avidin-HRP conjugate was added into each well and the plate was incubated once again for 30 minutes. After this second incubation, the wells were washed 5 times and 90 µl of tetramethylbenzidine (TMB) substrate was added to the wells. Once the liquid inside wells became blue, the plate was incubated for one last time for 15 minutes (this last incubation was done at room temperature for the amyloid beta assays). Fifty µl of stop solution was added to each well (except for the amyloid beta assays), which turned the liquid yellow. Next, the plate was read by a standard microplate reader at a wavelength of 540 nm (QA, IFN-γ, TXNIP) or 620 nm (AB_{40}/AB_{42}). From the pilot results, 10-40 µg of sample supernatant was loaded into each well alongside a 6-point serial dilution standard curve and blanks in duplicate and the ELISA plate was analyzed as described above.

4.2 Results

The amounts of $A\beta_{40}$ and AB_{42}, QA, INF-γ, and TXNIP were compared between male and female 3xTg-AD and WT mice, either treated with DWG-1036 or the vehicle, through ELISA assays and the results were analyzed with linear regression. A total of 6

female-Tg-DWG-1036, 5 female-Tg-vehicle, 4 female-WT-DWG-1036, 5 female-WT-vehicle, 2 male-Tg-DWG-1036, 9 male-WT-DWG-1036, and 8 male-WT-vehicle mice were used in these analyses.

4.2.1 Amyloid Beta 40: For the levels of $A\beta_{40}$ (Figure 50), there was a difference between the 3xTg-AD and WT control mice (AIC = 227.87, $p < 0.05$). As shown by the confidence intervals, 3xTg-AD mice had significantly more $A\beta_{40}$ than WT mice (95% CI = -42.324, -25.286). There were no differences between the treatment conditions or sexes (all $p > 0.05$).

4.2.2 Amyloid Beta 42: For the levels of $A\beta_{42}$ (Figure 51), there was a difference between 3xTg-AD and WT control mice (AIC = 214.18, $p < 0.05$). As shown by the confidence intervals, 3xTg-AD mice had significantly more $A\beta_{42}$ than WT mice (95% CI = -34.156, -17.903). There were no differences between the treatment conditions or sexes (all $p > 0.05$).

4.2.3 Quinolinic Acid: For the levels of QA (Figure 52), there were no main effects of genotype or sex (all $p > 0.05$). There was a trend for DWG-1036 treated mice to have higher levels of than vehicle treated mice (AIC = 206.69, $p = 0.053$), but the confidence intervals showed that the difference was not significant (95% CI = -16.851, 0.640).

4.2.4 Interferon Gamma: For the levels of INF-γ (Figure 53), there was a difference between 3xTg-AD and WT control mice (AIC = 138.96, $p = 0.037$). Confidence intervals showed higher levels of INF-γ in WT controls compared to 3xTg-AD mice (95% CI = 0.002, 8.710). There were no differences between the sexes or treatment conditions (all $p > 0.05$).

4.2.5 TXNIP: For the levels of TXNIP (Figure 54), there was a difference between 3xTg-AD and WT control mice (AIC = 425.34, $p < 0.05$). As shown by the confidence

intervals, 3xTg-AD mice had significantly more $A\beta_{40}$ compared to WT mice (95% CI = -524.689 -298.174). There were no differences between the treatment conditions or sexes (all $p > 0.05$).

We also performed correlation analyses between $A\beta_{40}$ and $A\beta_{42}$ levels, and TXNIP. As shown in Figures 55 and 56, there were significant positive correlations between $A\beta_{40}$ and TXNIP ($r = 0.560$, $df = 37$, $p < 0.005$) as well as $A\beta_{42}$ and TXNIP ($r = 0.632$, $df = 37$, $p < 0.005$,).

4.3 Conclusions of the Neurochemical Tests

4.3.1 Amyloid Beta 40 and 42: Along with hyperphosphorylated tau, increased levels of amyloid beta are one of the primary hallmarks of AD. We measured the levels of both non-toxic fragment $A\beta_{40}$ and the toxic $A\beta_{42}$ which is involved in AD pathogenesis, with an ELISA assay. Based on the findings of Oddo et al. (2003), we were expecting to detect significantly higher levels of both Aβ fragments in the brains of 3xTg-AD mice, compared to WT controls. Furthermore, based on our hypothesis for the role of IDO and KP in the pathogenesis of AD, $A\beta_{42}$ is upstream of the KP as the elevated levels of $A\beta_{42}$ increase IDO expression and the production of KP metabolites, hence, we were not expecting any changes in Aβ levels due to DWG-1036 treatment. Our results supported both hypotheses as the levels of $A\beta_{40}$ and $A\beta_{42}$ were significantly higher in 3xTg-AD mice by the time they were sacrificed at 7 months of age, and the amounts did not differ between the DWG-1036 or vehicle treated mice.

4.3.2 Quinolinic Acid: QA is one of the metabolites produced during the KP. It is believed to be involved in AD due to its neurotoxic properties and role in tau phosphorylation (Guillemin et al., 2005). Elevated levels of QA were shown in the

hippocampi of 3xTg-AD mice at 6-8 months of age by Wu et al. (2015). Based on these results, we were expecting higher levels of QA in the 3xTg-AD mice, compared to WT controls. Moreover, we were expecting the levels to be lower in the subjects treated with DWG-1036, since inhibiting IDO function should decrease KP activity and reduce the amount of metabolites produced.

Surprisingly, our results indicated the opposite of that, as there was a trend of higher QA levels in the mice treated with DWG-1036, compared to the vehicle. The levels were highest in 3xTg-AD mice treated with DWG-1036 and did not differ between 3xTg-AD and WT control mice treated with the vehicle. This increase in QA levels due to treatment with DWG-1036, suggests that the compound had the opposite effect on KP than we expected. This may be due to the pharmacokinetics of DWG-1036. As described above, the compound was cleared quite rapidly from the brain, which means that IDO was only inhibited for a short period of time. As further explained below in the general discussion, this may actually have increased KP activity. Based on these findings, DWG-1036 seems to fail as a treatment against AD as it actually increases QA which contributes to disease progression.

4.3.3 Interferon Gamma: As one of the primary modulators of IDO expression, IFN-γ is believed to contribute to the progression of AD. We were expecting higher levels of IFN-γ in the 3xTg-AD mice, as the expression of IFN-γ is increased in immune challenges, such as Aβ accumulation. Yet our results were in the opposite direction as WT mice had higher levels of IFN-γ compared to 3xTg-AD mice. This contradicts the findings in the literature as well, as Browne et al. (2013) showed IFN-γ production by the Aβ specific Th1 cells in the APP/PS1 mouse model of AD. Yet, the levels of IFN-γ may not be consistently high during the lifespan. By studying blood and ex-vivo brain samples from

AD patients, Belkhelfa et al. (2014) showed that IFN-γ levels are increased during the initial stages of AD, yet there was no difference between the healthy controls and patients at the later stages of the disease. Since Aβ accumulation is achieved by mutations in the 3xTg-AD mice, it starts at birth. Therefore, IFN-γ levels may be increasing as an initial response at an earlier age and then decreasing as the mice age.

4.3.4 TXNIP: As an immune reactivity marker, TXNIP is shown to link oxidative stress and inflammasome activation (Zhou et al., 2010). Levels of TXNIP have been shown to increase in 5xFAD mice as well as *in-vitro* following Aβ application (Gouget et al., 2011). Based on these results, we were expecting elevated levels of TXNIP in 3xTg-AD mice compared to WT controls, regardless of treatment condition. Our results supported this hypothesis as both male and female 3xTg-AD mice from DWG-1036 and vehicle treatment groups had significantly higher levels of TXNIP compared to WT mice. The strong positive correlation between Aβ and TXNIP suggests that Aβ might be directly increasing TXNIP expression by acting as a transcription factor, which might be a regulating factor for the immune deficits seen in AD.

CHAPTER 5: CONCLUSION

5.1 Behavioural Tests: The six tests explained in Chapter 3 were performed in order to evaluate the behavioural differences between 3xTg-AD and WT control mice, and how these differences are affected by the treatment with the IDO inhibitor DWG-1036.

Our results in the EPM have shown that 3xTg-AD mice are less nervous compared to WT controls, yet this may be caused by factors unrelated to anxiety such as painful whisker stimulation. Using other tests such as the open field and the light dark box, as well as neuroanatomical studies focusing on related brain regions may help to further understand the anxiety profile of the 3xTg-AD mice. Moreover, DWG-1036 treatment increased frequency and duration of various anxiety measures both in 3xTg-AD and WT mice and failed to reverse the preference for the open arms seen in 3xTg-AD mice. DWG-1036 is not an effective treatment for the anxiety related symptoms of AD seen in 3xTg-AD mice.

Results from the BM showed that 3xTg-AD and WT mice may be using different strategies to solve the maze, which may be masking the spatial memory deficits (which are caused by degradation in the hippocampus) in 3xTg-AD mice. Yet, treatment with DWG-1036 improved performance in both genotypes, possibly by rescuing neuronal loss. Thus, for spatial memory deficits, DWG-1036 may be an effective treatment.

Results from the FST and TST contradicted each other, possibly due to the confounding factor of cold tolerability in 3xTg-AD mice. Yet, the DWG-1036 treatment decreased some of the depression measures in both tests and reduced the frequency of immobility of 3xTg-AD mice in the TST, suggesting it is an effective treatment for depressive symptoms.

Our results from the Rotarod did not agree with the general findings in the literature as we did not find a performance enhancement in 3xTg-AD mice. This may be caused by the daily gavage treatment, as it may have affected the health of the mice and decreased their performance on the Rotarod.

The results from the trace fear conditioning task did not indicate any working memory deficits in 3xTg-AD mice, contradicting with previous findings. This may be due to the difference between our task, and those used in previous studies, as the working memory deficits may be hippocampal-dependent. On the other hand, all mice treated with DWG-1036 performed better than vehicle treated mice, suggesting that the compound is an effective treatment against working memory deficits.

In conclusion, DWG-1036 seems to be an effective treatment for various behavioural symptoms associated with AD such as spatial learning, depression and working memory deficits. Interestingly, the effect of the compound was not limited to 3xTg-AD mice in these tests, suggesting that DWG-1036 can be used as a general treatment against these disorders, independent of AD. Finally, the nature of the tests seems to have limited our ability to detect differences between genotypes. Hence, using more than one test for the same measure would increase the validity of the measures.

5.2 Neurochemical Tests: The four ELISA assays, explained in Chapter 4, were performed to study the neurochemical differences between 3xTg-AD and WT control mice and how they were affected by the DWG-1036 treatment.

Our findings regarding Aβ and TXNIP levels supported our hypothesis and agreed with the literature as the 3xTg-AD mice had higher levels of these AD markers. Since they are elevated with mutations and work upstream of IDO and KP, DWG-1036 treatment did not make a difference.

On the other hand, the results from the QA assay were contradicting with our expectations, as the levels were higher in the mice treated with the IDO inhibitor. We believe that this may be because of the insufficient inhibition of the KP, due to the short half-life of DWG-1036. Our inability to inhibit IDO entirely between consecutive gavage treatments may have actually increased the KP activity. Since the enzymatic activity is blocked for a short period of time, the body may have reacted by increasing the expression of the enzyme or through some other mechanism to counterbalance the effects of DWG-1036. This phenomenon is called homeostatic plasticity, which refers to the physiological changes that take place in order to accommodate for over- or under-stimulation in a specific pathway (D'Angelo, 2010). Unlike Hebbian plasticity (Hebb, 1949), when there are excessive levels of a signaling molecule, the levels of its receptor decrease and when the levels of the molecule decrease, the receptor expression increases to maintain homeostasis (Hazell et al., 2012). Thus, decreasing IDO activity with DWG-1036 for a short period of time may have increased enzyme activity after DWG-1036 was cleared and increased the amounts of KP metabolites produced.

Furthermore, the results for IFN-γ also contradicted with our hypothesis. As a mediator of immune response and IDO expression, we were expecting higher levels in 3xTg-AD mice, yet the levels were lower compared to WT controls. This may be due to the age of the mice. One study showed that IFN-γ is increased in the early stages of AD, hence the levels may have been decreased at 7 months of age.

To sum up, the results of our neurochemical analyses support the 3xTg-AD mouse model as a valid model for AD since the amyloid beta levels were significantly higher than WT mice. Yet, based on the QA levels DWG-1036 may not be an effective treatment against AD as it seems to increase KP activity instead of decreasing it.

5.3 Overall Conclusions, Limitations and Future Directions: In this study, we have examined the effects of a novel IDO inhibitor on the behaviour and neurochemistry of the 3xTg-AD mouse model. DWG-1036 was developed by Dr. Donald Weaver's group and was shown to penetrate to the brain as early as 15 minutes after administration and inhibit IDO activity (IC50 80μm). We started our tests with a pharmacokinetics and tolerability study. Then we treated male and female 3xTg-AD and WT control mice between 2 and 6 months of age. High mortality rates seen in the mice treated with DWG-1036 and lower weights seen in both treatment groups compared to the age, sex and genotype matched untreated mice, combined with the results of the tolerability study suggested that the compound may have undesirable side effects. This may have confounded the results of some of the test such as the Rotarod, as they rely on physical activity and motor performance.

Moreover, the mortality rates seen during the 4-month treatment period caused unequal sample sizes which decreased our statistical power and ability to compare the groups. For example, there were no male 3xTg-AD mice treated with the vehicle. We are planning to continue the study to get equal sample sizes.

These side effects of DWG-1036 also prevented the usage of a higher dose of treatment or multiple treatments per day. This may have decreased the inhibition of IDO and may have increased KP activity. Higher QA levels in the subjects treated with DWG-1036 may have caused this. Performing a full pharmacodynamics assay by treating 3xTg-AD and WT mice with different doses of DWG-1036 and then measuring IDO, Trp and kynurenine levels in the brain would be useful the understand the full inhibition profile of the compound, alongside with the IC50 value.

After 4 months of treatment, we tested the subjects in a test battery which consisted of tests measuring anxiety, spatial learning and memory, depression, motor performance, and working memory. The design of some of the tests may have decreased their reliability. For example, in the EPM, 3xTg-AD mice showed a preference for the open arms which may be due to the closed arms hurting their whiskers. Similarly, the duration of the acquisition phases of Barnes maze may not be appropriate to measure deficits in spatial learning. Yet overall, the results from the behavioural tests suggest that DWG-1036 may be an effective treatment against most of these deficits.

The neurochemical analyses for the markers associated with AD and KP were performed with ELISA assays. We have shown significant increases in Aβ levels in 3xTg-AD mice, which validates the model for AD. Yet, the behavioural results did not always reflect this increase in Aβ, as we did not find many genotype differences in our tests. This may be due to the design of the tests. Furthermore, as explained in the introduction, Aβ pathology precedes the behavioural deficits of AD, hence even though 3xTg-AD mice had significantly higher levels of Aβ, the neurological damage may not be severe enough to cause behavioural symptoms at 7 months of age. Repeating the tests at a later time point may result in greater genotype differences and treatment effects.

In conclusion, based on its side effects, as well as pharmacokinetic and neurochemical analyses, DWG-1036 does not seem to be an effective treatment against Alzheimer's disease. Yet, the evidence for the involvement of the kynurenine pathway in the progression of AD is overwhelming. By (1) modifying the compound to increase the half-life and the tolerability, (2) changing the protocols of some of the behavioural tests to increase their reliability, and (3) testing the mice at an older age, the involvement of KP in AD, as well as the therapeutic potential of IDO inhibitors can be demonstrated.

REFERENCES

Akaike A, Takada-Takatori Y, Kume T, Izumi Y (2010). Mechanisms of neuroprotective effects of nicotine and acetylcholinesterase inhibitors: role of alpha4 and alpha7 receptors in neuroprotection. *J Mol Neurosci.* 40(1-2):211-6.

Alberici A, Benussi A, Premi E, Borroni B, Padovani A (2014). Clinical, genetic, and neuroimaging features of Early Onset Alzheimer Disease: the challenges of diagnosis and treatment. *Curr Alzheimer Res.* 11(10):909-17.

Allinquant B, Hantraye P, Mailleux P, Moya K, Bouillot C, Prochiantz A (1995). Downregulation of amyloid precursor protein inhibits neurite outgrowth in vitro. *J Cell Biol.* 128, 919–927.

Alzheimer Society of Canada. (2016). http://www.alzheimer.ca/en/About-dementia/What-is-dementia/Dementia-numbers

Aman Y, Pitcher T, Simeoli R, Ballard C, Malcangio M (2016). Reduced thermal sensitivity and increased opioidergic tone in the TASTPM mouse model of Alzheimer's disease. *Pain.* 157(10):2285-96.

American Psychiatric Association. Diagnostic and statistical manual of mental disorders (5th ed.). Arlington, VA: American Psychiatric Publishing. 2013.

Andersen SL, Teicher MH (1999). Serotonin laterality in amygdala predicts performance in the elevated plus maze in rats. *Neuroreport.* 10(17):3497-500.

Andreadis A, Brown WM, Kosik KS (1992). Structure and novel exons of the human tau gene. *Biochemistry.* 31(43):10626-33.

Attar A, Liu T, Chan WT, Hayes J, Nejad M, Lei K, Bitan G (2013). A shortened Barnes maze protocol reveals memory deficits at 4-months of age in the triple-transgenic mouse model of Alzheimer's disease. *PLoS One.* 8(11):e80355.

Avila J, Lucas JJ, Perez M, Hernandez F (2004). Role of tau protein in both physiological and pathological conditions. *Physiol Rev.* 84(2):361-84.

Backman L, Small BJ, Fratiglioni L (2001). Stability of the pre-clinical episodic memory deficit in Alzheimer’s disease. *Brain* 124: 96–102.

Barnes CA (1979). Memory deficits associated with senescence: a neurophysiological and behavioral study in the rat. *J Comp Physiol Psychol.* 93(1):74-104.

Bartus RT, Dean RL 3rd, Beer B, Lippa AS (1982). The cholinergic hypothesis of geriatric memory dysfunction. *Science.* 217(4558):408-14.

Barrat F, Lesourd BM, Louise A, Boulouis HJ, Vincent-Naulleau S, Thibault D, Sanaa M, Neway T, Pilet CH (1997). Surface antigen expression in spleen cells of C57B1/6 mice during ageing: influence of sex and parity. *Clin Exp Immunol.* 107(3):593-600.

Bate C, Kempster S, Last V, Williams A. (2006). Interferon-γ increases neuronal death in response to amyloid-β_{1-42}. *J Neuroinflammation. 3*:7.

Baddeley A (1998). Recent developments in working memory. *Curr Opin Neurobiol.* 8:234-238.

Belkhelfa M et al., (2014). IFN-γ and TNF-α are involved during Alzheimer disease progression and correlate with nitric oxide production: a study in Algerian patients. *J Interferon Cytokine Res.* 34(11):839-47.

Bell R, Duke AA, Gilmore PE, Page D, Bègue L (2014). Anxiolytic-like effects observed in rats exposed to the elevated zero-maze following treatment with 5-HT2/5-HT3/5-HT4 ligands. *Sci Rep.* 4:3881.

Bencherif M, Narla ST, Stachowiak MS (2014). Alpha7 neuronal nicotinic receptor: a pluripotent target for diseases of the central nervous system. *CNS. Neurol. Disord. Drug. Targets.* 13(5):836-45.

Berry RW, Quinn B, Johnson N, Cochran EJ, Ghoshal N, Binder LI (2001). Pathological glial tau accumulations in neurodegenerative disease: review and case report. *Neurochem Int.* 39(5-6):469-79.

Bilke-Gorzo A (2014). Genetic mouse models of brain aging and Alzheimer's disease. *Pharmacol Ther.* 142(2):244-257.

Bliss TV, Lomo T (1973). Long-lasting potentiation of synaptic transmission in the dentate area of the anaesthetized rabbit following stimulation of the perforant path. *J.Physiol.* 232(2):331-56.

Blokland A (1995). Acetylcholine: a neurotransmitter for learning and memory? *Brain Res Brain Res Rev.* 21(3):285-300.

Blanchard RJ, Blanchard DC (1969). Crouching as an index of fear. *J Comp Physiol Psychol.* 67(3):370-5.

Bloom GS (2014). Amyloid-β and tau: the trigger and bullet in Alzheimer disease pathogenesis. *JAMA Neurol.* 71(4):505-8.

Boccia MM, Blake MG, Krawczyk MC, Baratti CM (2010). Hippocampal α7 nicotinic receptors modulate memory reconsolidation of an inhibitory avoidance task in mice. *Neuroscience.* 171(2):531-43.

Bolla LR, Filley CM, Palmer RM (2000). Dementia DDx. Office diagnosis of the four major types of dementia. *Geriatrics.* 55(1):34-7, 41-2, 45-6.

Bondolfi L, Calhoun M, Ermini F, Kuhn HG, Wiederhold KH, Walker L., et al. (2002). Amyloid-associated neuron loss and gliogenesis in the neocortex of amyloid precursor protein transgenic mice. *J Neurosci*. 22:515–522.

Borrello MA, Phipps RP (1996). Differential Thy-1 expression by splenic fibroblasts defines functionally distinct subsets. *Cell Immunol.* 173(2):198-206.

Bornstein E, Lenchner E, Donnenfeld A, Jodicke C, Keeler SM, Kapp S, Divon MY (2010). Complete trisomy 21 vs translocation Down syndrome: a comparison of modes of ascertainment. *Am J Obstet Gynecol.* 203(4): 391.e1-5.

Bradshaw, E. M. et al (2013). *CD33* Alzheimer's disease locus: altered monocyte function and amyloid biology. *Nature Neurosci.* 16: 848–850.

Brickell KL, Steinbart EJ, Rumbaugh M, Payami H, Schellenberg GD, Van Deerlin V, Yuan W, Bird TD (2006). Early-onset Alzheimer disease in families with late-onset Alzheimer disease: a potential important subtype of familial Alzheimer disease. *Arch Neurol.* 63(9):1307-11.

Broadbent NJ, Squire LR, Clark RE (2004). Spatial memory, recognition memory, and the hippocampus. *Proc Natl Acad Sci U S A.* 101(40):14515-20.

Brookmeyer R, Corrada MM, Curriero FC, Kawas C (2002). Survival following a diagnosis of Alzheimer disease. *Arch. Neurol.* (11):1764-7.

Brown AP, Dinger N, Levine BS (2000). Stress produced by gavage administration in the rat. *Contemp Top Lab Anim Sci.* 39(1):17-21.

Brown RE, Wong AA (2007). The influence of visual ability on learning and memory performance in 13 strains of mice. *Learn Mem.* 14:134-144.

Browne TC, McQuillan K, McManus RM, O'Reilly JA, Mills KH, Lynch MA (2013). IFN-γ Production by amyloid β-specific Th1 cells promotes microglial activation and increases plaque burden in a mouse model of Alzheimer's disease. *J Immunol.* 190(5):2241-51.

Buchman AS, Bennett DA (2011). Loss of motor function in preclinical Alzheimer's disease. *Expert Rev Neurother.* 11(5):665-76.

Buée L, Bussière T, Buée-Scherrer V, Delacourte A, Hof PR (2000). Tau protein isoforms, phosphorylation and role in neurodegenerative disorders. *Brain Res Brain Res Rev.* 33(1):95-130.

Burgess N, Maguire EA, O'Keefe J (2002). The human hippocampus and spatial and episodic memory. *Neuron.* 35(4):625-41.

Busshoff U, Hein A, Iglesias A, Dörries R, Régnier-Vigouroux A (2001). CD1 expression is differentially regulated by microglia, macrophages and T cells in the central nervous system upon inflammation and demyelination. *J Neuroimmunol.* 113(2):220-30.

Campion D et al., (1999). Early-onset autosomal dominant Alzheimer disease: prevalence, genetic heterogeneity, and mutation spectrum. *Am J Hum Genet.* 65(3):664-70.

Carpenedo R, Chiarugi A, Russi P, Lombardi G, Carlà V, Pellicciari R, Mattoli L, Moroni F (1994). Inhibitors of kynurenine hydroxylase and kynureninase increase cerebral formation of kynurenate and have sedative and anticonvulsant activities. *Neuro Science*. 61:237–43.

Caston J, Devulder B, Jouen F, Lalonde R (1999). Role of an enriched environment on the restoration of behavioral deficits in Lurcher mutant mice. *Dev Psychobiol.* 35:291-303.

Chen Y, Guillemin GJ (2009). Kynurenine pathway metabolites in humans: disease and healthy states. *Int J Tryptophan Res.* 2:1-19.

Chen CD, Oh SY, Hinman JD, Abraham CR (2006). Visualization of APP dimerization and APP-Notch2 heterodimerization in living cells using bimolecular fluorescence complementation. *J Neurochem.* 97(1):30-43.

Chen JX, Yan SD (2007). Amyloid-beta-induced mitochondrial dysfunction. *J Alzheimers Dis.* 12(2):177-84.

Chess AC, Simoni MK, Alling TE, Bucci DJ (2007). Elevations of endogenous kynurenic acid produce spatial working memory deficits. *Schizophr Bull.* 33(3):797-804.

Chiarini A, Dal Pra I, Whitfield JF, Armato U (2006). The killing of neurons by beta-amyloid peptides, prions, and pro-inflammatory cytokines. *Ital J Anat Embryol.* 111(4):221-46.

Chotiwat C, Kelso EW, Harris RB (2010). The effects of repeated restraint stress on energy balance and behavior of mice with selective deletion of CRF receptors. *Stress.* 13(3):203-13.

Cole LJ, Gravilescu M, Johnston LA, Gibson SJ, Farrell MJ, Egan GF (2011). The impact of Alzheimer's disease on the functional connectivity between brain regions underlying pain perception. *Eur J Pain.* 15:568e1–568e11.

Cornutiu G (2015). The epidemiological scale of Alzheimer's disease. *J Clin Med Res.* 7(9):657-66.

Corona AW, Norden DM, Skendelas JP, Huang Y, O'Connor JC, Lawson M, Dantzer R, Kelley KW, Godbout JP (2013). Indoleamine 2,3-dioxygenase inhibition attenuates lipopolysaccharide induced persistent microglial activation and depressive-like complications in fractalkine receptor (CX(3)CR1)-deficient mice. *Brain Behav Immun.* 31:134-42.

Cosi C, Mannaioni G, Cozzi A, Carlà V, Sili M, Cavone L, Maratea D, Moroni F (2011). G-protein coupled receptor 35 (GPR35) activation and inflammatory pain: Studies on the antinociceptive effects of kynurenic acid and zaprinast. *Neuropharmacology.* 60(7-8):1227-31.

Cowen PJ, Browning M (2015). What has serotonin to do with depression? *World Psychiatry.* 14(2):158-60.

Cozzi A, Carpenedo R, Moroni F (1999). Kynurenine hydroxylase inhibitors reduce ischemic brain damage: studies with (m-nitrobenzoyl)-alanine (mNBA) and 3,4-dimethoxy-[-N-4-(nitrophenyl)thiazol-2yl]- benzene- sulfonamide (Ro 61–8048) in models of focal or global brain ischemia. *J Cereb Blood Flow Metab*. 19:771–7.

Craig LA, Hong NS, McDonald RJ (2011). Revisiting the cholinergic hypothesis in the development of Alzheimer's disease. *Neurosci Biobehav. Rev.* 35(6):1397-409.

Cutler DJ (1987). Definition of mean residence times in pharmacokinetics. *Biopharm Drug Dispos.* 8(1):87-97.

Dai W, Gupta SL (1990). Regulation of indoleamine 2,3-dioxygenase gene expression in human fibroblasts by interferon-gamma. Upstream control region discriminates between interferon-gamma and interferon- alpha. *J Biol Chem*. 265:19871–7.

D'Angelo (2010). Homeostasis of intrinsic excitability: making the point. *J Physiol.* 588(6): 901–902.

Dauphinot V, Delphin-Combe F, Mouchoux C, Dorey A, Bathsavanis A, Makaroff Z, Rouch I, Krolak-Salmon P (2015). Risk factors of caregiver burden among patients with Alzheimer's disease or related disorders: a cross-sectional study. *J Alzheimers Dis*. 44(3):907-16.

DaRocha-Souto B, Scotton TC, Coma M, Serrano-Pozo A, Hashimoto T, Serenó L, Rodríguez M, Sánchez B, Hyman BT, Gómez-Isla T (2011). Brain oligomeric β-amyloid but not total amyloid plaque burden correlates with neuronal loss and astrocyte inflammatory response in amyloid precursor protein/tau transgenic mice. *J Neuropathol Exp Neurol.* 70(5):360-76.

Davies P, Maloney AJ (1976). Selective loss of central cholinergic neurons in Alzheimer's disease. *Lancet.* 2(8000):1403.

Dawkins E, Small DH (2014). Insights into the physiological function of the β-amyloid precursor protein: beyond Alzheimer's disease. *J Neurochem.* 129(5):756-69.

De Bie J, Lim CK, Guillemin GJ (2016). Progesterone alters kynurenine pathway activation in IFN-γ-activated macrophages – relevance for neuroinflammatory diseases. *Int J Tryptophan Res.* 9:89–93.

de la Monte SM, Tong M (2014). Brain metabolic dysfunction at the core of Alzheimer's disease. *Biochem. Pharmacol.* 88(4):548-59.

Dennert G, Hyman R (1980). Functional Thy-1+ cells in cultures of spleen cells from nu/nu mice. *Eur J Immunol.* 10(8):583-9.

Desai MK, Guercio BJ, Narrow WC, Bowers WJ (2011). An Alzheimer's disease-relevant presenilin-1 mutation augments amyloid-beta-induced oligodendrocyte dysfunction. *Glia.* 59(4):627-40.

Deng Y, Li B, Liu Y, Iqbal K, Grundke-Iqbal I, Gong CX (2009) Dysregulation of insulin signaling, glucose transporters, O-GlcNAcylation, and phosphorylation of tau and neurofilaments in the brain: Implication for Alzheimer's disease. *Am J Pathol.* 175(5):2089-98.

Desai SS (1997). Down syndrome: a review of the literature. *Oral Surg Oral Med Oral Pathol Oral Radiol Endod.* 84(3):279-85.

DiNatale BC, Murray IA, Schroeder JC, Flaveny CA, Lahoti TS, Laurenzana EM, Omiecinski CJ, Perdew GH (2010). Kynurenic acid is a potent endogenous aryl hydrocarbon receptor ligand that synergistically induces interleukin-6 in the presence of inflammatory signaling. *Toxicol Sci.* 115(1):89-97.

Dostal, CR, Carson Sulzer M, Kelley KW, Freund GG, McCusker RH. (2017). Glial and tissue-specific regulation of Kynurenine Pathway dioxygenases by acute stress of mice. *Neurobiol Stress.* 7:1-15.

D'Souza I, Schellenberg GD (2005). Regulation of tau isoform expression and dementia. *Biochim Biophys Acta.* 1739(2-3):104-15.

Duarte AI, Moreira PI, Oliveira CR (2012). Insulin in central nervous system: more than just a peripheral hormone. *J Aging Res.* 2012:384017.

Eckman CB et al., (1997). A new pathogenic mutation in the APP gene (I716V) increases the relative proportion of A beta 42(43). *Hum Mol Genet.* 6(12):2087-2089.

Einarsson EÖ, Nader K (2012). Involvement of the anterior cingulate cortex in formation, consolidation, and reconsolidation of recent and remote contextual fear memory. *Learn Mem.* 19(10):449-52.

Fahnestock M, Garzon D, Holsinger RM, Michalski B (2002). Neurotrophic factors and Alzheimer's disease: are we focusing on the wrong molecule? *J Neural Transm Suppl.* (62):241-52.

Fanselow MS (1980). Conditioned and unconditional components of post-shock freezing. *Pavlov J Biol Sci.* 15(4):177-82.

Feldman HH, Jacova C, Robillard A, Garcia A, Chow T, Borrie M, Schipper HM, Blair M, Kertesz A, Chertkow H (2008). Diagnosis and treatment of dementia: 2. Diagnosis. *CMAJ.* 178(7):825-36.

Fernandez-Martinez M, Molano A, Castro J, Zarranz JJ (2010). Prevalence of neuropsychiatric symptoms in mild cognitive impairment and Alzheimer's disease, and its relationship with cognitive impairment. *Curr Alzheimer Res.* 7:517–526.

Ferri CP et al., (2005). Global prevalence of dementia: a Delphi consensus study. *Lancet.* 366(9503):2112- 2117.

Fertan E, Brown RE (2014). Age-related changes in working memory and anxiety like behaviours in the Hebb-Williams Maze in the Triple Transgenic Mouse Model of Alzheimer's Disease. *Unpublished 3000X/Y project.*

Filali M, Lalonde R, Theriault P, Julien C, Calon F, Planel E (2012). Cognitive and non-cognitive behaviors in the triple transgenic mouse model of Alzheimer's disease expressing mutated APP, PS1, and Mapt (3xTg-AD). *Behav Brain Res.* 234(2):334-42.

Filley CM, Rollins YD, Anderson CA, Arciniegas DB, Howard KL, Murrell JR, Boyer PJ, Kleinschmidt-DeMasters BK, Ghetti B (2007). The genetics of very early onset Alzheimer disease. *Cogn Behav Neurol.* 20(3):149-56.

Flanigan TJ, Xue Y, Kishan Rao S, Dhanushkodi A, McDonald MP (2014). Abnormal vibrissa-related behavior and loss of barrel field inhibitory neurons in 5xFAD transgenics. *Genes Brain Behav.* 13(5):488-500.

Fletcher DA, Mullins RD (2010). Cell mechanics and the cytoskeleton. *Nature.* 463(7280):485-92.

Fogarty MP, McCormack RM, Noonan J, Murphy D, Gowran A, Campbell VA (2010). A role for p53 in the beta-amyloid-mediated regulation of the lysosomal system. *Neurobiol Aging.* 31(10):1774-86.

Frandemiche ML, De Seranno S, Rush T, Borel E, Elie A, Arnal I, Lanté F, Buisson A (2014). Activity-dependent tau protein translocation to excitatory synapse is disrupted by exposure to amyloid-beta oligomers. *J Neurosci.* 34(17):6084-97.

Frankland PW, Bontempi B (2005). The organization of recent and remote memories. *Nat Rev Neurosci.* 6(2):119-30.

Fraser LM (2013). Locomotor behaviour, emotionality, and cognition in the 3xTg-AD mouse model of Alzheimer's disease: A cross-sectional study. PhD thesis. http://dalspace.library.dal.ca/handle/10222/28080

Fujigaki S, Saito K, Sekikawa K, Tone S, Takikawa O, Fujii H, Wada H, Noma A, Seishima M (2001). Lipopolysaccharide induction of indoleamine 2,3-dioxygenase is mediated dominantly by an IFN-gamma- independent mechanism. *Eur J Immunol*. 31:2313–8.

Fukui S, Schwarcz R, Rapoport SI, Takada Y, Smith QR (1991). Blood-brain barrier transport of kynurenines: implications for brain synthesis and metabolism. *J Neurochem.* 56(6):2007-17.

Garzon DJ, Fahnestock M (2007). Oligomeric amyloid decreases basal levels of brain-derived neurotrophic factor (BDNF) mRNA via specific downregulation of BDNF transcripts IV and V in differentiated human neuroblastoma cells. *J Neurosci.* 27(10):2628-35.

Gentleman SM, Nash MJ, Sweeting CJ, Graham DI, Roberts GW (1993). Beta-amyloid precursor protein (beta APP) as a marker for axonal injury after head injury. *Neurosci Lett.* 160, 139–144.

Gibson GE, Sheu KF, Blass JP (1998). Abnormalities of mitochondrial enzymes in Alzheimer disease. *J Neural Transm (Vienna).* 105(8-9):855-70.

Gimonet D, Grailhe R, Coninx P, Antonicelli F, Haye B, Liautaud-Roger F (2003). Functional role of nicotinic acetylcholine receptors in apoptosis in HL-60 cell line. *Eur. J. Pharmacol.* 482(1-3):25-9.

Giorgi C et al., (2012). Mitochondrial Ca(2+) and apoptosis. *Cell Calcium.* 52(1):36-43.

Glenner GG, Wong CW (1984). Alzheimer's disease: initial report of the purification and characterization of a novel cerebrovascular amyloid protein. *Biochem Biophys Res Commun.* 16;120(3):885-90.

Goate A et al., (1991). Segregation of a missense mutation in the amyloid precursor protein gene with familial Alzheimer's disease. *Nature.* 349(6311):704-706.

Goedert M, Jakes R (1990). Expression of separate isoforms of human tau protein: correlation with the tau pattern in brain and effects on tubulin polymerization. *EMBO J.* 9(13):4225-30.

Gotz J, Deters N, Doldissen A, Bokhari L, Ke Y, Wiesner A, Schonrock N, Ittner LM (2007). A decade of tau transgenic animal models and beyond. *Brain Pathol.* 17(1):91-103.

Gouget T, Djelloul M, Boucraut J, Weinhard L, Baranger K, Rivera S, Khrestchatisky M, Perrone L (2011). TXNIP, the major player in insulin resistance, is early over-expressed in the brain of the 5XFAD Alzheimer's mice model and is induced by Aβ *in vitro:* Emerging role of TXNIP and inflammation in Alzheimer's Disease progression. *Alzheimers Dement.* 7(4):S684.

Götz J, Chen F, van Dorpe J, Nitsch RM (2001). Formation of neurofibrillary tangles in P301l tau transgenic mice induced by Abeta 42 fibrils. *Science.* 293(5534):1491-5.

Grigoryan G, Biella G, Albani D, Forloni G, Segal M (2014). Stress impairs synaptic plasticity in triple-transgenic Alzheimer's disease mice: rescue by ryanodine. *Neurodegener Dis.* 13(2-3):135-8.

Guerin D, Sacquet J, Mandairon N, Jourdan F, Didier A (2009). Early locus coeruleus degeneration and olfactory dysfunctions in Tg2576 mice. *Neurobiol Aging.* 30:272–283.

Guillemin GJ, Brew BJ, Noonan CE, Takikawa O, Cullen KM. Indoleamine 2,3 dioxygenase and quinolinic acid immunoreactivity in Alzheimer's disease hippocampus (2005). *Neuropathol Appl Neurobiol*. 31:395–404.

Guillemin GJ, Cullen KM, Lim CK, Smythe GA, Garner B, Kapoor V, Takikawa O, Brew BJ (2007). Characterization of the kynurenine pathway in human neurons. *J Neurosci.* 27(47):12884-92.

Guillemin GJ, Smythe GA, Veas LA, Takikawa O, Brew BJ (2003). A beta 1-42 induces production of quinolinic acid by human macrophages and microglia. *Neuroreport.* 14(18):2311-5.

Ha J, Kim EJ, Lim S, Shin DW, Kang YJ, Bae SM, Yoon HK, Oh KS (2012). Altered risk-aversion and risk-taking behaviour in patients with Alzheimer's disease. *Psychogeriatrics.* 12(3):151-8.

Haass C, Lemere CA, Capell A, Citron M, Seubert P, Schenk D, Lannfelt L, Selkoe DJ (1995). The Swedish mutation causes early-onset Alzheimer's disease by beta-secretase cleavage within the secretory pathway. *Nat Med.* 1(12):1291-1296.

Hampel H et al., (2011). The future of Alzheimer's disease: the next 10 years. *Prog. Neurobiol.* 95:718-728.

Han CJ, O'Tuathaigh CM, van Trigt L, Quinn JJ, Fanselow MS, Mongeau R, Koch C, Anderson DJ (2003). Trace but not delay fear conditioning requires attention and the anterior cingulate cortex. *Proc Natl Acad Sci U S A.* 100(22):13087-92.

Harada A, Oguchi K, Okabe S, Kuno J, Terada S, Ohshima T, Sato-Yoshitake R, Takei Y, Noda T, Hirokawa N (1994). Altered microtubule organization in small-calibre axons of mice lacking tau protein. *Nature.* 369(6480):488-91.

Hardy J, Allsop D (1991) Amyloid deposition as the central event in the etiology of Alzheimer's disease. *Trends in Pharmac* 12: 383 – 388.

Hargreaves KM, Pardridge WM (1988). Neutral amino acid transport at the human blood-brain barrier. *J Biol Chem*. 263:19392–7.

Hatchett CS, Tyler S, Armstrong D, Dawbarn D, Allen SJ (2007). Familial Alzheimer's disease presenilin 1 mutation M146V increases gamma secretase cutting of p75NTR in vitro. *Brain Res.* 1147:248-55.

Hasselmo, ME (2006). The Role of Acetylcholine in Learning and Memory. *Curr Opin Neurobiol. 16*(6):710–715.

Hazell GG, Hindmarch CC, Pope GR, Roper JA, Lightman SL, Murphy D, O'Carroll AM, Lolait SJ (2012). G protein-coupled receptors in the hypothalamic paraventricular and supraoptic nuclei--serpentine gateways to neuroendocrine homeostasis. *Front Neuroendocrinol.* 33(1):45-66.

Hebb D (1949). The Organization of Behavior. New York: Wiley & Sons.

Henneman WJ, Sluimer JD, Barnes J, van der Flier WM, Sluimer IC, Fox NC, Scheltens P, Vrenken H, Barkhof F (2009). Hippocampal atrophy rates in Alzheimer disease: added value over whole brain volume measures. *Neurology.* 72(11):999-1007.

Heyes MP, Achim CL, Wiley CA, Major EO, Saito K, Markey SP (1996). Human microglia convert 1-tryptophan into the neurotoxin quinolinic acid. *Biochem J*. 320(Pt 2):595–7.

Heyes MP, Chen CY, Major EO, Saito K (1997). Different kynurenine pathway enzymes limit quinolinic acid formation by various human cell types. *Biochem J*. 326(Pt 2):351–6.

Henry JD, Crawford JR, Phillips LH (2004). Verbal fluency performance in dementia of the Alzheimer's type: A meta-analysis. *Neuropsychologia* 42: 1212–1222.

Heppner FL, Ransohoff RM, Becher B (2015). Immune attack: the role of inflammation in Alzheimer disease. *Nat Rev Neurosci.* 16(6):358-72.

Hilmas C, Pereira EF, Alkondon M, Rassoulpour A, Schwarcz R, Albuquerque EX (2001). The brain metabolite kynurenic acid inhibits alpha7 nicotinic receptor activity and increases non-alpha7 nicotinic receptor expression: physiopathological implications. *J Neuro Sci*. 21:7463–73.

Huang Y, Mahley RW (2014). Apolipoprotein E: structure and function in lipid metabolism, neurobiology, and Alzheimer's diseases. *Neurobiol Dis.* 72 Pt A:3-12.

Huang YA, Zhou B, Wernig M, Südhof TC (2017). ApoE2, ApoE3, and ApoE4 differentially stimulate APP transcription and Aβ secretion. *Cell.* 168(3):427-441.e21.

Humbert IA, McLaren DG, Kosmatka K, Fitzgerald M, Johnson S, Porcaro E, Kays S, Umoh EO, Robbins J (2010). Early deficits in cortical control of swallowing in Alzheimer's disease. *J Alzheimers Dis.* 19(4):1185-97.

Hutton M et al., (1998). Association of missense and 5'-splice-site mutations in tau with the inherited dementia FTDP-17. *Nature.* 393(6686):702-5.

Hymson DL, Hynes MD (1982). Evidence that ethanol-induced impairment of Rota-rod performance is not mediated by opioid mechanisms. *Prog Neuropsychopharmacol Biol Psychiatry.* 6:159-165.

Ibach B, Haen E (2004). Acetylcholinesterase inhibition in Alzheimer's Disease. *Curr Pharm Des.* 10(3):231-51.

ICD-10 World Health Organization. 2001.

Iemolo F, Duro G,4 Rizzo C, Castiglia L, Hachinski V, Caruso C (2009). Pathophysiology of vascular dementia. *Immun.Ageing.* 6: 13.f

Igoumenou A, Ebmeier KP (2012). Diagnosing and managing vascular dementia. *Practitioner.* 256(1747):13-6, 2.

Ikegami S, Harada A, Hirokawa N (2000). Muscle weakness, hyperactivity, and impairment in fear conditioning in tau-deficient mice. *Neurosci Lett.* 279(3):129-32.

Iqbal K, Liu F, Gong CX, Grundke-Iqbal I (2010). Tau in Alzheimer disease and related tauopathies. *Curr Alzheimer Res.* 7(8):656-64.

Izumi Y, Yamada KA, Matsukawa M, Zorumski CF (2003). Effects of insulin on long-term potentiation in hippocampal slices from diabetic rats. *Diabetologia.* 46(7):1007-12.

Jawhar S, Trawicka A, Jenneckens C, Bayer TA, Wirths O (2012). Motor deficits, neuron loss, and reduced anxiety coinciding with axonal degeneration and intraneuronal Aβ aggregation in the 5XFAD mouse model of Alzheimer's disease. *Neurobiol Aging.* 33(1):196.e29-40.

Joachim CL, Morris JH, Selkoe DJ (1988). Clinically diagnosed Alzheimer's disease: autopsy results in 150 cases. *Ann Neurol.* (1):50-56.

Jones BJ, Roberts DJ (1968). The quantitative measurement of motor co-ordination in naive mice using an accelerating rotarod. *J Pharm Pharmac.* 20: 302-304.

Jonsson, T. et al (2013). Variant of *TREM2* associated with the risk of Alzheimer's disease. *N Engl J Med.* 368: 107–116.

Kahlson MA, Colodner KJ (2015). Glial Tau Pathology in Tauopathies: Functional Consequences. *J Exp Neurosci*, *9*(Suppl 2), 43–50.

Karantzoulis S, Galvin JE (2011). Distinguishing Alzheimer's disease from other major forms of dementia. *Expert Rev Neurother.* 11(11):1579-91.

Keeler JF, Pretsell DO, Robbins TW (2014). Functional implications of dopamine D1 vs. D2 receptors: A 'prepare and select' model of the striatal direct vs. indirect pathways. *Neuroscience.* 282:156-75.

Kapitein LC, Hoogenraad CC (2015). Building the neuronal microtubule cytoskeleton. *Neuron.* 87(3):492-506.

Kar A, Kuo D, He R, Zhou J, Wu JY (2005). Tau alternative splicing and frontotemporal dementia. *Alzheimer Dis Assoc Disord.* 19 Suppl 1:S29-36.

Khan TK, Alkon DL (2015). Peripheral Biomarkers of Alzheimer's Disease. *J. Alzheimers. Dis.* 44(3):729-44.

Kim JP, Choi DW (1987). Quinolinate neurotoxicity in cortical cell culture. *Neuroscience*. 23:423–32.

Kim EJ, Horovitz O, Pellman BA, Tan LM, Li Q, Richter-Levin G, Kim JJ (2013). Dorsal periaqueductal gray-amygdala pathway conveys both innate and learned fear responses in rats. *Proc Natl Acad Sci U S A.* 110(36):14795-800.

Klimova B, Maresova P, Valis M, Hort J, Kuca K (2015). Alzheimer's disease and language impairments: social intervention and medical treatment. *Clin Interv Aging.* 10:1401-7.

Koenigsknecht J, Landreth G (2004). Microglial phagocytosis of fibrillar beta-amyloid through a beta1 integrin-dependent mechanism. J *Neurosci.* 24(44):9838-46.

Kohen R, Nyska A (2002). Oxidation of biological systems: oxidative stress phenomena, antioxidants, redox reactions, and methods for their quantification. *Toxicol Pathol.* 30(6):620-50.

Kohn MA, Michaels AD (2005). Likelihood ratio reporting. *Mayo Clin Proc.* 80(4):563; author reply 563-4.

Koike MA, Lin AJ, PhamJ, Nguyen E, Yeh JJ, Rahimian R, Tromberg BJ, Choi B, Green KN, LaFerla, F. M. (2012). APP Knockout Mice Experience Acute Mortality as the Result of Ischemia. *PLoS ONE*, *7*(8), e42665.

Kollias G, Spanopoulou E, Grosveld F, Ritter M, Beech J, Morris R (1987). Differential regulation of a Thy-1 gene in transgenic mice. *Proc Natl Acad Sci U S A.* 84(6):1492-6.

Kontush A (2001). Amyloid-beta: an antioxidant that becomes a pro-oxidant and critically contributes to Alzheimer's disease. *Free Radic Biol Med.* 31(9):1120-31.

Koo EH, Sisodia SS, Archer DR, Martin LJ, Weidemann A, Beyreuther K, Fischer P, Masters CL, Price DL (1990). Precursor of amyloid protein in Alzheimer disease undergoes fast anterograde axonal transport. *Proc Natl Acad Sci. U S A.* 87(4):1561-5.

Kosik KS, Orecchio LD, Bakalis S, Neve RL (1989). Developmentally regulated expression of specific tau sequences. *Neuron.* 2(4):1389-97.

Kovacs GG (2015). Invited review: Neuropathology of tauopathies: principles and practice. *Neuropathol Appl Neurobiol.* 41(1):3-23

Kroner Z (2009). The relationship between Alzheimer's disease and diabetes: Type 3 diabetes? *Altern Med Rev.* 14(4):373-9.

Krstic D et al., (2012). Systemic immune challenges trigger and drive Alzheimer-like neuropathology in mice. *J Neuroinflammation.* 9:151.

Kumar DK et al., (2016). Amyloid-β peptide protects against microbial infection in mouse and worm models of Alzheimer's disease. *Sci Transl Med.* 8(340):340ra72.

Laßek M, Weingarten J, Acker-Palmer A, Bajjalieh S, Müller U, Volknandt W (2014). Amyloid Precursor Protein Knockout Diminishes Synaptic Vesicle Proteins at the Presynaptic Active Zone in Mouse Brain. *Curr Alzheimer Res.* 11(10):971-80.

LaFerla FM (2012). APP knockout mice experience acute mortality as the result of ischemia. *PLoS One.*7(8): e42665.

Lagadec S, Rotureau L, Hémar A, Macrez N, Delcasso S, Jeantet Y, Cho YH (2012). Early temporal short-term memory deficits in double transgenic APP/PS1 mice. *Neurobiol Aging.* 33(1):203.e1-11.

Lam B, Masellis M, Freedman M, Stuss DT, Black SE (2013). Clinical, imaging, and pathological heterogeneity of the Alzheimer's disease syndrome. *Alzheimers Res Ther.* 5(1):1.

LaPointe NE, Morfini G, Pigino G, Gaisina IN, Kozikowski AP, Binder LI, Brady ST (2009). The amino terminus of tau inhibits kinesin-dependent axonal transport: implications for filament toxicity. *J Neurosci Res.* 87(2):440-51.

Lawrence JL, Tong M, Alfulaij N, Sherrin T, Contarino M, White MM, Bellinger FP, Todorovic C, Nichols RA (2014). Regulation of Presynaptic Ca2+, Synaptic Plasticity and Contextual Fear Conditioning by a N-terminal β-Amyloid Fragment. *J Neurosci.* 34(43):14210-8.

LaMarec N, Lalonde R (1997). Sensorimotor learning and retention during equilibrium tests in Purkinje cell degeneration mutant mice. *Brain Res.* 768:310-316.

Lever AR, Park H, Mulhern TJ, Jackson GR, Comolli JC, Borenstein JT, Hayden PJ, Prantil-Baun R (2015). Comprehensive evaluation of poly(I:C) induced inflammatory response in an airway epithelial model. *Physiol Rep.* 3(4). pii: e12334.

Lewis J et al., (2000). Neurofibrillary tangles, amyotrophy and progressive motor disturbance in mice expressing mutant (P301L) tau protein. *Nat Genet.* 25(4):402-425.

Lewis J et al., (2001). Enhanced neurofibrillary degeneration in transgenic mice expressing mutant tau and APP. *Science.* 293(5534):1487-91.

Li R, Wei F, Yu J (2009). IDO inhibits T-cell function through suppressing Vav1 expression and activation. *Cancer Biol Ther.* 8:1402–1408.

Lim GP (2000). Ibuprofen suppresses plaque pathology and inflammation in a mouse model for Alzheimer's disease. J *Neurosci.* 20(15):5709-14

Lipsky RH, Marini AM (2007). Brain-derived neurotrophic factor in neuronal survival and behavior-related plasticity. *Ann N Y Acad Sci.* 1122:130-43.

Liu F, Gong CX (2008). Tau exon 10 alternative splicing and tauopathies. *Mol Neurodegener.* 3:8.

Luciana M, Burgund ED, Berman M, Hanson KL (2001). Effects of tryptophan loading on verbal, spatial and affective working memory functions in healthy adults. *J Psychopharmacol.* 15(4):219-30.

Luo X, Shui Y, Wang F, Yamamoto R, Kato N (2017). Impaired retention of depression-like behavior in a mouse model of Alzheimer's disease. *IBRO Reports.* 2:81-86.

Lustbader JW et al., (2004). ABAD directly links Abeta to mitochondrial toxicity in Alzheimer's disease. *Science.* 304(5669):448-52.

Maccioni RB, Cambiazo V (1995). Role of microtubule-associated proteins in the control of microtubule assembly. *Physiol Rev.* 75(4):835-64.

Mann DM, Iwatsubo T, Ihara Y, Cairns NJ, Lantos PL, Bogdanovic N, Lannfelt L, Winblad B, Maat-Schieman ML, Rossor MN (1996). Predominant deposition of amyloid-beta 42(43) in plaques in cases of Alzheimer's disease and hereditary cerebral hemorrhage associated with mutations in the amyloid precursor protein gene. *Am. J. Pathol.* 148(4):1257-66.

Manook A, Yousefi BH, Willuweit A, Platzer S, Reder S, Voss A, et al. (2012). Small-animal PET imaging of amyloid-beta plaques with [11C]PiB and its multi-modal validation in an APP/PS1 mouse model of Alzheimer's disease. *PLoS.One.* 7:31310.

Maren S, Phan KL, Liberzon I (2013). The contextual brain: implications for fear conditioning, extinction and psychopathology. *Nat Rev Neurosci.* 14(6):417-28

Marrero MB, Bencherif M (2009). Convergence of alpha 7 nicotinic acetylcholine receptor-activated pathways for anti-apoptosis and anti-inflammation: central role for JAK2 activation of STAT3 and NF-kappaB. *Brain. Res.* 1256:1-7.

Marschner A, Kalisch R, Vervliet B, Vansteenwegen D, Büchel C (2008). Dissociable roles for the hippocampus and the amygdala in human cued versus context fear conditioning. *J Neurosci.* 28(36):9030-6.

Mastrangelo MA, Sudol KL, Narrow WC, Bowers WJ (2009). Interferon-{gamma} differentially affects Alzheimer's disease pathologies and induces neurogenesis in triple transgenic-AD mice. Am J Pathol. 175(5):2076-88.

McDonald RJ, White NM (1993). A triple dissociation of memory systems: hippocampus, amygdala, and dorsal striatum. *Behav Neurosci.* 107(1):3-22.

McKhann G, Drachman D, Folstein M, Katzman R, Price D, Stadlan EM (1984). Clinical diagnosis of Alzheimer's disease: report of the NINCDS-ADRDA Work Group under the auspices of Department of Health and Human Services Task Force on Alzheimer's Disease. *Neurology*. 34(7):939-944.

McKhann GM et al., (2011). The diagnosis of dementia due to Alzheimer's disease: recommendations from the National Institute on Aging-Alzheimer's Association workgroups on diagnostic guidelines for Alzheimer's disease. *Alzheimers Dement.* 7(3):263-9.

McMenamy RH (1965). Binding of indole analogues to human serum albumin. Effects of fatty acids. *J Biol Chem*. 240:4235–43.

Miller AL, Leach MC (2015). The Mouse Grimace Scale: A Clinically Useful Tool? *PLoS One.* 10(9):e0136000.

Mirra SS et al., (1999). Tau pathology in a family with dementia and a P301L mutation in tau. *J Neuropathol Exp Neurol.* 58(4):335-45.

Moffett JR, Espey MG, Gaudet SJ. Namboodiri MA (1993). Antibodies to quinolinic acid reveal localization in select immune cells rather than neurons or astroglia. *Brain Res*. 623:337–40.

Moffett JR, Namboodiri MA (2003). Tryptophan and the immune response. *Immunol Cell Biol.* 81(4):247-65.

Monastero R, Mangialasche F, Camarda C, Ercolani S, Camarda R (2009). A systematic review of neuropsychiatric symptoms in mild cognitive impairment. *J Alzheimers Dis.* 18(1):11-30.

Monfort P, Gomez-Gimenez B, Llansola M, Felipo V (2015). Gender differences in spatial learning, synaptic activity, and long-term potentiation in the hippocampus in rats: molecular mechanisms. *ACS Chem Neurosci.* 6(8):1420-7.

Montacute R, Foley K, Forman F, Else KJ, Cruickshank SM, Allan SM (2017). Enhanced susceptibility of triple transgenic Alzheimer's disease (3xTg-AD) mice to acute infection. *J Neuroinflammation.* 14: 50.

Montgomery KC. The relation between fear induced by novel stimulation and exploratory behavior. *J Comp Physiol Psychol.* 1955;48:254–260.

Moon YW, Hajjar J, Hwu P, Naing A (2015). Targeting the indoleamine 2,3-dioxygenase pathway in cancer. *J Immunother Cancer.* 3:51.

Morgan D, Munireddy S, Alamed J, DeLeon J, Diamond DM, Bickford P, Hutton M, Lewis J, McGowan E, Gordon MN (2008). Apparent behavioral benefits of tau overexpression in P301L tau transgenic mice. *J Alzheimers Dis.* 15(4):605-14.

Moroni F, Fossati S, Chiarugi A, Cozzi A (2007). Kynurenic acid actions in brain and periphery. *International Congress Series*. 1304:305–13.

Moroni F, Russi P, Carlá V, Lombardi G (1988). Kynurenic acid is present in the rat brain and its content increases during development and aging processes. *Neurosci Lett.* 94(1-2):145-50.

Morris JC, Storandt M, McKeel DW Jr, Rubin EH, Price JL, Grant EA, Berg L (1996). Cerebral amyloid deposition and diffuse plaques in "normal" aging: Evidence for pre-symptomatic and very mild Alzheimer's disease. *Neurology* 46: 707 – 719.

Morris GP, Clark IA, Vissel B (2014). Inconsistencies and controversies surrounding the amyloid hypothesis of Alzheimer's disease. *Acta Neuropathol Commun.* 2:135.

Mosienko V, Bert B, Beis D, Matthes S, Fink H, Bader M, Alenina N (2012). Exaggerated aggression and decreased anxiety in mice deficient in brain serotonin. *Transl Psychiatry.* 2:e122

Mullan M, Crawford F, Axelman K, Houlden H, Lilius L, Winblad B, Lannfelt L (1992). A pathogenic mutation for probable Alzheimer's disease in the APP gene at the N-terminus of beta-amyloid. *Nat Genet.* 1(5):345-347.

Mullane K, Williams M (2013). Alzheimer's therapeutics: continued clinical failures question the validity of the amyloid hypothesis-but what lies beyond? *Biochem Pharmacol.* 85(3):289-305.

Munn DH, Shafizadeh E, Attwood JT, Bondarev I, Pashine A, Mellor AL (1999). Inhibition of T cell proliferation by macrophage tryptophan catabolism. *J Exp Med*. 189:1363–72.

Munn DH, Zhou M, Attwood JT, Bondarev I, Conway SJ, Marshall B, Brown C, Mellor AL (1998). Prevention of allogeneic fetal rejection by tryptophan catabolism. *Science.* 281:1191–1193.

Müller NG, Knight RT (2006). The functional neuroanatomy of working memory: contributions of human brain lesion studies. *Neuroscience.* 139(1):51-8.

Müller-Spahn F (2003). Behavioural disturbances in dementia. *Dialogues Clin Neurosci.* 5(1): 49–59.

Müller U, Winter P, Graeber MB (2013). A presenilin 1 mutation in the first case of Alzheimer's disease. *Lancet. Neurol.* 12(2):129-30.

Nagele RG, D'Andrea MR, Anderson WJ, Wang HY (2002). Intracellular accumulation of beta-amyloid (1-42) in neurons is facilitated by the alpha 7 nicotinic acetylcholine receptor in Alzheimer's disease. *Neuroscience.* 110(2):199-211.

Nasrallah IM, Wolk DA (2014). Multimodality imaging of Alzheimer disease and other neurodegenerative dementias. *J Nucl Med.* 55(12):2003-11.

Nochlin D, van Belle G, Bird TD, Sumi SM (1993). Comparison of the severity of neuropathologic changes in familial and sporadic Alzheimer’s disease. *Alzheimer Dis Assoc Disord*. 7: 212-222.

Nunan J, Small DH (2000). Regulation of APP cleavage by alpha-, beta- and gamma-secretases. *FEBS Lett.* 483(1): 6-10.

Oakley H, Cole SL, Logan S, Maus E, Shao P, Craft J, et al. (2006). Intraneuronal beta-amyloid aggregates, neurodegeneration, and neuron loss in transgenic mice with five familial Alzheimer's disease mutations: potential factors in amyloid plaque formation. *J Neurosci.* 26:10129–10140.

O'Brien RJ, Wong PC (2011). Amyloid precursor protein processing and Alzheimer's disease. *Annu Rev Neurosci.* 34:185-204.

Oddo S at al., (2003) Triple-transgenic model of Alzheimer's disease with plaques and tangles: intracellular Aβ and synaptic dysfunction. *Neuron.* 39:409-421.

Oh ES, Savonenko AV, King JF, Fangmark Tucker SM, Rudow GL, Xu G, Borchelt DR, Troncoso JC (2009). Amyloid precursor protein increases cortical neuron size in transgenic mice. *Neurobiol. Aging.* 30(8):1238-44.

Ohyagi Y et al., (2005). Intracellular Abeta42 activates p53 promoter: a pathway to neurodegeneration in Alzheimer's disease. *FASEB J.* 19(2):255-7.

Okuda S, Nishiyama N, Saito H, Katsuki H (1998). 3-Hydroxykynurenine, an endogenous oxidative stress generator, causes neuronal cell death with apoptotic features and region selectivity. *J Neurochem.* 70(1):299-307.

O'Leary TP, Brown RE (2013). Optimization of apparatus design and behavioral measures for the assessment of visuo-spatial learning and memory of mice on the Barnes maze. *Learn Mem.* 20(2):85-96.

O'Leary TP, Gunn RK, Brown RE (2013). What are we measuring when we test strain differences in anxiety in mice? *Behav Genet.* 43(1):34-50.

Olivares D, Deshpande VK, Shi Y, Lahiri DK, Greig NH, Rogers JT, Huang X (2012). N-methyl D-aspartate (NMDA) receptor antagonists and memantine treatment for Alzheimer's disease, vascular dementia and Parkinson's disease. *Curr Alzheimer Res.* 9(6):746-58.

Olsauskas-Kuprys R, Zlobin A, Osipo C (2013). Gamma secretase inhibitors of Notch signaling. *Onco. Targets. Ther.* 6:943–955.

Ovsepian SV, Herms J (2013). Cholinergic neurons-keeping check on amyloid β in the cerebral cortex. *Front Cell Neurosci.* 7:252.

Pallardó FV et al., (2006). Multiple evidence for an early age pro-oxidant state in Down Syndrome patients. *Biogerontology.* 7(4):211-20.

Panegyres PK, Chen HY (2013). Differences between early and late onset Alzheimer's disease. *Am J Neurodegener Dis. 2*(4), 300–306.

Parri HR, Hernandez CM, Dineley KT (2011). Research update: Alpha7 nicotinic acetylcholine receptor mechanisms in Alzheimer's disease. *Biochem Pharmacol.* 82(8):931-42.

Parsons MP, Raymond LA (2014). Extrasynaptic NMDA receptor involvement in central nervous system disorders. *Neuron.* 82(2):279-93.

Pearson SJ, Reynolds GP (1992). Increased brain concentrations of a neurotoxin, 3-hydroxykynurenine, in Huntington's disease. *Neurosci Lett.* 144(1-2):199-201.

Pellow S, Chopin P, File SE, Briley M. Validation of open:closed arm entries in an elevated plus-maze as a measure of anxiety in the rat. *J Neurosci Methods.* 1985;14:149–167.

Peng S, Garzon DJ, Marchese M, Klein W, Ginsberg SD, Francis BM, Mount HT, Mufson EJ, Salehi A, Fahnestock M (2009). Decreased brain-derived neurotrophic factor depends on amyloid aggregation state in transgenic mouse models of Alzheimer's disease. *J Neurosci.* 29(29):9321-9.

Penrose LS (1949). The incidence of mongolism in the general population. *J Ment Sci.* 95(400):685-8.

Perrin RJ, Fagan AM, Holtzman DM (2009). Multimodal techniques for diagnosis and prognosis of Alzheimer’s disease. *Nature* 461: 916–922.

Petit-Demouliere B, Chenu F, Bourin M. Forced swimming test in mice: a review of antidepressant activity. *Psychopharmacology. (Berl).* 177:245–255.

Piaceri I, Nacmias B, Sorbi S (2013). Genetics of familial and sporadic Alzheimer's disease. *Front Biosci (Elite Ed).* 5:167-77.

Pietropaolo S, Sun Y, Li R, Brana C, Feldon J, Yee BK (2009). Limited impact of social isolation on Alzheimer-like symptoms in a triple transgenic mouse model. *Behav Neurosci.* 123(1):181-95.

Pickering G, Jourdan D, Dubray C (2005). Acute versus chronic pain treatment in Alzheimer’s disease. *Eur J Pain.* 10:379–384.

Poppek D, Keck S, Ermak G, Jung T, Stolzing A, Ullrich O, Davies KJ, Grune T (2006). Phosphorylation inhibits turnover of the tau protein by the proteasome: influence of RCAN1 and oxidative stress. *Biochem J.* 400(3):511-20.

Porsolt RD, Bertin A, Jalfre M. Behavioral despair in mice: a primary screening test for antidepressants. *Arch Int Pharmacodyn Ther.* 229:327–336.

Portelius E, Price E, Brinkmalm G, Stiteler M, Olsson M, Persson R, Westman-Brinkmalm A, Zetterberg H, Simon AJ, Blennow K (2011). A novel pathway for amyloid precursor protein processing. *Neurobiol. Aging.* 32(6):1090-1098.

Praticò D, Clark CM, Liun F, Rokach J, Lee VY, Trojanowski JQ (2002). Increase of brain oxidative stress in mild cognitive impairment: a possible predictor of Alzheimer disease. *Arch Neurol.* 59(6):972-6.

Prasher VP, Farrer MJ, Kessling AM, Fisher EM, West RJ, Barber PC, Butler AC (1998). Molecular mapping of Alzheimer-type dementia in Down's syndrome. *Ann Neurol* 43: 380 – 383.

Preston AR, Eichenbaum H (2013). Interplay of hippocampus and prefrontal cortex in memory. *Curr Biol.* 23(17):R764-73.

Prince M, Ali GC, Guerchet M, Prina AM, Albanese E, Wu YT (2016). Recent global trends in the prevalence and incidence of dementia, and survival with dementia. *Alzheimers Res Ther.* 8(1):23.

Price JL et al., (2009). Neuropathology of nondemented aging: presumptive evidence for preclinical Alzheimer disease. *Neurobiol Aging.* 30(7):1026-36.

Pugh PL, Richardson JC, Bate ST, Upton N, Sunter D (2007). Non-cognitive behaviours in an APP/PS1 transgenic model of Alzheimer's disease. *Behav Brain Res.* 178:18–28.

Qiu WQ, Zhu H (2014). Amylin and its analogs: a friend or foe for the treatment of Alzheimer's disease? *Front Aging Neurotici.* 6:186.

Rahman A, Ting K, Cullen KM, Braidy N, Brew BJ, Guillemin GJ (2009). The excitotoxin quinolinic acid induces tau phosphorylation in human neurons. *PLoS One.* 4(7):e6344.

Ramachandraih CT, Subramanyam N, Bar KJ, Baker G, Yeragani VK (2011). Antidepressants: From MAOIs to SSRIs and more. *Indian J Psychiatry.* 53(2):180–182.

RapoportM, DawsonHN, BinderLI, VitekMP, Ferreira A (2002). Tau is essential to β -amyloid-induced neurotoxicity. *Proc Natl Acad Sci U S A*. 99(9):6364-6369.

Raudino F (2013). Non-cognitive symptoms and related conditions in the Alzheimer's disease: a literature review. *Neurol Sci.* 34(8):1275-82.

Réus GZ, Jansen K, Titus S, Carvalho AF, Gabbay V, Quevedo J (2015). Kynurenine pathway dysfunction in the pathophysiology and treatment of depression: Evidences from animal and human studies. *J Psychiatr Res.* 68:316-28.

Rhein V, Baysang G, Rao S, Meier F, Bonert A, Müller-Spahn F, Eckert A (2009). Amyloid-beta leads to impaired cellular respiration, energy production and mitochondrial electron chain complex activities in human neuroblastoma cells. *Cell Mol Neurobiol.* 29(6-7):1063-71.

Rice FL, Van der Loos H (1977). Development of the barrels and barrel field in the somatosensory cortex of the mouse. J Comp Neurol. 171(4):545-60.

Roberson ED, Scearce-Levie K, Palop JJ, Yan F, Cheng IH, Wu T, Gerstein H, Yu GQ, Mucke L (2007). Reducing endogenous tau ameliorates amyloid beta-induced deficits in an Alzheimer's disease mouse model. *Science.* 316(5825):750-4.

Rovelet-Lecrux A et al., (2006). APP locus duplication causes autosomal dominant early-onset Alzheimer disease with cerebral amyloid angiopathy. *Nat Genet*. 38: 24 – 26.

Ruddick JP, Evans AK, Nutt DJ, Lightman SL, Rook GA, Lowry CA (2006). Tryptophan metabolism in the central nervous system: medical implications. *Expert Rev Mol Med*. 8:1–27.

Runyan JD, Moore AN, Dash PK (2004). A role for prefrontal cortex in memory storage for trace fear conditioning. *J Neurosci.* 24(6):1288-95.

Rupp C, Beyreuther K, Maurer K, Kins S (2014). A presenilin 1 mutation in the first case of Alzheimer's disease: Revisited. *Alzheimers. Dement.* 10(6):869-72.

Ryazantseva M, Skobeleva K, Kaznacheyeva E (2013). Familial Alzheimer's disease-linked presenilin-1 mutation M146V affects store-operated calcium entry: does gain look like loss? *Biochimie.* 95(7):1506-9.

Savitz J, Drevets WC, Wurfel BE, Ford BN, Bellgowan PS, Victor TA, Bodurka J, Teague TK, Dantzer R (2015). Reduction of kynurenic acid to quinolinic acid ratio in both the depressed and remitted phases of major depressive disorder. *Brain Behav Immun.* 46:55-9.

Scherder EJ, Sergeant JA, Swaab DF (2003). Pain processing in dementia and its relation to neuropathology. *Lancet Neurol.* 2(11):677-86.

Serpente M, Bonsi R, Scarpini E, Galimberti D (2014). Innate immune system and inflammation in Alzheimer's disease: from pathogenesis to treatment. *Neuroimmunomodulation.* 21(2-3):79-87.

Scoville WB, Milner B (1957). Loss of recent memory after bilateral hippocampal lesions. *J Neurol Neurosurg Psychiatry.* 20(1):11-21.

Schwarz MJ, Guillemin GJ, Teipel SJ, Buerger K, Hampel H (2013). Increased 3-hydroxykynurenine serum concentrations differentiate Alzheimer's disease patients from controls. *Eur Arch Psychiatry Clin Neurosci.* 263(4):345-52.

Schwarcz R, Whetsell WO Jr, Mangano RM (1983). Quinolinic acid: an endogenous metabolite that produces axon-sparing lesions in rat brain. *Science*. 219:316–8.

Selkoe DJ (1991) The molecular pathology of Alzheimer's disease. *Neuron* 6: 487 – 498.

Selkoe DJ, Hardy J (2016). The amyloid hypothesis of Alzheimer's disease at 25 years. *EMBO Mol Med.* 8(6):595-608.

Senechal Y, Kelly PH, Dev KK (2008). Amyloid precursor protein knockout mice show age-dependent deficits in passive avoidance learning. *Behav. Brain. Res.* 10;186(1):126-32.

Shoemark DK, Allen SJ (2015). The Microbiome and Disease: Reviewing the Links between the oral microbiome, aging, and Alzheimer's Disease. *J Alzheimers Dis.* 43(3):725-38.

Shore DI, Stanford L, MacInnes WJ, Klein RM, Brown RE (2001). Of mice and men: virtual Hebb-Williams mazes permit comparison of spatial learning across species. *Cogn Affect Behav Neurosci.* 1(1):83-9.

Simpson C, Carter P (2015). The impact of living arrangements on dementia caregivers' sleep quality. *Am J Alzheimers Dis Other Demen.* 30(4):352-9.

Slattery DA, Cryan JF (2012). Using the rat forced swim test to assess antidepressant-like activity in rodents. *Nat Protoc.* 7(6):1009-14.

Small DH, Nurcombe V, Reed G, Clarris H, Moir R, Beyreuther K, Masters CL (1994). A heparin-binding domain in the amyloid protein precursor of Alzheimer's disease is involved in the regulation of neurite outgrowth. *J Neurosci.* 14, 2117–2127.

Small BJ, Fratiglioni L, Viitanen M, Winblad B, Backman L (2000). The course of cognitive impairment in preclinical Alzheimer disease: Three and 6-year follow-up of a population-based sample. *Arch Neurol* 57: 839–844.

Smits LL, Pijnenburg YA, Koedam EL, van der Vlies AE, Reuling IE, Koene T, Teunissen CE, Scheltens P, van der Flier WM (2012). Early onset Alzheimer's disease is associated with a distinct neuropsychological profile. *J Alzheimers Dis.* 30(1):101-8.

Soderstrom NC, Bjork RA (2015). Learning versus performance: an integrative review. *Perspect Psychol Sci.* 10(2):176-99.

Soliman H, Mediavilla-Varela M, Antonia S (2010). Indoleamine 2,3-dioxygenase: is it an immune suppressor? *Cancer J.* 16(4):354-9.

Solito E, Sastre M (2012). Microglia function in Alzheimer's disease. *Front Pharmacol.* 3:14.

Sowunmi A, Gbotosho GO, Happi CT, Folarin O, Okuboyejo T, Michael O, Fatunmbi B (2011). Use of area under the curve to evaluate the effects of antimalarial drugs on malaria-associated anemia after treatment. *Am J Ther.* 18(3):190-7.

Spanopoulou E, Giguere V, Grosveld F (1988). Transcriptional unit of the murine Thy-1 gene: different distribution of transcription initiation sites in brain. *Mol Cell Biol.* 8(9):3847-56.

Spellman T, Rigotti M, Ahmari SE, Fusi S, Gogos JA, Gordon JA (2015). Hippocampal-prefrontal input supports spatial encoding in working memory. *Nature.* 522(7556):309-14.

Steiner J et al., (2011). Severe depression is associated with increased microglial quinolinic acid in subregions of the anterior cingulate gyrus: evidence for an immune-modulated glutamatergic neurotransmission? *J Neuroinflammation.* 8:94.

Stelzmann RA, Schnitzlein HN, Murtagh FR (1995). An English translation of Alzheimer's 1907 paper, "Uber eine eigenartige Erkankung der Hirnrinde" *Clin. Anat.* 8:429-431.

Steru L, Chermat R, Thierry B, Simon P (1985). The tail suspension test: a new method for screening antidepressants in mice. *Psychopharmacology (Berl).* 85(3):367-70.

Stevens LM, Brown RE (2014). Reference and working memory deficits in the 3xTg-AD mouse between 2 and 15-months of age: A cross-sectional study. *Behav Brain Res*. 2278C:496-505.

Sterniczuk R, Antle MC, Laferla FM, Dyck RH (2010). Characterization of the 3xTg-AD mouse model of Alzheimer's disease: part 1. Behavioral and cognitive changes. *Brain Res.* 1348:139-148.

Sterniczuk R, Antle MC, Laferla FM, Dyck RH (2010). Characterization of the 3xTg-AD mouse model of Alzheimer's disease: part 2. Behavioral and cognitive changes. *Brain Res.* 1348:149-155.

Stone TW, Perkins MN (1981). Quinolinic acid: a potent endogenous excitant at amino acid receptors in CNS. *Eur J Pharmacol*. 72:411–2.

Stone TW (1993). Neuropharmacology of quinolinic and kynurenic acids. *Pharmacol Rev*. 45:309–79.

Stover KR, Campbell MA, Van Winssen CM, Brown RE (2015). Analysis of motor function in 6-month-old male and female 3xTg-AD mice. *Behav Brain Res.* 281:16-23.

Stover KR, Campbell MA, Van Winssen CM, Brown RE (2015). Early detection of cognitive deficits in the 3xTg-AD mouse model of Alzheimer's disease. *Behav Brain Res.* 289:29-38.

Subramanian S, Ayala P, Wadsworth TL, Harris CJ, Vandenbark AA, Quinn JF, Offner H (2010). CCR6: a biomarker for Alzheimer's-like disease in a triple transgenic mouse model. *J Alzheimers Dis.* 22(2):619-29.

Takeuchi T, Owa T, Nishino T, Kamei C (2010). Assessing anxiolytic-like effects of selective serotonin reuptake inhibitors and serotonin-noradrenaline reuptake inhibitors using the elevated plus maze in mice. *Methods Find Exp Clin Pharmacol.* 32(2):113-21.

Talantova M et al., (2013). Aβ induces astrocytic glutamate release, extrasynaptic NMDA receptor activation, and synaptic loss. *Proc Natl Acad Sci U S A.* 110(27):2518-2527.

Talarico G et al., (2010). The London APP mutation (Val717Ile) associated with early shifting abilities and behavioral changes in two Italian families with early-onset Alzheimer's disease. *Dement. Geriatr Cogn Disord.* 29(6):484-490.

Tam JH, Seah C, Pasternak SH (2014). The Amyloid precursor protein is rapidly transported from the Golgi apparatus to the lysosome and where it is processed into beta-amyloid. *Mol Brain.* 7:54.

Tanzi RE (2012). The genetics of Alzheimer disease. *Cold. Spring. Harb. Perspect. Med.* 2(10): a006296.

Taylor MW, Feng GS (1991). Relationship between interferon-gamma, indoleamine 2,3-dioxygenase, and tryptophan catabolism. *FASEB J.* 5(11):2516-22.

Thambisetty M at al., (2010) Association of plasma clusterin concentration with severity, pathology, and progression in Alzheimer disease. *Arch Gen Psychiatry.* 67:739-748.

Thannickal VJ, Fanburg BL (2000). Reactive oxygen species in cell signaling. *Am J Physiol Lung Cell Mol Physiol.* 279(6):L1005-28.

Thompson SA, Smith O, Linn DM, Linn CL (2006). Acetylcholine neuroprotection against glutamate-induced excitotoxicity in adult pig retinal ganglion cells is partially mediated through alpha4 nAChRs. *Exp Eye Res.* 83(5):1135-45.

Thornton E, Vink R, Blumbergs PC, Van Den Heuvel C (2006). Soluble amyloid precursor protein alpha reduces neuronal injury and improves functional outcome following diffuse traumatic brain injury in rats. *Brain Res.* 1094(1):38-46.

Tokuhiro S, Tomita T, Iwata H, Kosaka T, Saido TC, Maruyama K, Iwatsubo T (1998). The presenilin 1 mutation (M146V) linked to familial Alzheimer's disease attenuates the neuronal differentiation of NTera 2 cells. *Biochem Biophys Res Commun.* 244(3):751-5.

Tu S, Okamoto S, Lipton SA, Xu H (2014). Oligomeric Aβ-induced synaptic dysfunction in Alzheimer's disease. *Mol Neurodegener.* 9:48.

Turner PV, Vaughn E, Sunohara-Neilson J, Ovari J, Leri F (2012). Oral gavage in rats: animal welfare evaluation. *J Am Assoc Lab Anim Sci.* 51(1):25-30.

Vara D, Pula G (2014). Reactive oxygen species: physiological roles in the regulation of vascular cells. *Curr Mol Med.* 14(9):1103-25.

Velez-Pardo C, Jimenez Del Rio M, Lopera F (1998). Familial Alzheimer's disease: oxidative stress, beta-amyloid, presenilins, and cell death. *Gen Pharmacol.* 31(5):675-81.

Vignini A, Sartini D, Morganti S, Nanetti L, Luzzi S, Provinciali L, Mazzanti L, Emanuelli M (2011). Platelet amyloid precursor protein isoform expression in Alzheimer's disease: evidence for peripheral marker. *Int. J. Immunopathol. Pharmacol.* 24(2):529-34.

Violet M et al., (2014). A major role for Tau in neuronal DNA and RNA protection *in vivo* under physiological and hyperthermic conditions. *Front Cell Neurosci.* 8: 84.

Vlad SC, Miller DR, Kowall NW, Felson DT (2008). Protective effects of NSAIDs on the development of Alzheimer disease. *Neurology.* 70(19):1672-7.

Vorhees CV, Williams MT (2014). Assessing spatial learning and memory in rodents. *ILAR J.* 55(2):310-32

Wagenmakers EJ, Farrell S (2004). AIC model selection using Akaike weights. Psychon Bull Rev. 11(1):192-6.

Wang Y, Mandelkow E (2016). Tau in physiology and pathology. Nat Rev *Neurosci.* 17(1):5-21.

Wang J, Simonavicius N, Wu X, Swaminath G, Reagan J, Tian H, Ling L (2006). Kynurenic acid as a ligand for orphan G protein-coupled receptor GPR35. *J Biol Chem.* 281(31):22021-8.

Wang X, Wang W, Li L, Perry G, Lee HG, Zhu X (2014). Oxidative stress and mitochondrial dysfunction in Alzheimer's disease. *Biochim Biophys Acta.* 1842(8):1240-7.

Wang Z, Wang B, Yang L, Guo Q, Aithmitti N, Songyang Z, Zheng H (2009). Presynaptic and postsynaptic interaction of the amyloid precursor protein promotes peripheral and central synaptogenesis. *J Neurosci.* 29, 10788–10801.

Wang X, Su B, Zheng L, Perry G, Smith MA, Zhu X (2009). The role of abnormal mitochondrial dynamics in the pathogenesis of Alzheimer's disease. *J Neurochem.* 109 Suppl 1:153-9.

Ward SM, Himmelstein DS, Lancia JK, Binder LI (2012). Tau oligomers and tau toxicity in neurodegenerative disease. *Biochem Soc Trans.* 40(4):667-71.

Weingarten MD, Lockwood AH, Hwo SY, Kirschner MW (1975). A protein factor essential for microtubule assembly. *Proc Natl Acad Sci U S A.* 72(5):1858-62.

Weintraub S, Wicklund AH, Salmon DP (2012). The neuropsychological profile of Alzheimer disease. *Cold Spring Harb Perspect Med.* 2(4): a006171.

Wichers MC, Maes M (2004). The role of indoleamine 2,3-dioxygenase (IDO) in the pathophysiology of interferon-alpha-induced depression. *J Psychiatry Neurosci.* 29(1):11-7.

Williams AF, Gagnon J (1982). Neuronal cell Thy-1 glycoprotein: homology with immunoglobulin. *Science.* 216(4547):696-703.

Winton M, Lee E, Sun E, Wong M, Leight S, Zhang B, Trojanowski J, Lee V (2011) Intraneuronal APP, not free Aβ peptides in 3xTg-AD mice: implications for tau versus Aβ-mediated Alzheimer neurodegeneration. *J Neurosci.* 31:7691-7699.

Wiseman FK, Al-Janabi T, Hardy J, Karmiloff-Smith A, Nizetic D, Tybulewicz VLJ, Fisher EMC, Strydom A (2015). A genetic cause of Alzheimer disease: mechanistic insights from Down syndrome. *Nat Rev Neurosci.* 16(9): 564–574.
Wong P, Cai H, Borchelt D, Price D (2002) Genetically engineered mouse models of neurodegenerative diseases. *Nature Neurosci.* 5:633-639.

Wu W, Nicolazzo JA, Wen L, Chung R, Stankovic R, Bao SS, Lim CK, Brew BJ, Cullen KM, Guillemin GJ (2013). Expression of tryptophan 2,3-dioxygenase and production of kynurenine pathway metabolites in triple transgenic mice and human Alzheimer's disease brain. *PLoS One.* 8(4):e59749.

Wu L, Rosa-Neto P, Hsiung GY, Sadovnick AD, Masellis M, Black SE, Jia J, Gauthier S (2012). Early-onset familial Alzheimer's disease (EOFAD). *Can. J. Neurol. Sci.* 39(4):436-45.

Wyss-Coray T (2006). Inflammation in Alzheimer disease: driving force, bystander or beneficial response? *Nat Med.* 12(9):1005-15.

Xie L, Helmerhorst E, Taddei K, Plewright B, Van Bronswijk W, Martins R (2002). Alzheimer's beta-amyloid peptides compete for insulin binding to the insulin receptor. *J Neurosci.* 22(10): RC221.

Yamada A, Akimoto H, Kagawa S, Guillemin GJ, Takikawa O (2009). Proinflammatory cytokine interferon-gamma increases induction of indoleamine 2,3-dioxygenase in monocytic cells primed with amyloid beta peptide 1-42: implications for the pathogenesis of Alzheimer's disease. *J Neurochem.* 110(3):791-800.

Yamamoto M, Kiyota T, Horiba M, Buescher JL, Walsh SM, Gendelman HE, Ikezu T (2007). Interferon-gamma and tumor necrosis factor-alpha regulate amyloid-beta plaque deposition and beta-secretase expression in Swedish mutant APP transgenic mice. *Am J Pathol.* 170(2):680-92.

Yasui H, Takai K, Yoshida R, Hayaishi O (1986). Interferon enhances tryptophan metabolism by inducing pulmonary indoleamine 2,3-dioxygenase: its possible occurrence in cancer patients. *Proc Natl Acad Sci U S A*. 83:6622–6.

Yasuno F, Imamura T, Hirono N, Ishii K, Sasaki M, Ikejiri Y, Hashimoto M, Shimomura T, Ya- mashita H, Mori E (1998). Age at onset and regional cerebral glucose metabolism in Alzheimer's disease. *Dement Geriatr Cogn Disord.* 9: 63-67.

Yu D, Tao BB, Yang YY, Du LS, Yang SS, He XJ, Zhu YW, Yan JK, Yang Q (2015). The IDO inhibitor coptisine ameliorates cognitive impairment in a mouse model of Alzheimer's disease. *J Alzheimers Dis.* 43(1):291-302.

Zhang Y, McLaughlin R, Goodyer C, LeBlanc A (2002). Selective cytotoxicity of intracellular amyloid beta peptide1-42 through p53 and Bax in cultured primary human neurons. *J Cell Biol.* 156(3): 519-29.

Zhou R, Tardivel A, Thorens B, Choi I, Tschopp J (2010). Thioredoxin-interacting protein links oxidative stress to inflammasome activation. Nat Immunol. 11(2):136-40.

APPENDIX A – TABLES

Table 1. Nine 3xTg-AD and 15 WT control mice were used in the PK study. 22 mice received DWG-1036 at a dose of 80mg/kg with an injection volume of 0.01ml/g, via oral gavage and sacrificed at 0.25, 0.5, 1, 4, 8, or 12 hours after treatment for brain tissue and plasma analyses. Two additional mice were treated with the vehicle and sacrificed 0.5 hours after as negative controls. BQL stands for below quantifiable levels.

Mouse #	Sex	Genotype	Sacrifice Time	Plasma (mg)	Brain (mg)
3461	f	tg	0.25	13204.1	53500
3469	f	wt	0.25	6089.7	22149
3470	f	wt	0.25	9665.1	64389.5
3471	f	wt	0.25	13077.8	59704.5
3487	f	wt	0.5	9882.1	75671
3488	f	wt	0.5	12027	56795.5
3489	f	wt	0.5	10714.4	76791.5
3525	m	tg	1	7411	22263.5
3526	m	tg	1	9946.6	49616.5
3544	m	wt	1	12610.7	64053.5
3548	f	wt	2	7385.9	36582
3550	f	wt	2	4102.2	16696.5
3527	m	tg	2	8731.2	38296.5
3551	f	wt	4	3252.6	12105
3528	m	tg	4	1755.3	5495.5
3539	f	wt	8	20.7	115.5
3540	f	wt	8	19.6	116.5
3541	f	wt	8	20.1	113
3454	m	tg	12	BQL	BQL
3547	f	wt	12	BQL	BQL
3455	m	tg	12	BQL	BQL
3451 (control)	m	tg	0.5	0	0
3453 (control)	m	tg	0.5	0	0

Table 2. Two 3xTg-AD and 8 WT mice were used in the tolerability study.

Mouse #	Dosage (mg/kg)	sex	genotype
3482	Control (H2O)	m	wt
3483	Control (H2O)	m	wt
3492	DWG-1036 (30)	m	wt
3493	DWG-1036 (30)	m	wt
3459	DWG-1036 (60)	m	tg
3460	DWG-1036 (60)	m	tg
3480	DWG-1036 (80)	m	wt
3481	DWG-1036 (80)	m	wt
3542	DWG-1036 (80 x 2)	f	wt
3543	DWG-1036 (80 x 2)	f	wt

Table 3. A total of 21 transgenic (3xTg-AD, JAX #34830) and 53 WT control (129C57BL/6) mice were treated either with DWG-1036 or the vehicle for 4 months to be used in the behavioural and neurochemical tests.

Genotype / Treatment	DWG-1036	Distilled water (vehicle)
3xTg-AD	10 female 6 male	5 female 0 male
129C57BL/6	19 female 13 male	11 female 10 male

APPENDIX B – FIGURES

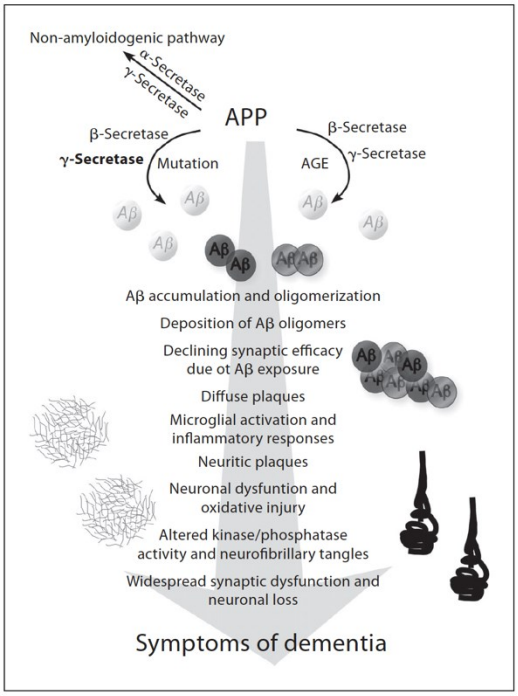

Figure 1. Aβ is formed when APP is cleaved by β and ɣ secratases. It accumulates in the extra cellular space and acts as a neuromodulater. This causes the hyper-phosphorylation of tau protein as well as oxidative stress and immune reactivity. AB_{42} may also stimulate the neuron and cause excito-toxicity. (Figure taken from Herrup, 2012, p.34, Figure 1).

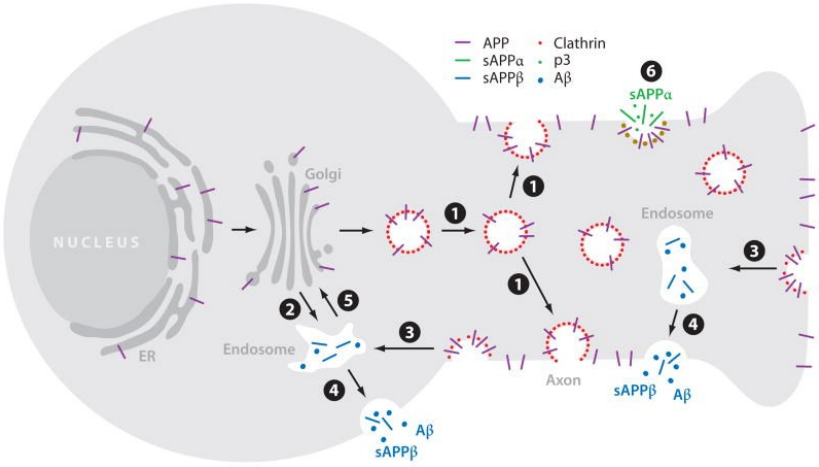

Figure 2. APP is synthesized in the Golgi apparatus and carried to the axon terminals with fast axonal transport (1), and very rapidly metabolized with different pathways. Cleavage by α and ɣ secretaries occurs on the cell surface (6). APP may also be taken back into the cell with endosomes (3) which are carried to the Golgi apparatus and lysosomes (5) and get cleaved by β and ɣ secratases. Residues, including Aβ, are then carried to the extra cellular space with endosomes (2, 4). (Figure taken from O'Brien and Wong, 2011, p. 22, Figure 3).

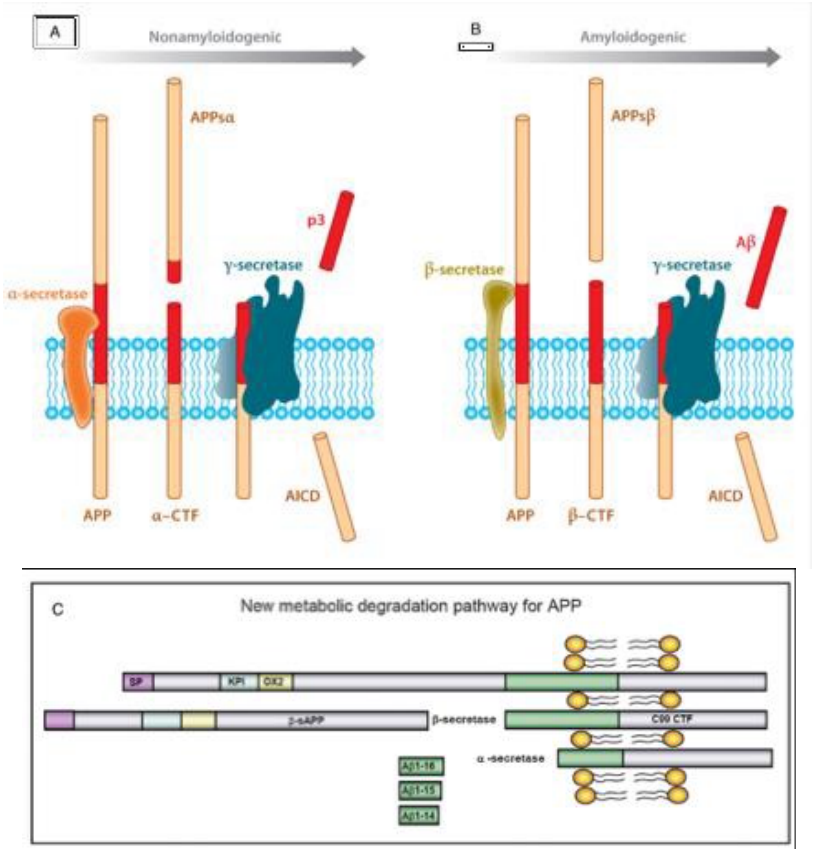

Figure 3. Non-amyloid pathway involves α and ɣ secretases at the cell membrane. First, α-secretase cuts the protein within the amyloid sequence, releasing the ectodomaine, later ɣ-secretase cleaves at the trans- membrane part of the protein. APP may also be endocytosed and taken to the Golgi apparatus and lysosomes respectively, where it is cleaved by β-secretase at the N-terminus and ɣ-secretase at the trans-membrane domain. A third cleavage pathway involves the α and β secretases. This pathway produces Aβ fragments 15-16 amino acids in length. (Figures A-B taken from O'Brien and Wong, 2011 p.21, Figure 2; C is taken from Portelius et al., 2011, p.1096, Figure 7).

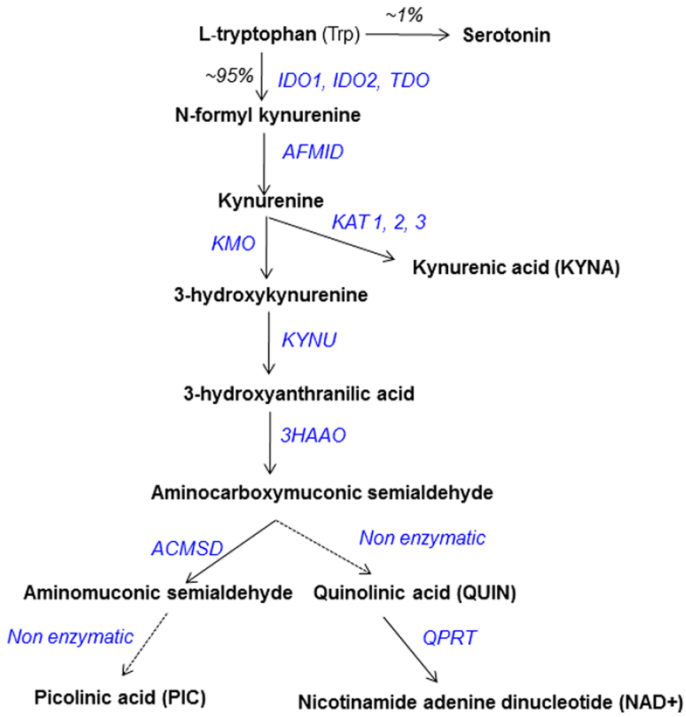

Figure 4. The kynurenine pathway. 95% of tryptophan is degraded into NAD with this pathway. IDO1 is the first and rate limiting enzyme, which was targeted in our study with the inhibitor DWG-1036. While kynurenic acid is neuroprotective, 3-hydroxykynurenine and quinolinic acid have toxic effects.

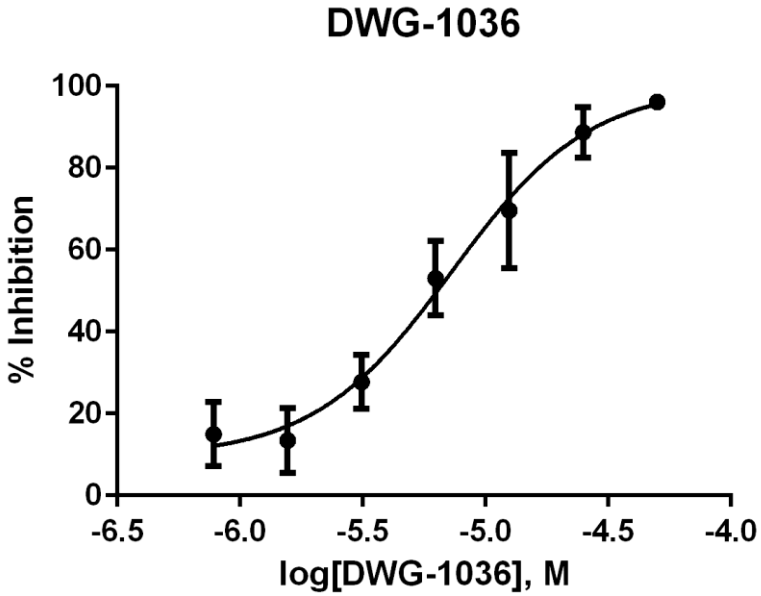

Figure 5. IC-50 value of DWG-1036 was calculated as 7µm in a cell based assay. The *in-vivo* value was 80µm. IC-50 is a measure for enzymatic inhibition and reflects how much compound is needed to cut 50% percent of the targeted enzyme activity.

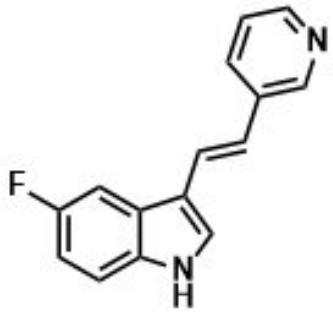

Figure 6. Molecular shape of DWG-1036. The chemical formula of the compound is $C_{15}H_{11}FN_2$ and the molecular weight is 238.265 g/mol.

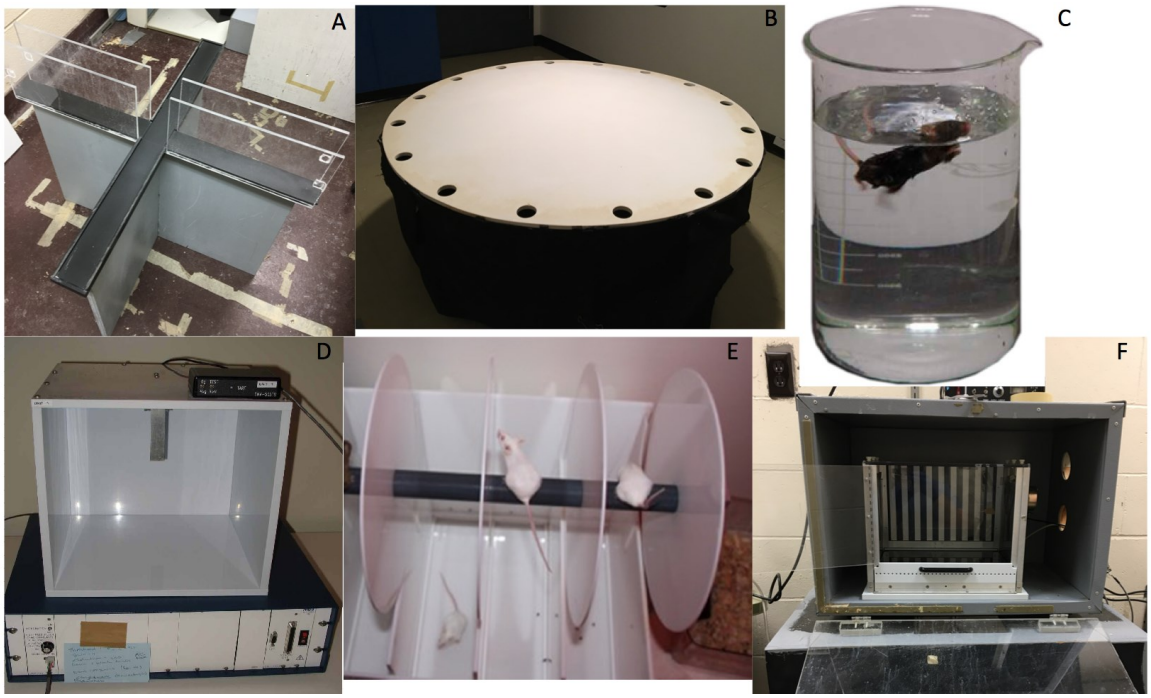

Figure 7. Behavioural tests used in this study. 7A: The elevated plus maze was used to measure anxiety and locomotor activity. 7B: The Barnes maze was used to measure spatial learning and memory. 7C: The forced swim test and the tail suspension test (7D) measured depressive-like behaviour. 7E: The Rotarod measured motor learning and coordination. 7F: The trace fear conditioning measured working memory.

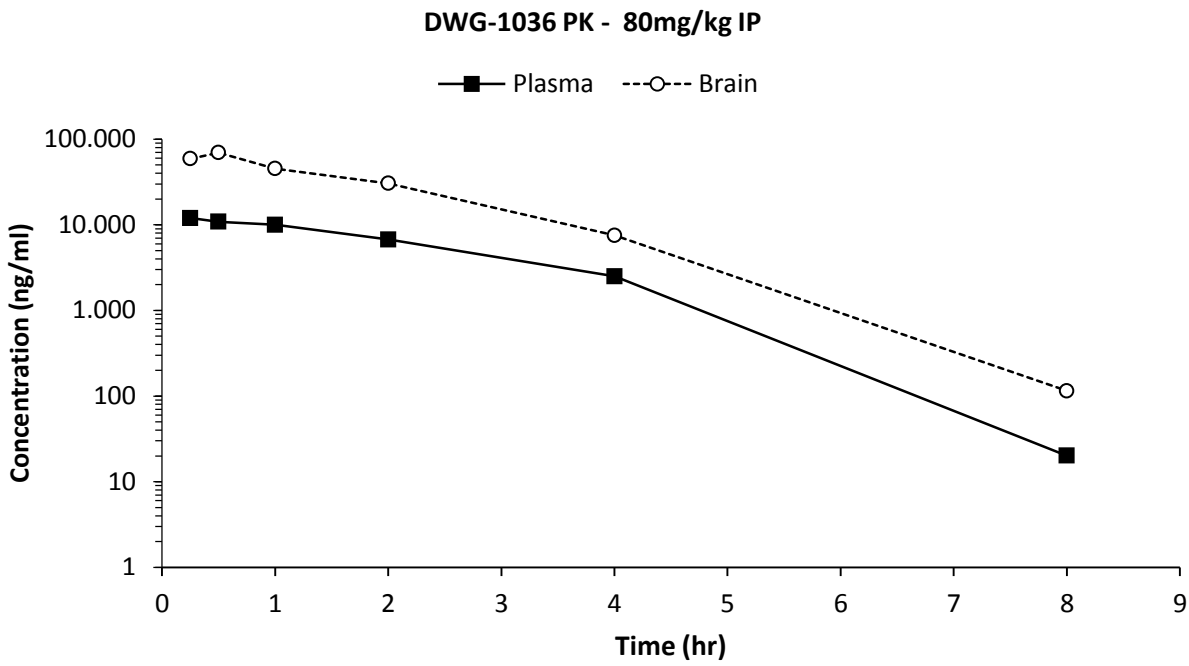

Figure 8. Results of the pharmacokinetics study showed that DWG-1036 is cleared from the brains of male and female 3xTg-AD and WT mice at statistically similar rates. DWG-1036 was at detectable levels (mean = 59,198 ng/ml) in the brain 15 minutes after administration and reached the highest levels after 30 minutes (mean = 69,753). The half-life of DWG-1036 was calculated as 1.24 hours and it was no longer detectable 12 hours after treatment.

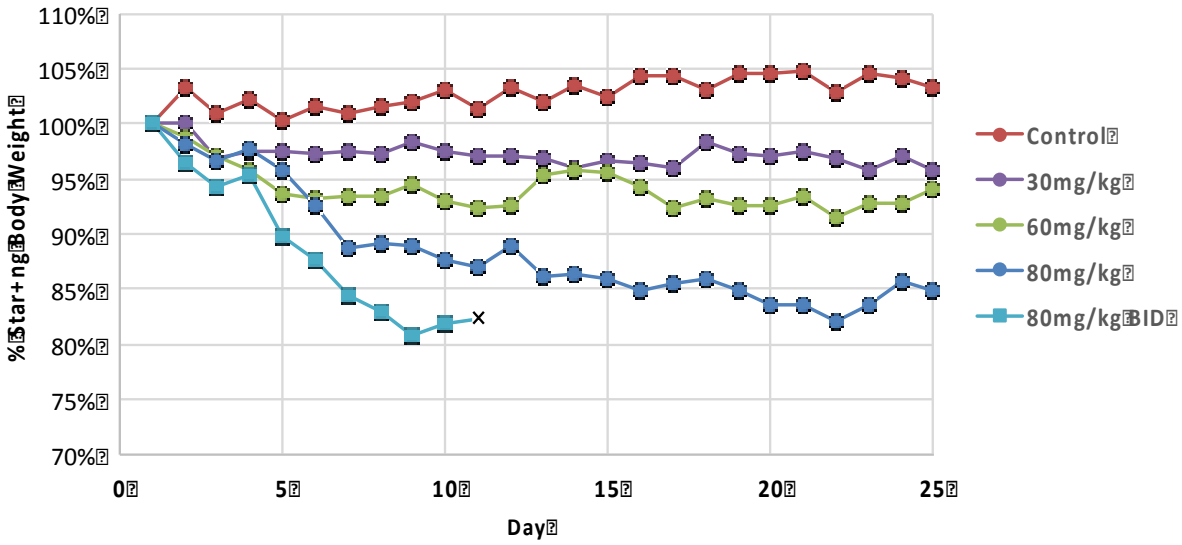

Figure 9. According to the 25-day tolerability study, there was a main effect of dose ($F(3, 99) = 33.699$, $p = 0.003$) on the body weights of the DWG-1036 treated mice, as the subjects receiving higher doses lost more weight. BID stands for treatment twice a day.

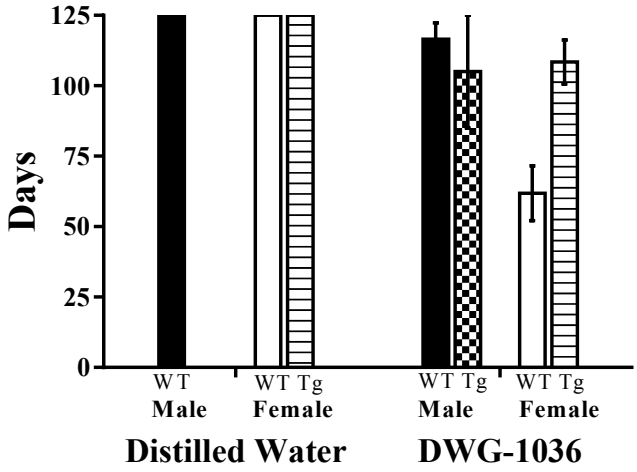

Figure 10. Mean (±SEM) number of days mice from different treatment, genotype, and sex groups survived during DWG-106 or vehicle treatment. A total of 22 mice died during treatment or removed from the study for weight loss. 4 of them were female 3xTg-AD mice receiving DWG-106, 14 of them were female WT mice receiving DWG-106, 1 of them was a female WT mouse, receiving vehicle, 2 of them were male 3xTg-AD mice receiving DWG-106, and 1 of them was a male WT mouse receiving the vehicle.

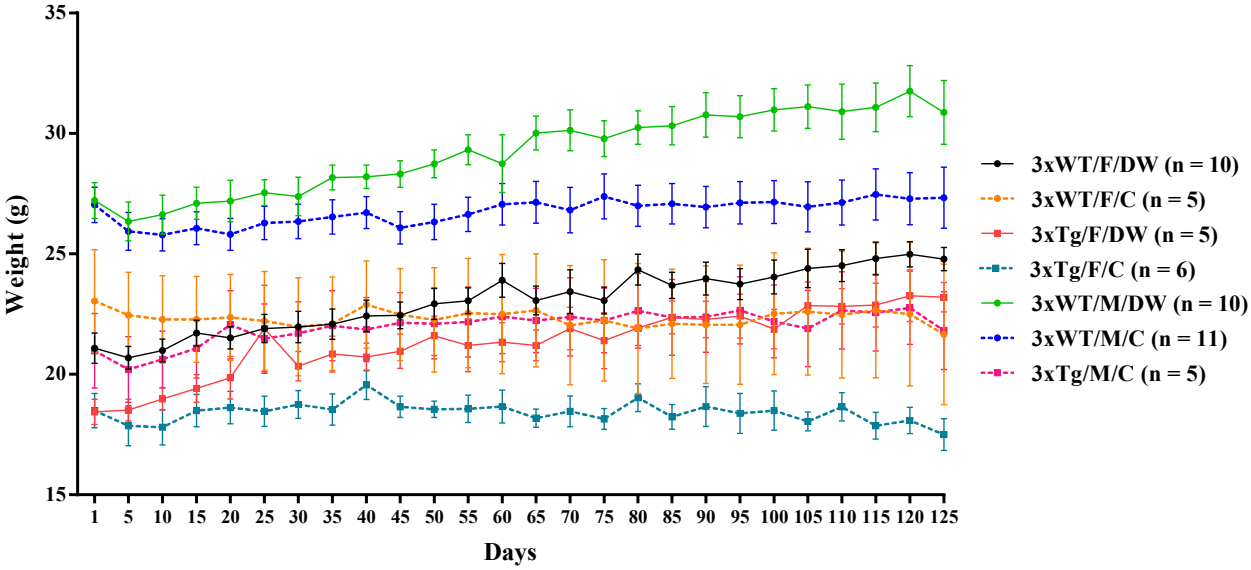

Figure 11. Mean (±SEM) weights of the mice during the 4-month treatment. Male WT mice receiving the vehicle were larger than all the other mice, and female 3xTg-AD mice receiving DWG-106 were the smallest. Other groups ranked in between in the order of male-Tg-DWG-106 > female-WT-vehicle > female-WT-DWG-106 > male-Tg-DWG-106 > female-Tg-vehicle.

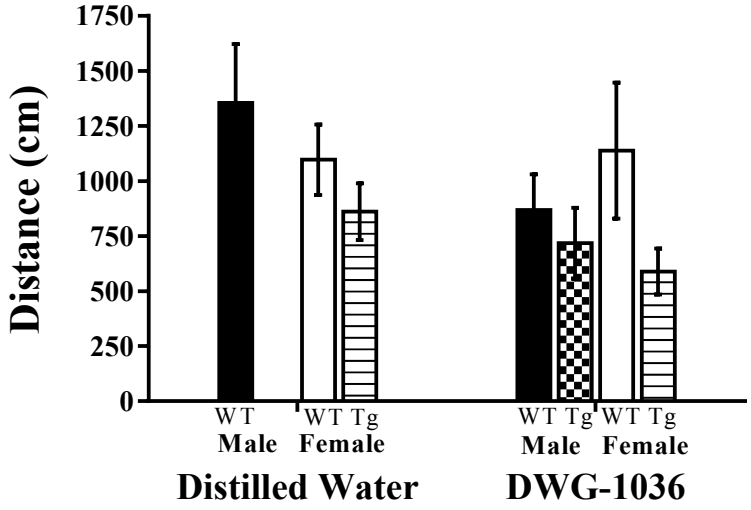

Figure 12. Mean (±SEM) distance moved by the mice on the elevated plus maze. Although there were no significant differences between the groups, there was a trend of WT mice moving more compared to the 3xTg-AD mice (CI 95% = -42.840, 647.754).

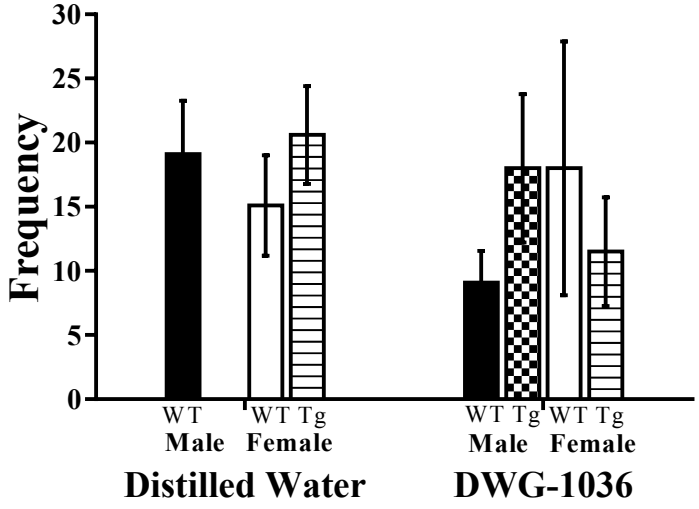

Figure 13. Mean (±SEM) frequency of open arm visits in the elevated plus maze. There were no significant differences between the groups yet there was a trend of WT female mice visiting the open arms more frequently compared to the WT male mice, while the opposite was true for the 3xTg-AD mice (CI 95% = -35.391, 4.573).

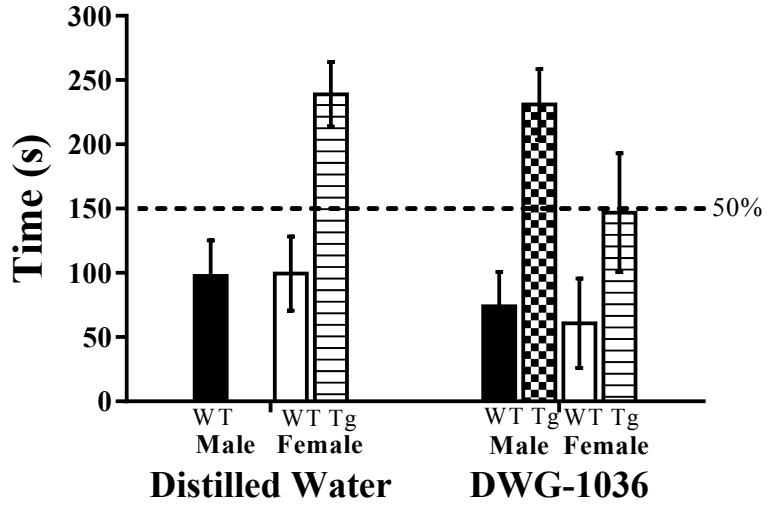

Figure 14. Mean (±SEM) duration of time spent in the open arms of the elevated plus maze. 3xTg-AD mice spent more time in the OA's, compared to the WT mice (CI 95% = -188.031, -79.689). There was also a trend of vehicle treated mice spending more time on the OA's compared to the DWG-106 treated mice (CI 95% = -9.337, 93.229).

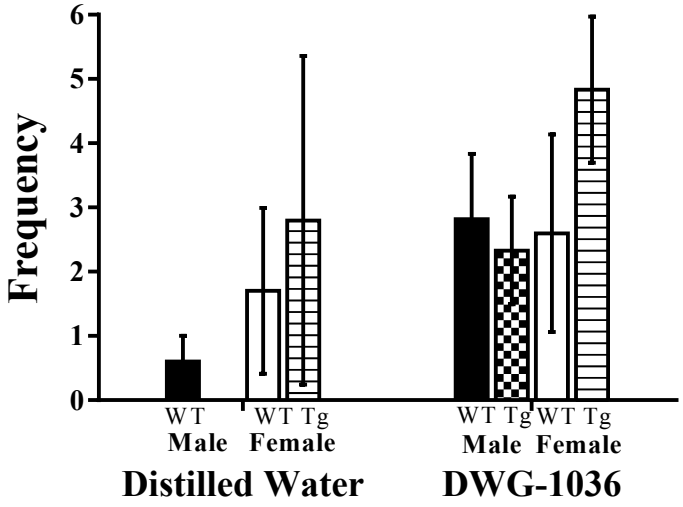

Figure 15. Mean (±SEM) freezing frequency of the mice in the elevated plus maze. There were no significant differences between the groups, but there was a trend of DWG-106 treated mice freezing more frequently then vehicle treated controls (CI 95% = -3.621, 0.275).

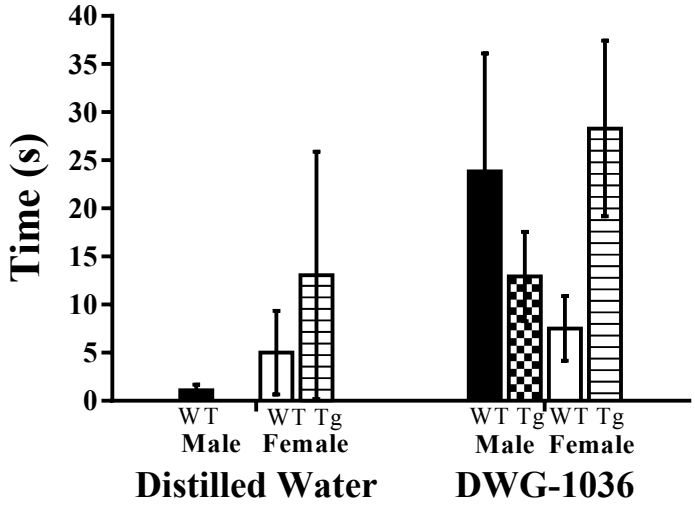

Figure 16. Mean (±SEM) freezing duration of the mice in the elevated plus maze. DWG-106 treated mice froze longer than water treated controls (CI 95% = -27.615, 0.064). There was also a trend of WT female mice freezing less than 3xTg-AD mice, but there was no such difference for the male mice (CI 95% = -5.260, 68.663).

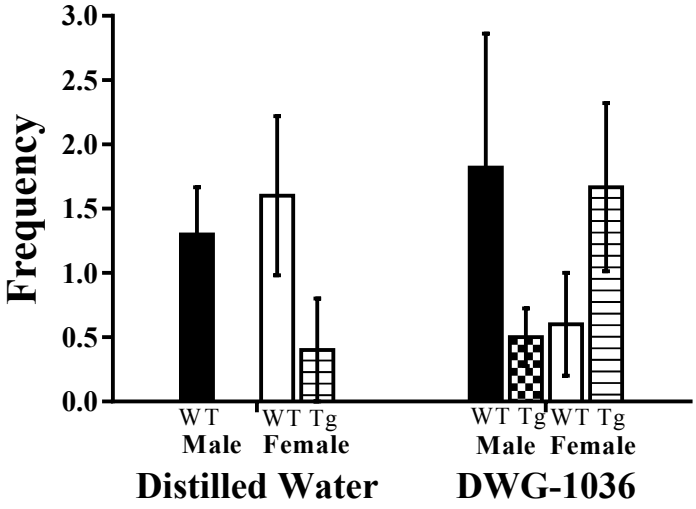

Figure 17. Mean (±SEM) stretch attend posture frequency of the mice in the elevated plus maze. There were no differences between the groups.

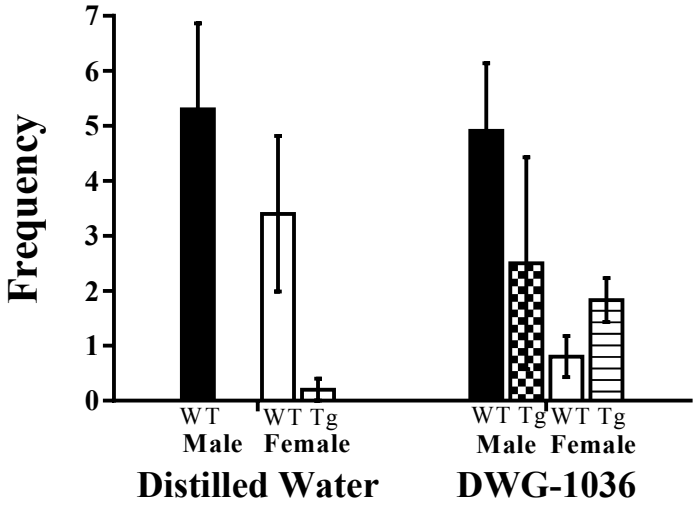

Figure 18. Mean (±SEM) rearing frequency of the mice in the elevated plus maze. Male mice reared more than the female mice (CI 95% = 0.126, 4.624).

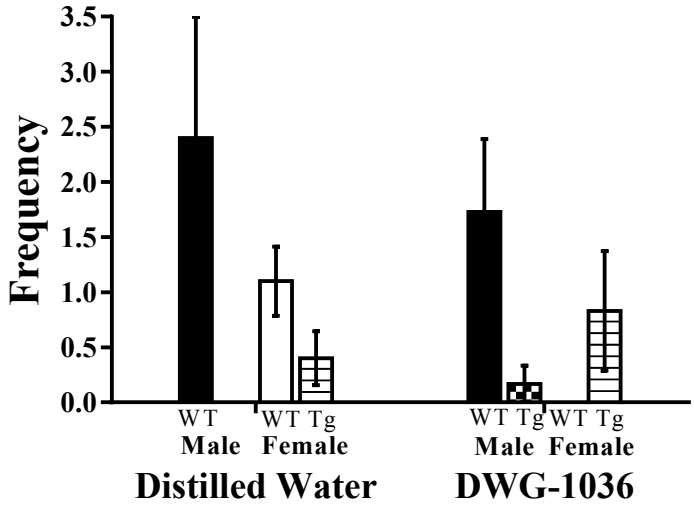

Figure 19. Mean (±SEM) grooming frequency of the mice in the elevated plus maze. There was no difference between the groups.

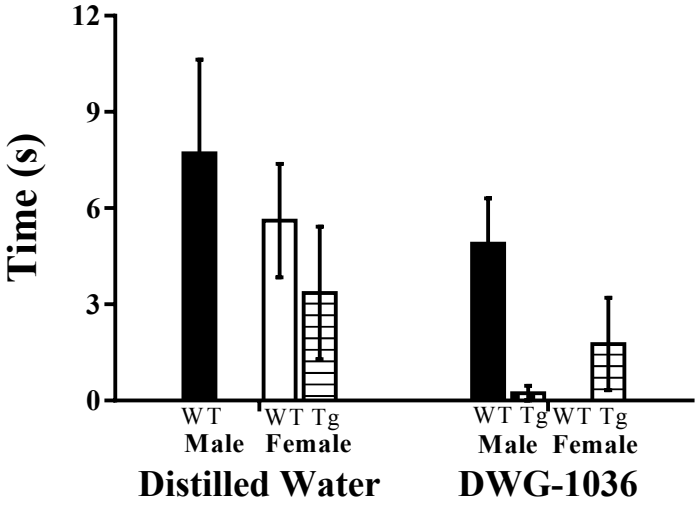

Figure 20. Mean (±SEM) grooming duration of the mice in the elevated plus maze. The distilled water treated mice groomed more than the DWG-106 treated mice (CI 95% = 0.333, 6.853).

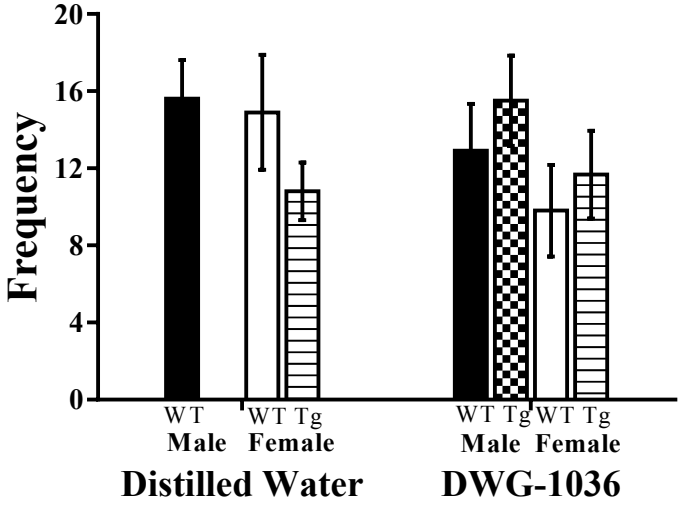

Figure 21. Mean (±SEM) head dip frequency of the mice in th elevated plus maze. There were no differences between the groups.

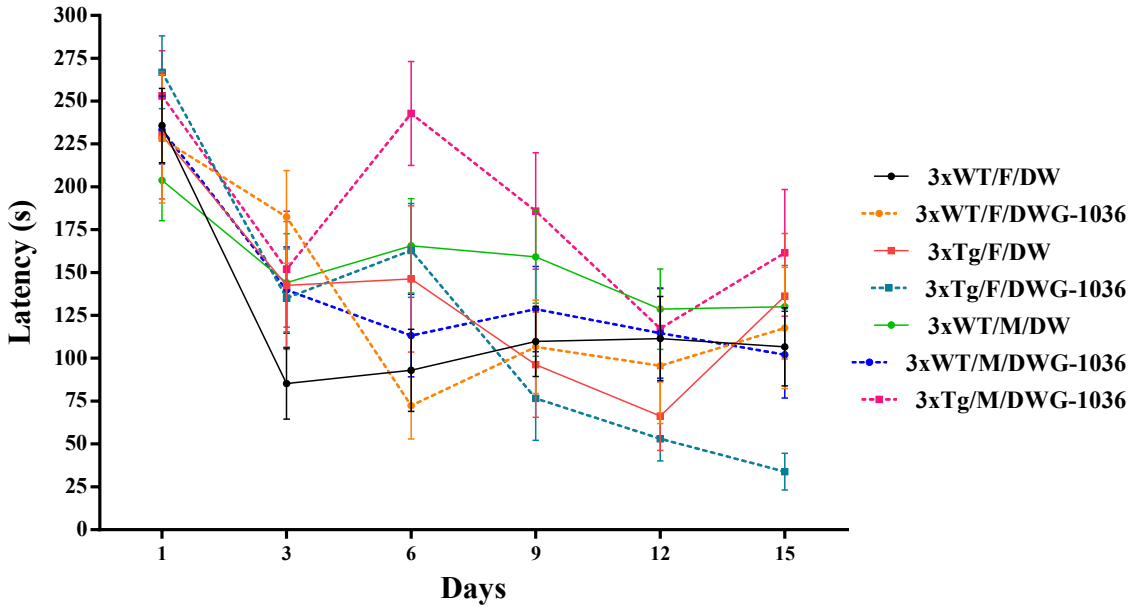

Figure 22. Mean (±SEM) latency of the mice to locate the escape hole in the Barnes maze acquisition trial. All mice got faster at locating the correct hole over the 15-day period (CI 95% = -6.876, -5.060) with females improving more than the males (95% CI = 0.975, 4.832). The DWG-106 treated mice improved more over time compared to the vehicle treated mice (95% CI = 1.008, 4.832) and the 3xTg-AD mice improved more than the WT mice (95% CI = 0.121, 4.337).

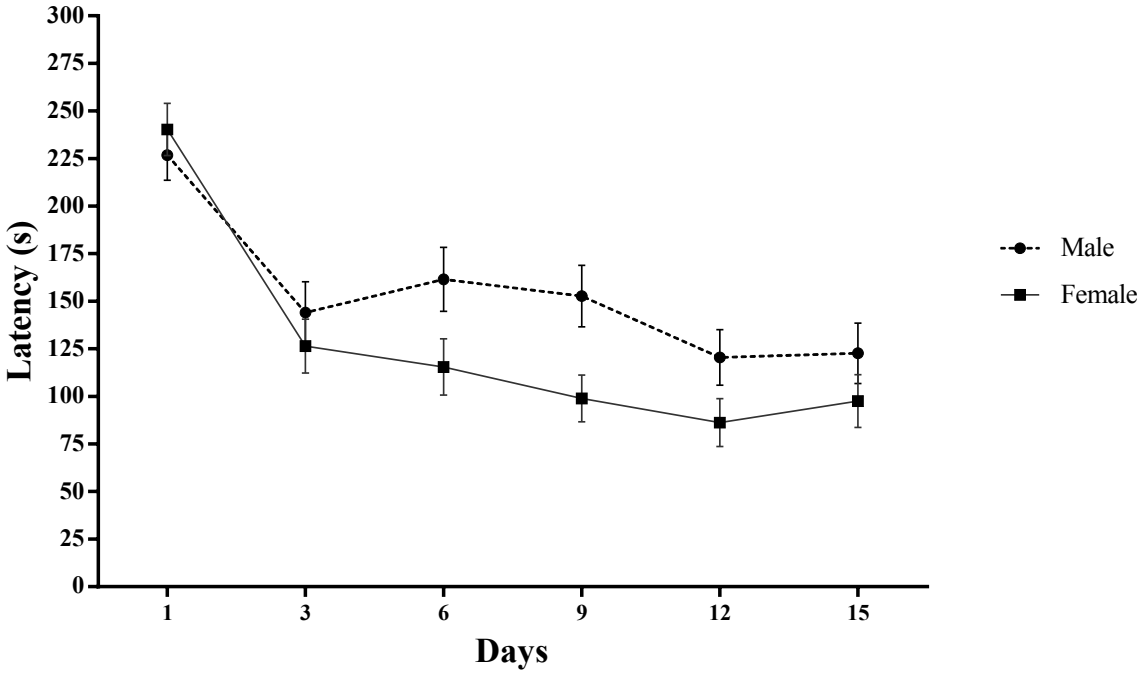

Figure 23. Mean (±SEM) latency of the male and female mice to locate the escape hole in the Barnes maze acquisition trial. Females improved more than the males over the 15-day period (95% CI = 0.975, 4.832).

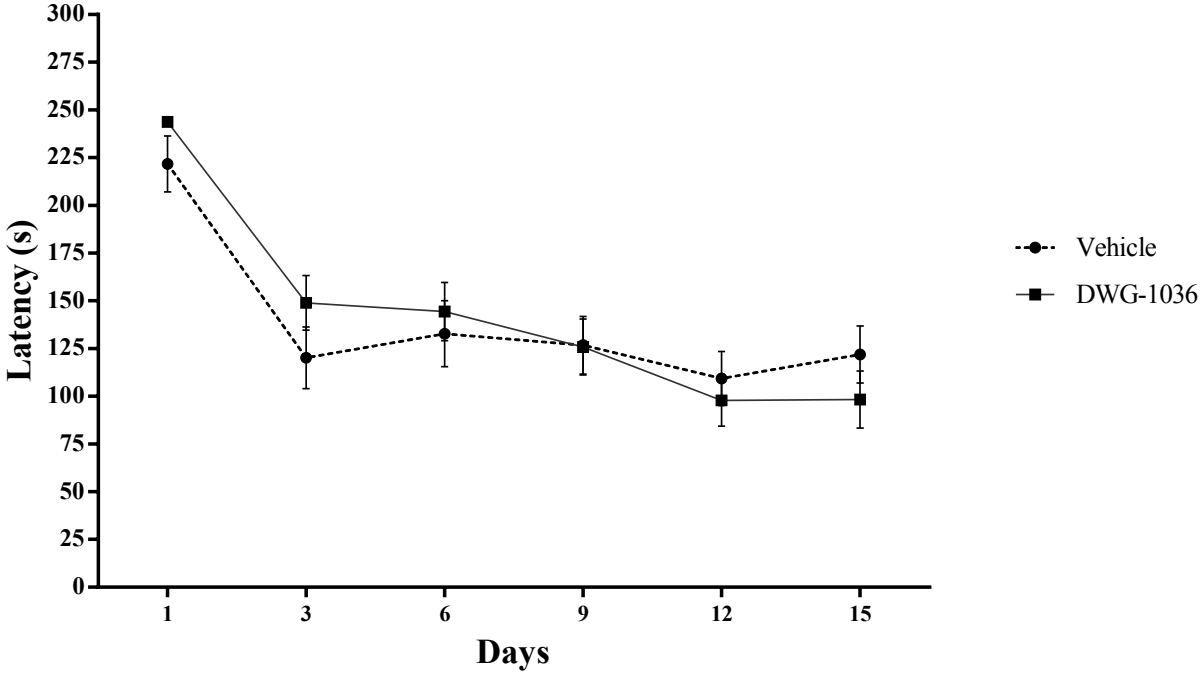

Figure 24. Mean (±SEM) latency of the mice to locate the escape hole in the Barnes maze acquisition trial. The DWG-106 treated mice improved more over time compared to the vehicle treated mice (95% CI = 1.008, 4.832).

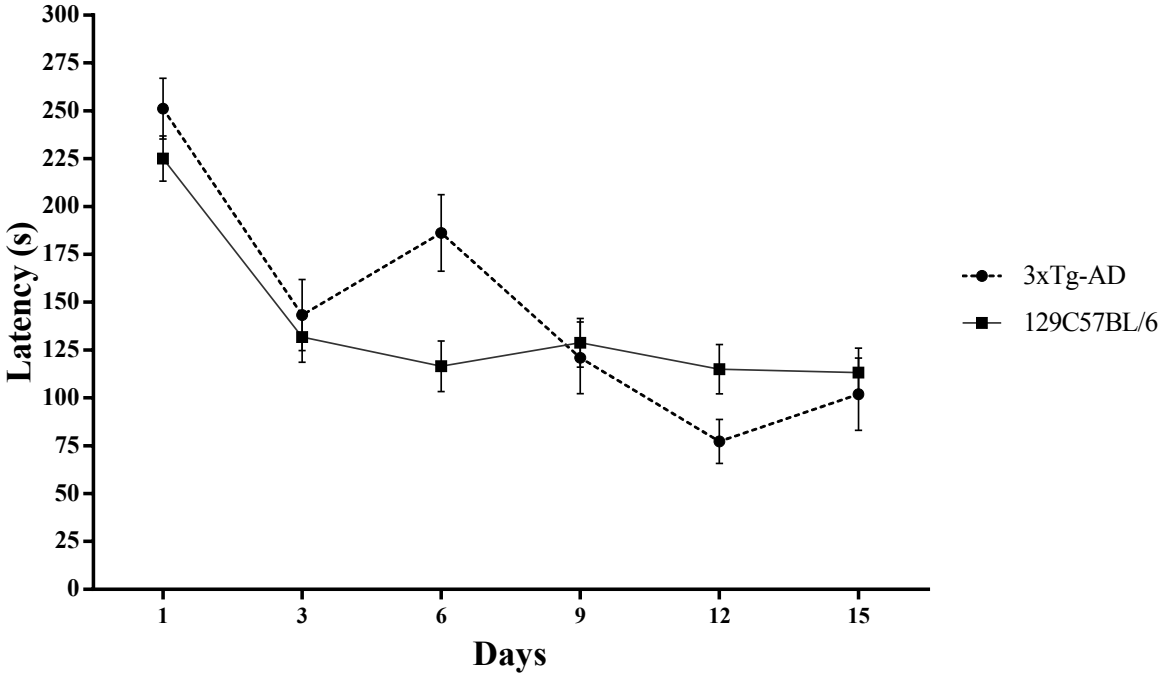

Figure 25. Mean (±SEM) latency of the mice to locate the escape hole in the Barnes maze acquisition trial. The 3xTg-AD mice improved more than the WT mice (95% CI = 0.121, 4.337).

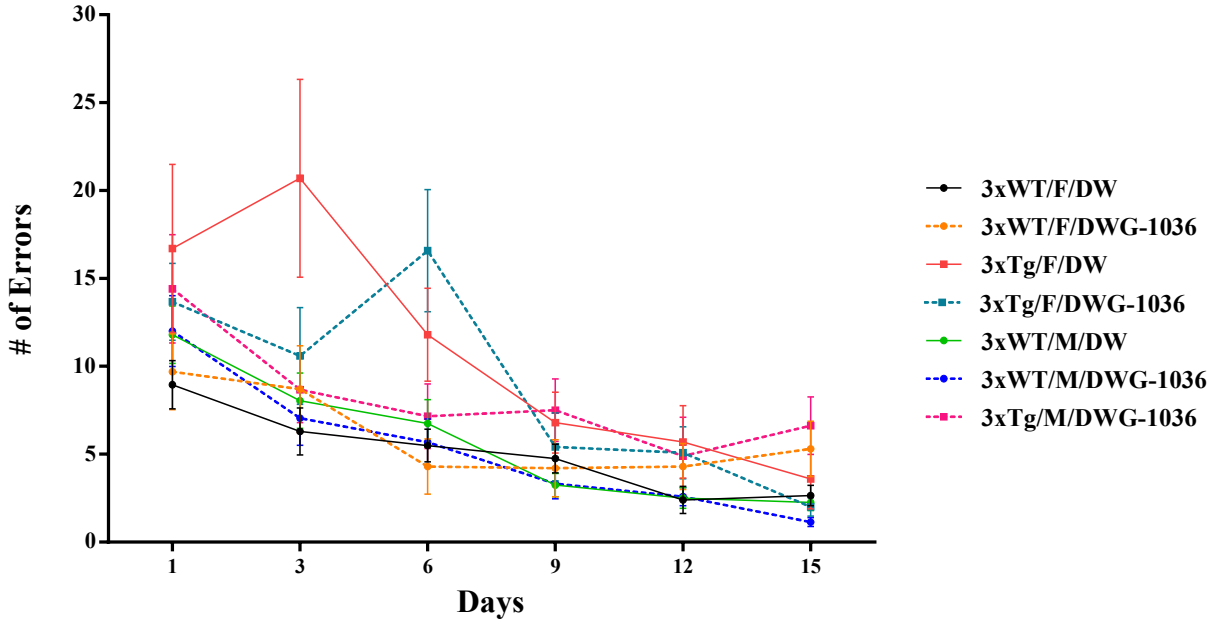

Figure 26. Mean (±SEM) number of wrong head dips over the 15-day period of BM acquisition trial. The number of errors decreased more for the 3xTgAD mice over the 15 days compared to the WT controls (95% CI = 0.038, 0.376). The DWG-106 treated WT mice improved more than the other groups (95% CI = 0.018, 0.861).

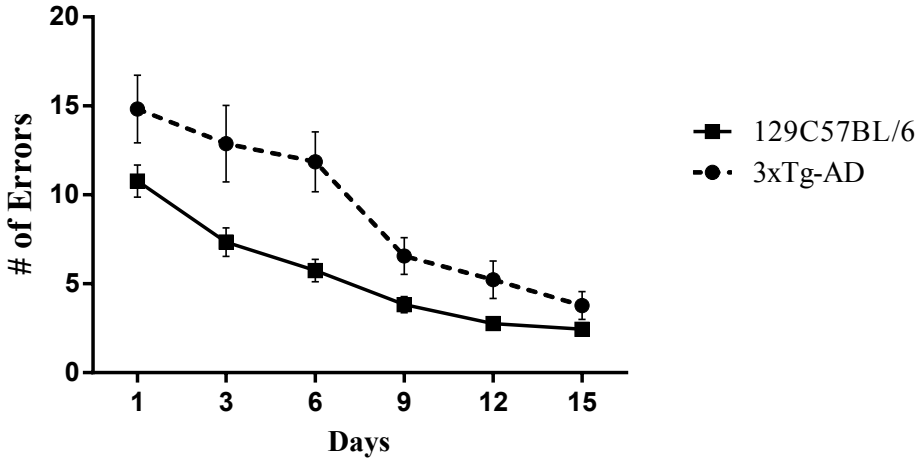

Figure 27. Mean (±SEM) number of wrong head dips over the 15-day period of BM acquisition trial. The number of errors decreased more for the 3xTgAD mice over the 15 days compared to the WT controls (95% CI = 0.038, 0.376).

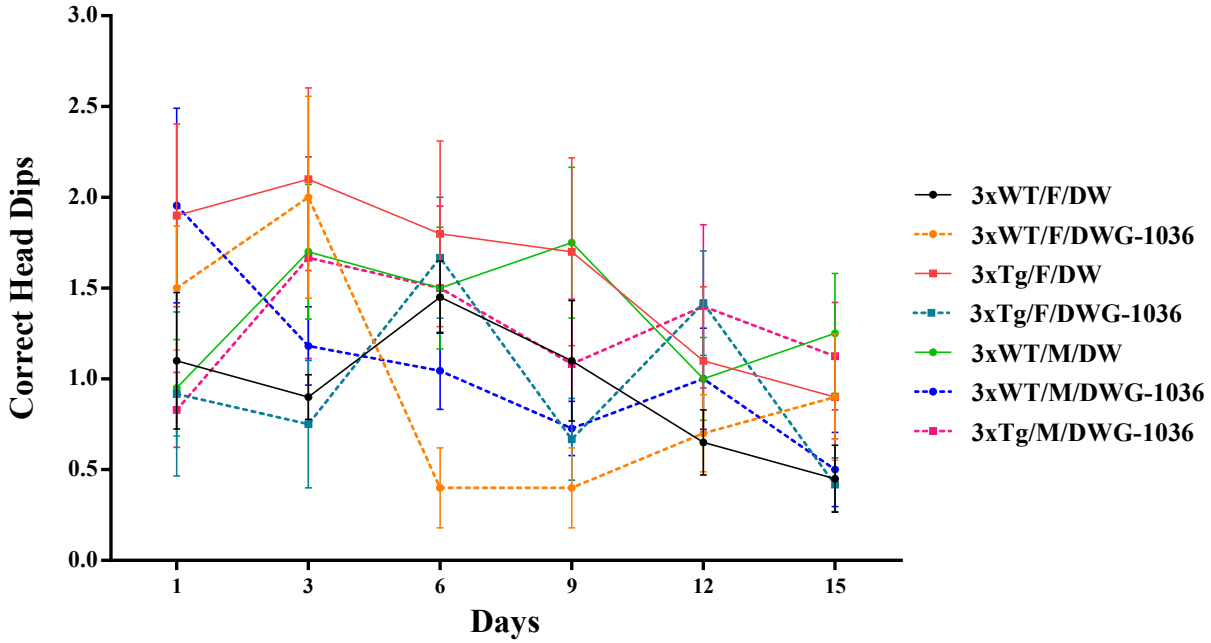

Figure 28. Mean (±SEM) number of correct head dips over the 15-day period of BM acquisition trial. All mice deceased their number of head dips into the correct hole over the 15-day period (95% CI = -0.070, -0.045) and the greatest change was in the 3xTg-AD mice receiving DWG-106 (95% CI = 0.012, 0.163).

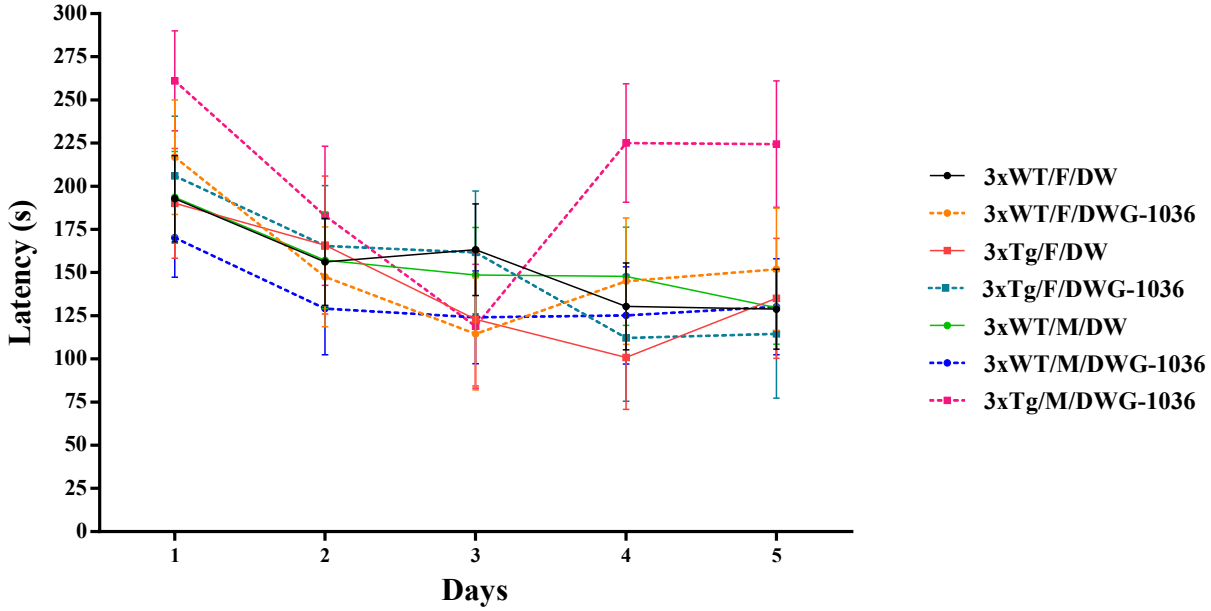

Figure 29. Mean (±SEM) latency of the mice to locate the escape hole in the Barnes maze reversal acquisition trial. All mice got faster over the 5-day period (95% CI = -17.736, -9.570).

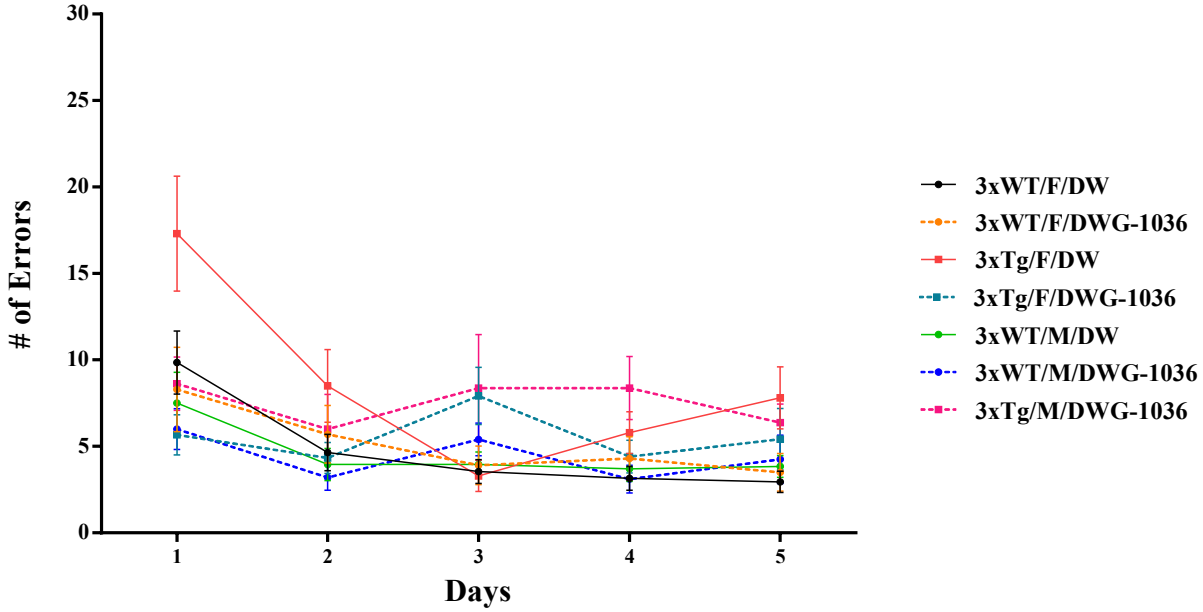

Figure 30. Mean (±SEM) number of wrong head dips over the 5-day period of BM reversal acquisition trial. All mice improved over the 5-day period (95% CI = -1.176, -0.580) and the WT mice made less errors compared to the 3xTg-AD mice (95% CI = -4.270, -0.840). There was also a treatment by day interaction as the vehicle treated mice improved more (95% CI = -1.437, -0.199).

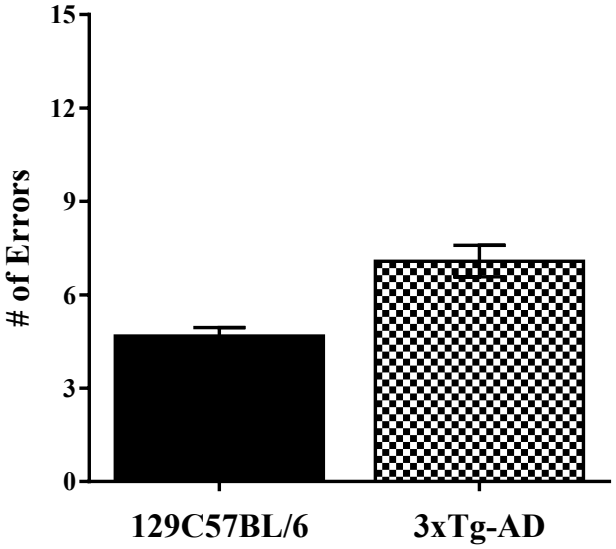

Figure 31. Mean (±SEM) number of wrong head dips over the 5-day period of BM reversal acquisition trial. The WT mice made less errors compared to the 3xTg-AD mice (95% CI = -4.270, -0.840).

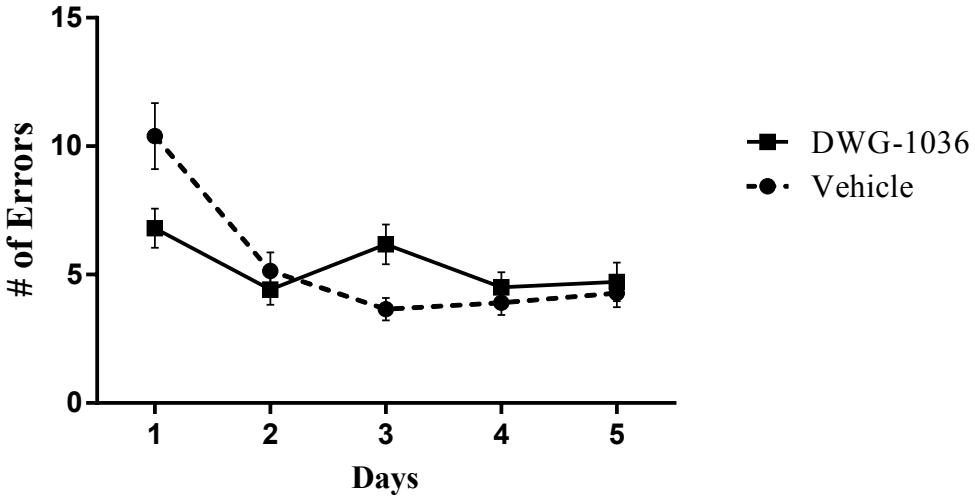

Figure 32. Mean (±SEM) number of wrong head dips over the 5-day period of BM reversal acquisition trial. Vehicle treated mice improved more compared to the DWG-1036 treated ones (95% CI = -1.437, -0.199).

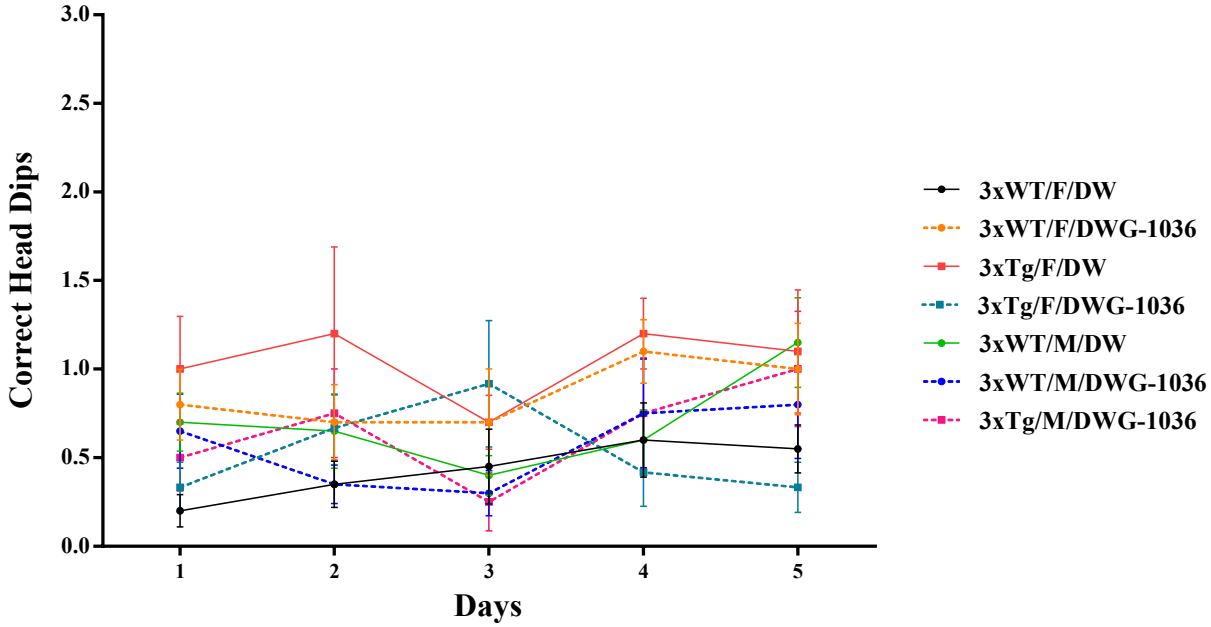

Figure 33. Mean (±SEM) number of correct head dips over the 5-day period of BM reversal acquisition trial. The WT mice treated with DWG-106 did more correct head dips compared to the WT mice treated with vehicle but the 3xTg-AD mice treated with DWG-106 did less correct head dips compared to the 3xTg-AD mice treated with vehicle (95% CI = -1.800, -0.074).

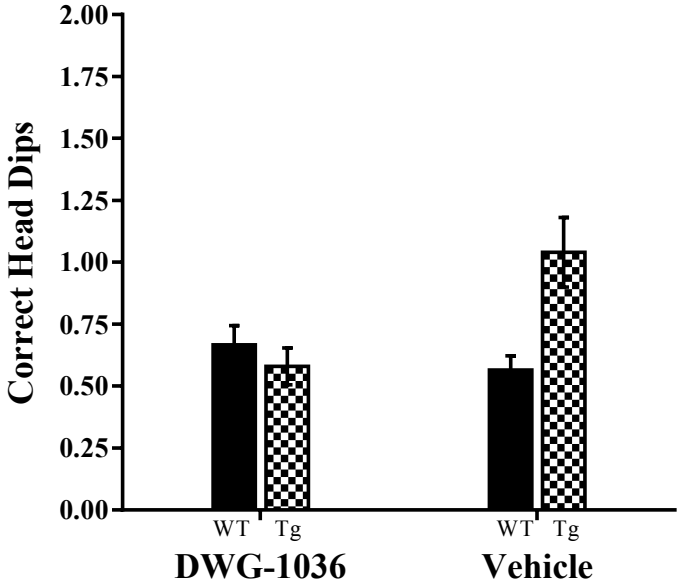

Figure 34. Mean (±SEM) number of correct head dips over the 5-day period of BM reversal acquisition trial. The WT mice treated with DWG-106 did more correct head dips compared to the WT mice treated with vehicle but the 3xTg-AD mice treated with DWG-106 did less correct head dips compared to the 3xTg-AD mice treated with vehicle (95% CI = -1.800, -0.074).

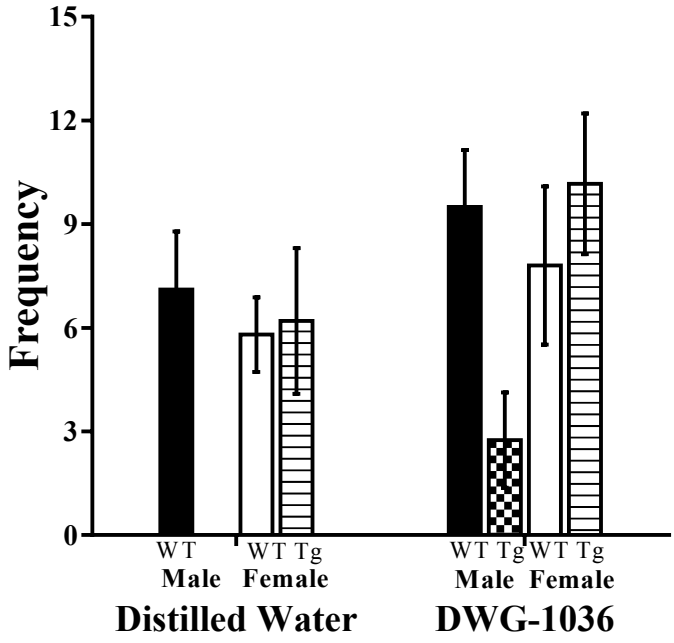

Figure 35. Mean (±SEM) frequency of correct hole visits in the probe trial of Barnes maze. Male 3xTg-AD mice visited the correct hole less than the other groups (95% CI = 1.108, 17.125).

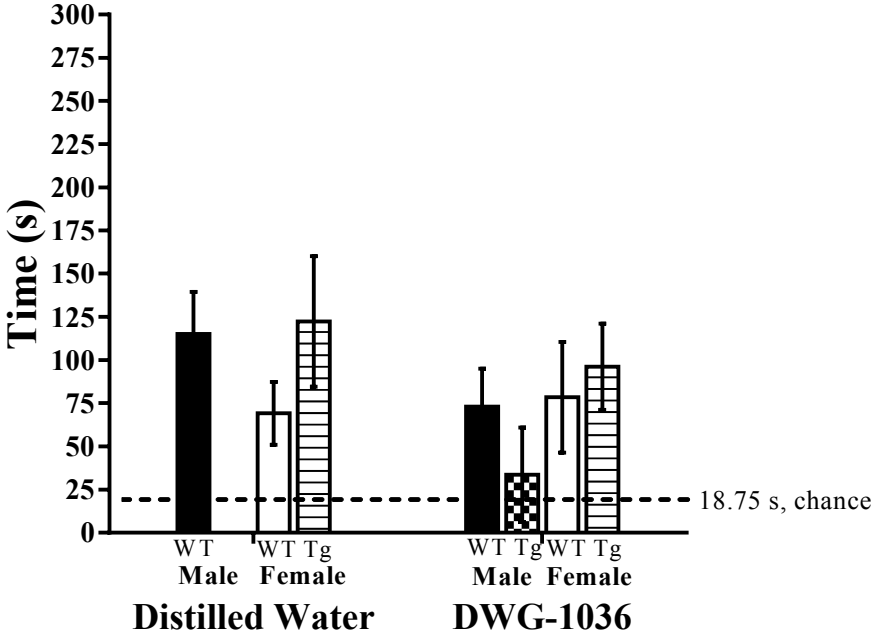

Figure 36. Mean (±SEM) duration of time spent by the correct hole in the probe trial of Barnes maze. There were no differences between the groups.

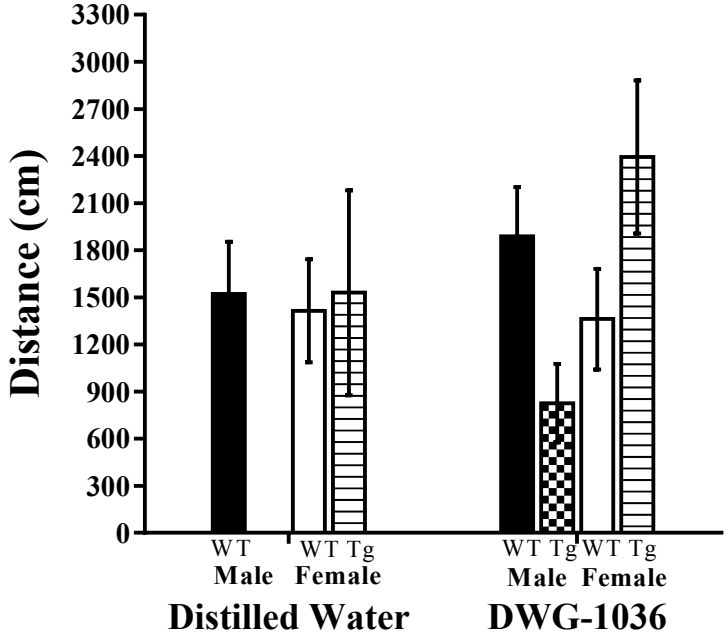

Figure 37. Mean (±SEM) distance moved by the mice in the probe trial of Barnes maze. The female 3xTg-AD mice moved more compared to the male 3xTg-AD mice but the female WT mice moved less than the male WT mice (95% CI = 308.229, 3876.784).

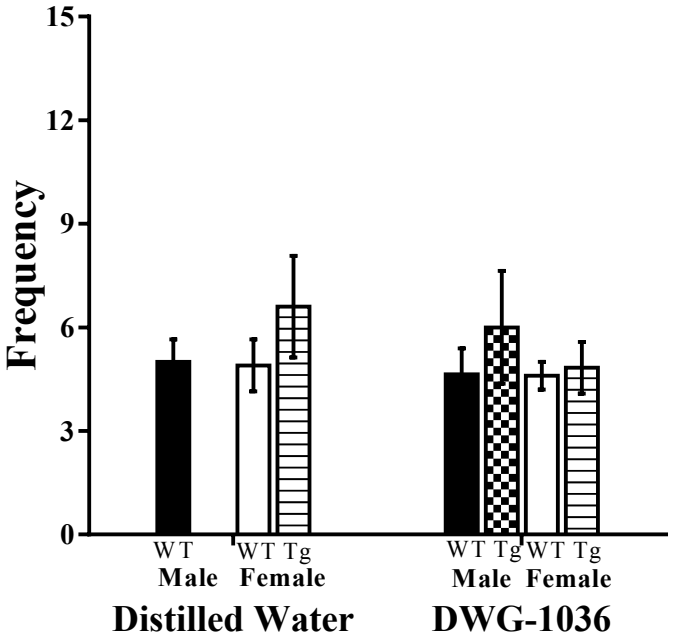

Figure 38. Mean (±SEM) frequency of correct hole visits in the curtain probe trial of Barnes maze. All groups visited the correct hole similar number of times.

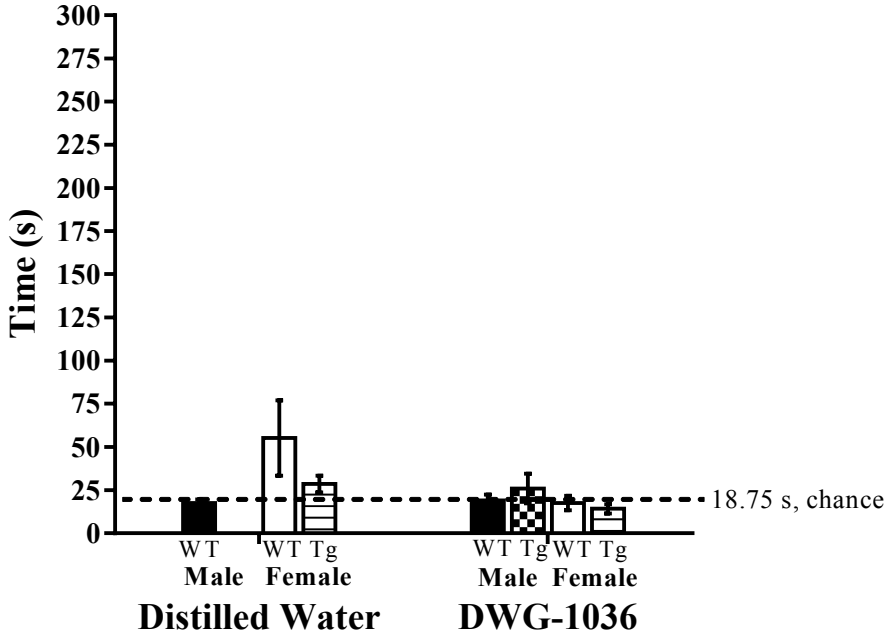

Figure 39. Mean (±SEM) duration of time spent by the correct hole in the curtain probe trial of the Barnes maze. There was no difference between the groups.

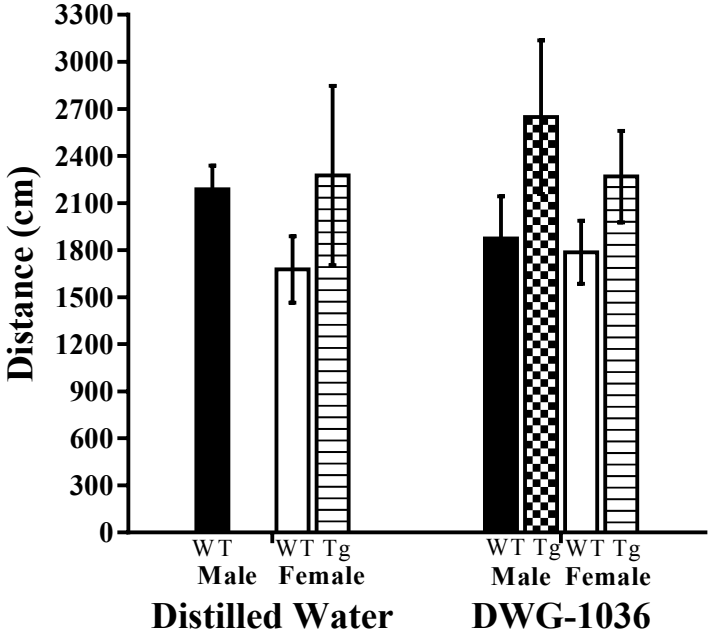

Figure 40. Mean (±SEM) distance moved by the mice in the curtain probe trial of Barnes maze. The 3xTg-AD mice moved more than the WT mice (95% CI = -1124.428, -104.094).

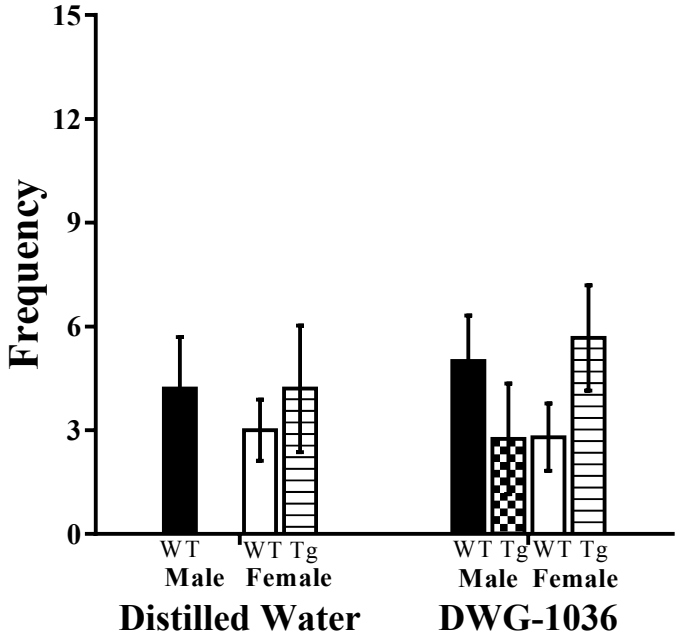

Figure 41. Mean (±SEM) frequency of correct hole visits in the reversal probe trial of Barnes maze. All groups visited the correct hole similar number of times.

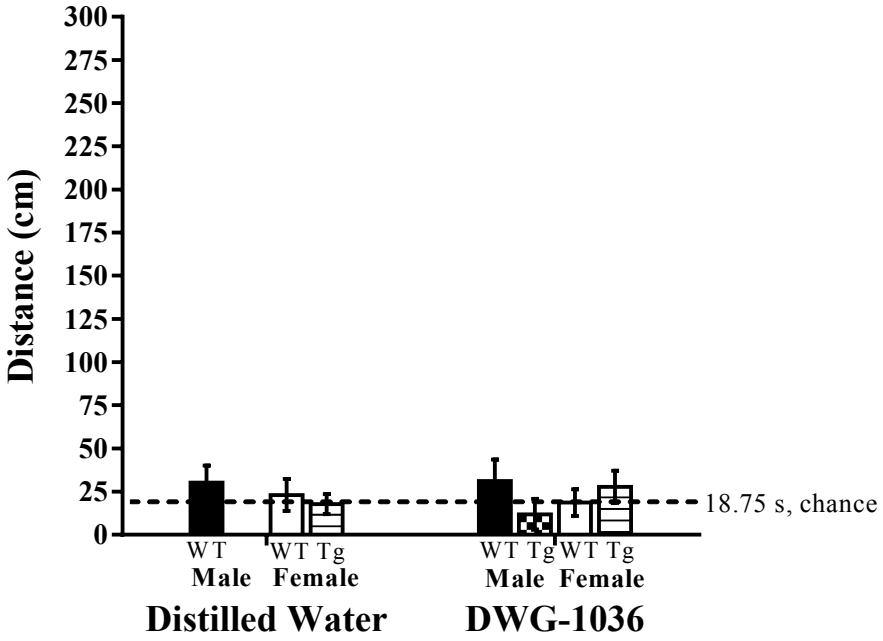

Figure 42. Mean (±SEM) duration of time spent by the correct hole in the reversal probe trial of the Barnes maze. There was no difference between the groups.

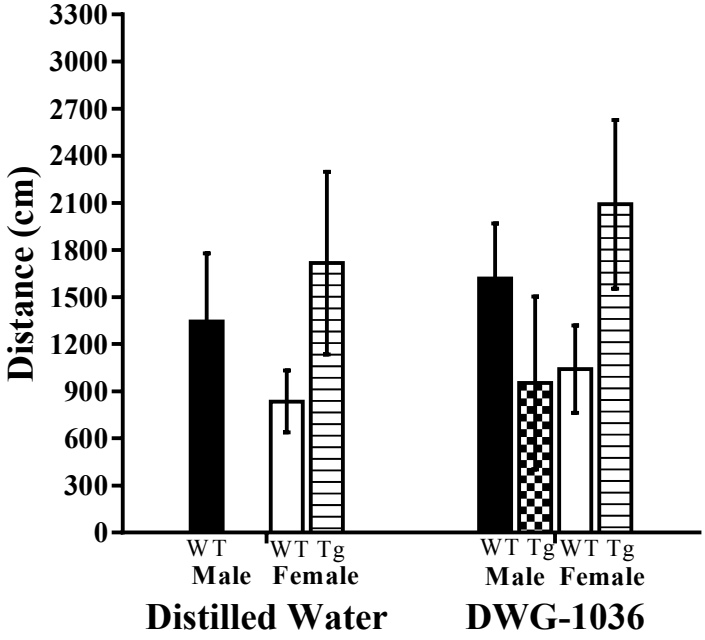

Figure 43. Mean (±SEM) distance moved by the mice in the reversal probe trial of Barnes maze. The female 3xTg-AD mice moved more than the male 3xTg-AD mice but the female WT mice moved less than the male WT mice (95% CI = -117.609, 3546.580).

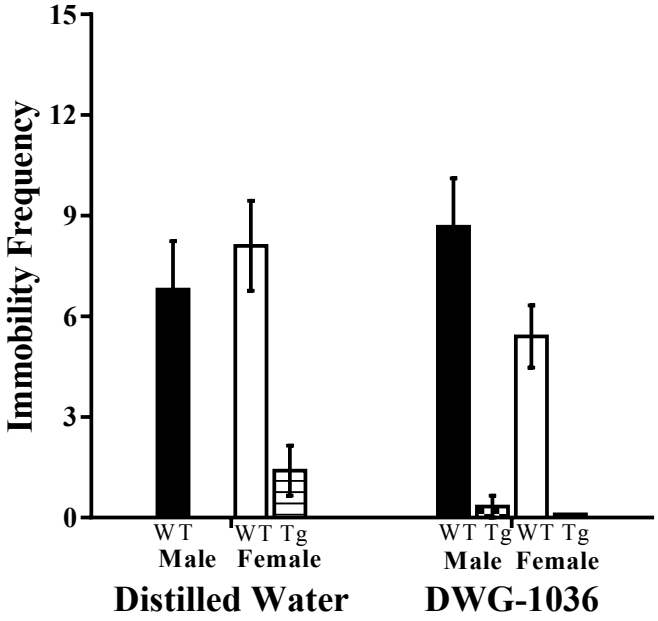

Figure 44. Mean (±SEM) frequency of immobile bots in the forced swim test. The WT control mice were more frequently immobile compared to the 3xTg-AD mice (CI 95% = 4.147, 9.192).

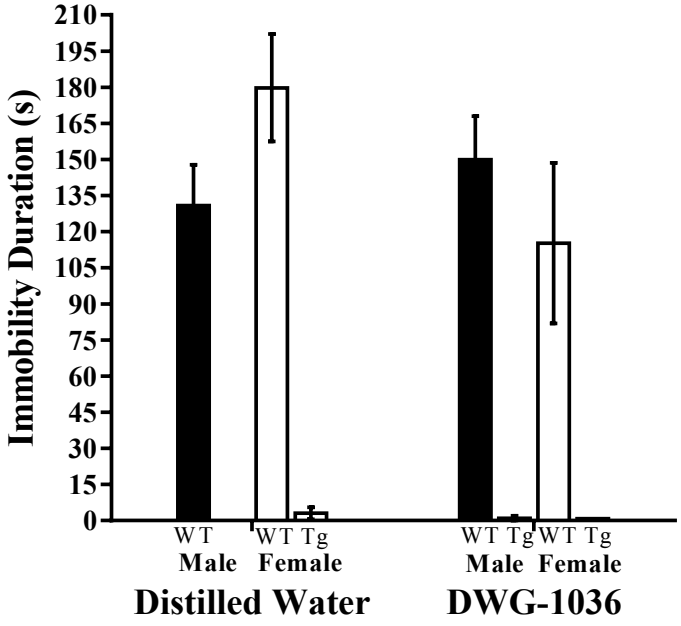

Figure 45. Mean (±SEM) duration of immobility in the forced swim test. WT control mice were immobile for longer periods of time compared to the 3xTg-AD mice (CI 95% = 110.035, 186.505). Moreover, the male mice receiving DWG-106 were immobile for longer periods of time compared to the female mice receiving the compound, yet there was no such difference for the mice receiving the vehicle (CI 95% = -160.675, -6.540).

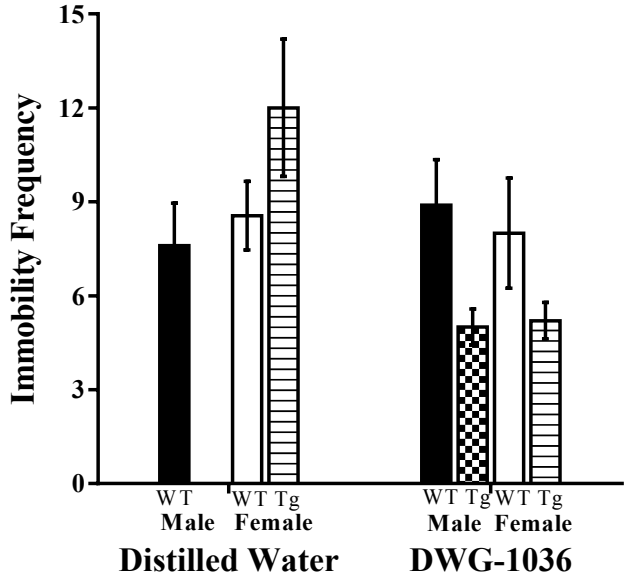

Figure 46. Mean (±SEM) frequency of immobile bots in the tail suspension. The 3xTg-AD mice receiving DWG-106 were immobile less frequently compared to the 3xTg-AD mice receiving vehicle, but there was no such difference for the WT mice (95% CI = -12.797, 0.308).

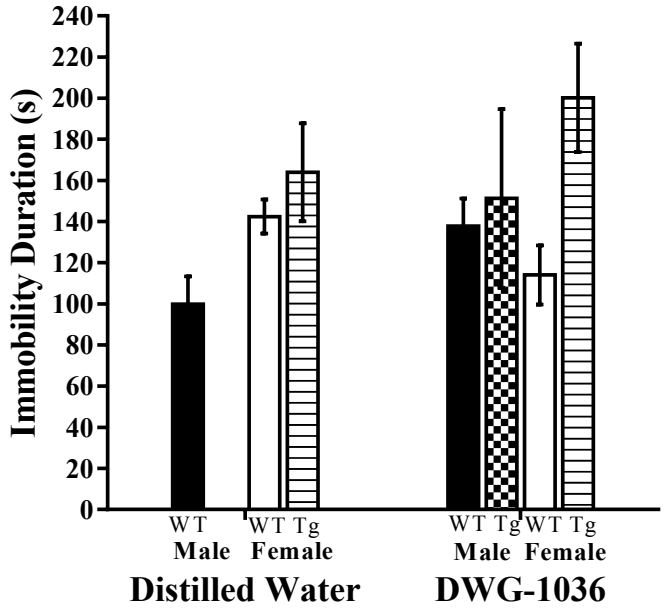

Figure 47. Mean (±SEM) duration of immobility in the tail suspension test. The 3xTg-AD mice were immobile for longer periods of time (95% CI = -72.209, -8.202). Moreover, there was a treatment by sex interaction as the male mice receiving DWG-106 were immobile for longer periods of time compared to the male mice receiving vehicle, yet there was no such difference for the female mice (CI 95%= -131.943, -0.876).

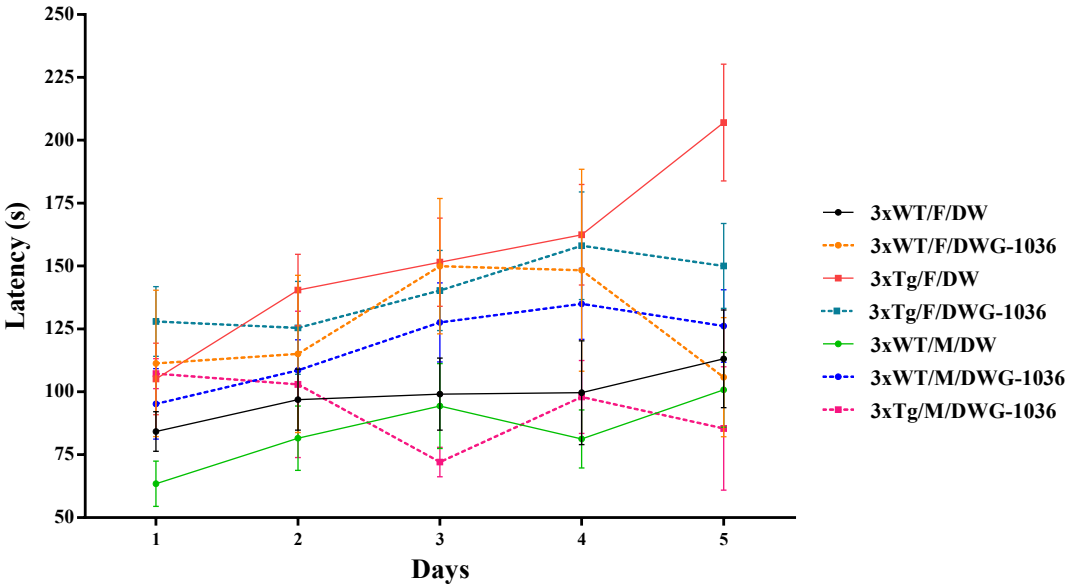

Figure 48. Mean (±SEM) latency to fall down from the rotarod over the 5-day period. All the mice got better over the 5-day period (95% CI = 5.211, 10.325).

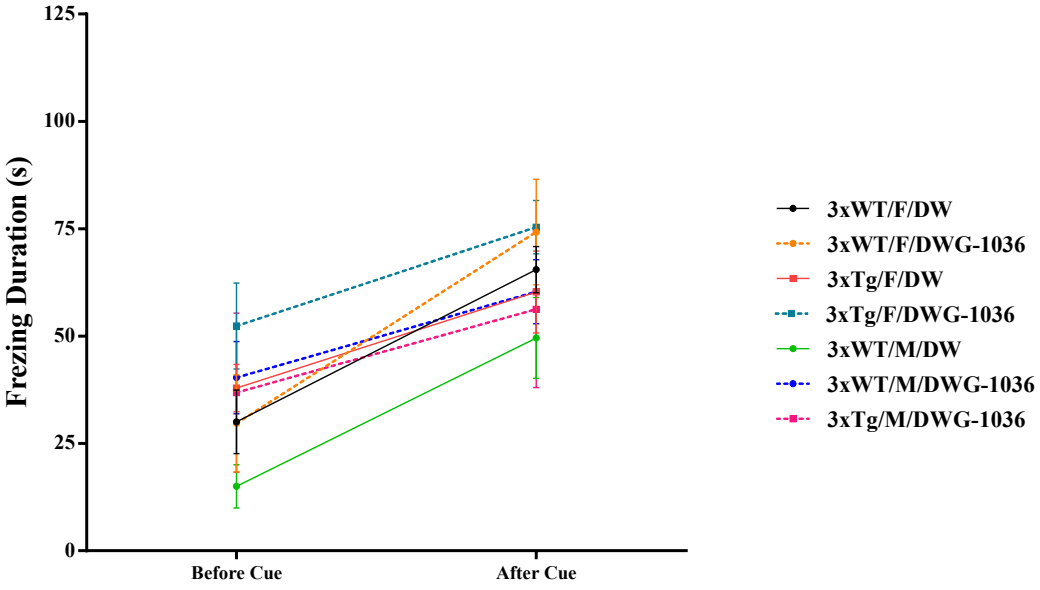

Figure 49. Mean (±SEM) time frozen in the trace fear conditioning. All the mice spent more time frozen after the tone cue (95% CI = -35.034, -22.837) and the DWG-106 treated mice spent more time frozen compared to the vehicle treated mice (95% CI = -24.711, -1.492).

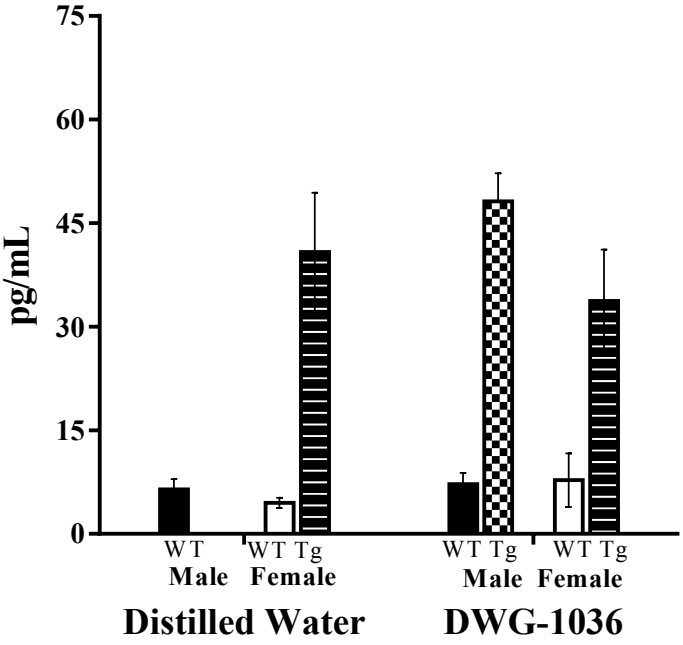

Figure 50. According to the ELISA analyses at 7 months of age, 3xTg-AD mice had significantly more $A\beta_{40}$ compared to WT mice (95% CI = -42.324, -25.286).

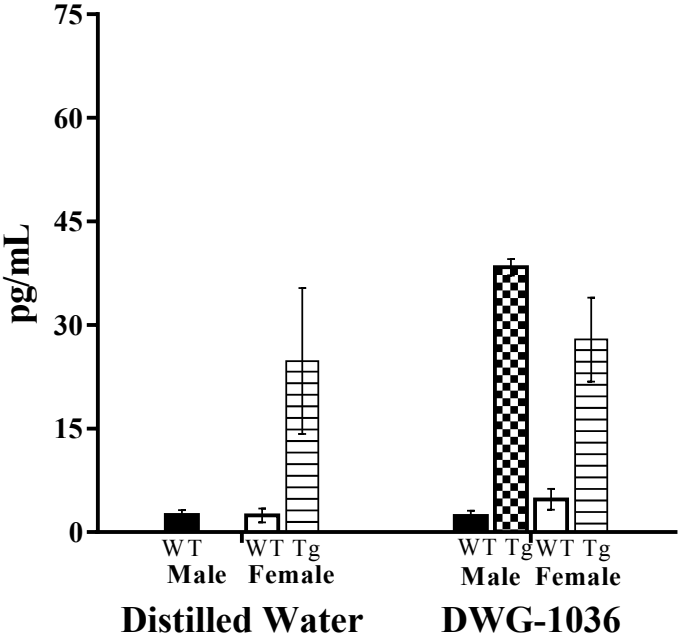

Figure 51. According to the ELISA analyses at 7 months of age, 3xTg-AD mice had significantly more $A\beta_{42}$ compared to WT mice (95% CI = -34.156, -17.903).

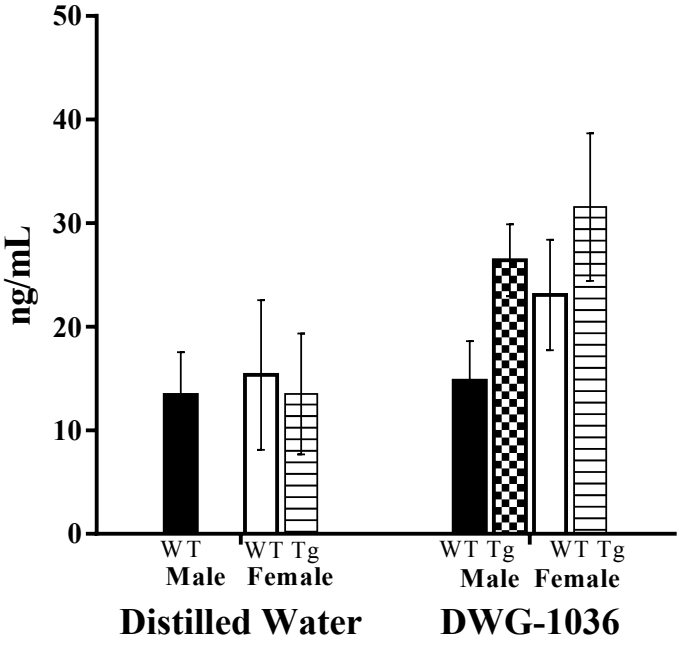

Figure 52. According to the ELISA analysis at 7 months of age, there was a trend of DWG-1036 treated mice having higher levels of quinolinic acid compared to vehicle treated mice (95% CI = -16.851, 0.640).

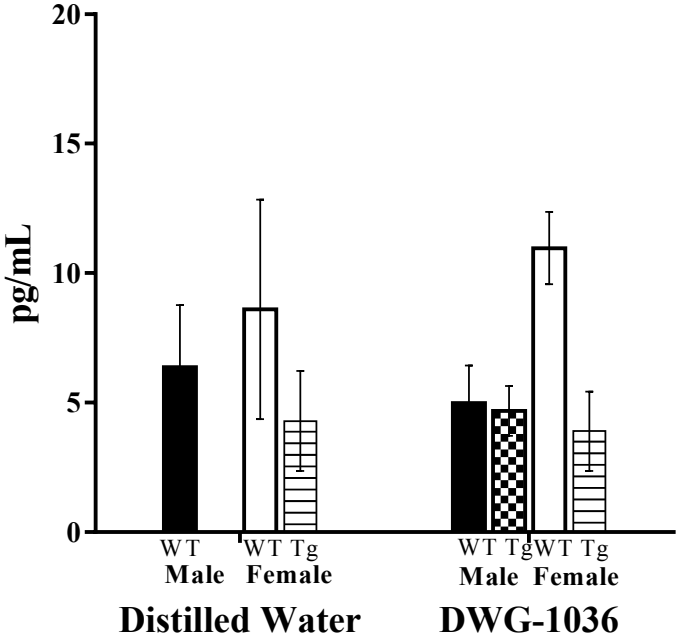

Figure 53. According to the ELISA analysis at 7 months of age, WT control mice had higher levels of INF-γ compared to 3xTg-AD mice (95% CI = 0.002, 8.710).

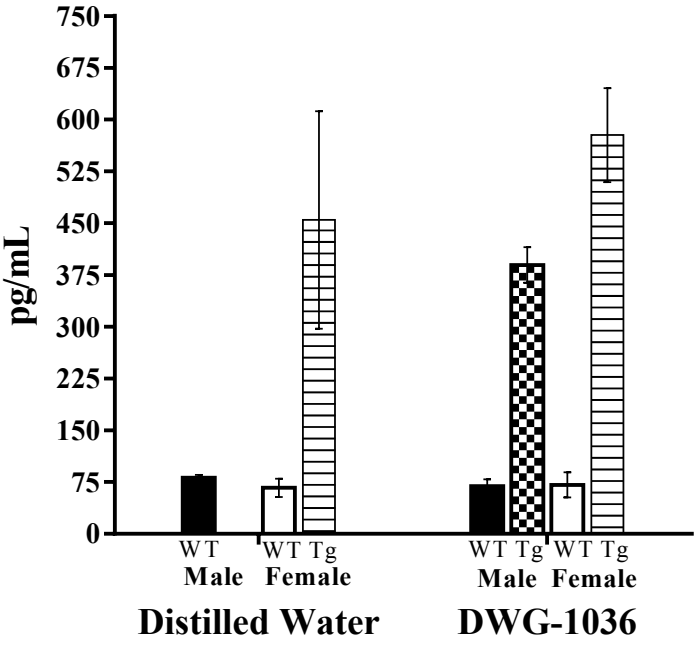

Figure 54. According to the ELISA analysis at 7 months of age, 3xTg-AD mice had significantly more TXNIP compared to WT mice (95% CI = -524.689 -298.174).

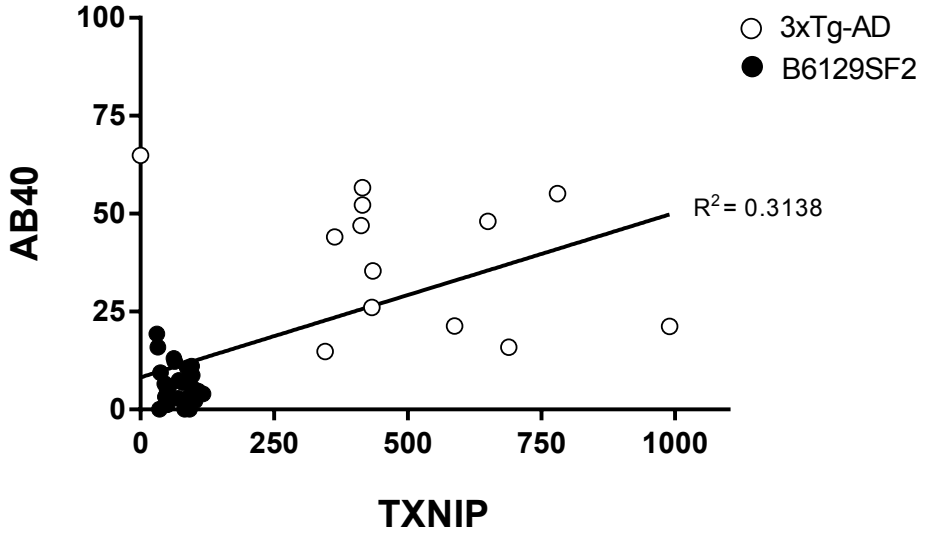

Figure 55. There was a positive correlation between $A\beta_{40}$ and TXNIP levels ($r = 0.560$, $p < 0.05$).

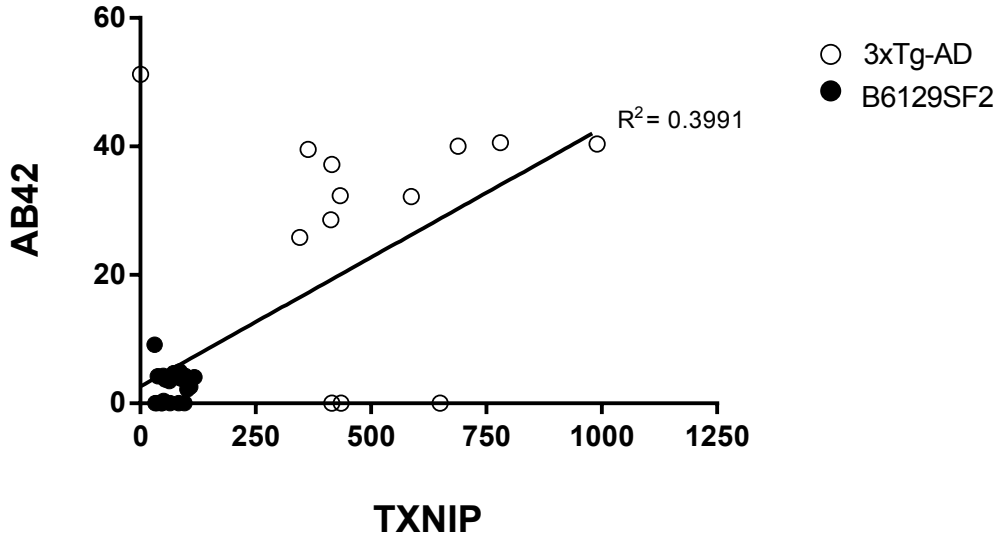

Figure 56. There was a positive correlation between $A\beta_{42}$ and TXNIP levels ($r = 0.632$, $p < 0.05$).